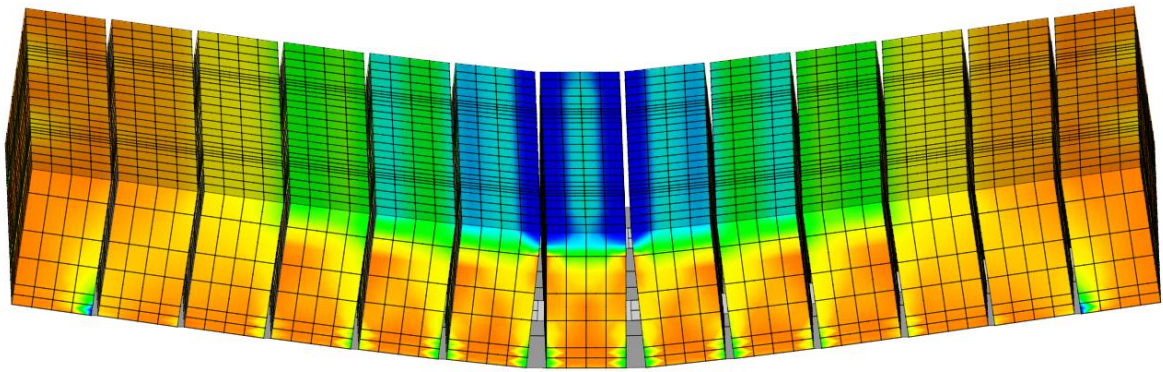


TU Delft & Quake-Shield

# Combining existing independent seismic reinforcing methods for clay brick masonry

Knowledge development of the behaviour of reinforced masonry by using Finite Element Modelling



Edwin Meulman  
15-4-2016



# Combining existing independent seismic reinforcing methods for clay brick masonry

Master thesis  
By  
Edwin Meulman



Delft University of Technology  
Faculty of Mechanical Engineering  
Master track: Materials Engineering and Applications

Quake-Shield

April 15, 2016

Graduation committee

Prof. dr. ir. J.G. Rots, Delft University of Technology - Section of Structural Mechanics  
Dr. Ir. P.C.J. Hoogenboom, Delft University of Technology - Section of Structural Mechanics  
Dr.ir. A. Van Beek, Delft University of Technology - Section of Materials and Environment  
Ir. Drs. Ö. Türkmen, Royal Oosterhof Holman – Department of infra  
Dr.ir. M. Hermans, Delft University of Technology - Section of Metals Processing, Microstructure and Properties



## Abstract

In the last decades induced earthquakes are taking place more frequently in Groningen. This is due to gas extraction from the soil. Buildings are damaged by the earthquakes and building collapse is possible in the near future. Houses in Groningen are commonly built up out of single leaf masonry cavity walls and are not designed for earthquake loads. Oosterhof Holman and SealteQ Group have designed a masonry reinforcing method that is called Quake-Shield. Quake-Shield is a unique reinforcing method and consists out of a combination of two existing independent seismic reinforcing measures.

These two existing independent seismic reinforcing measures are: NSM FRP strips and an EB FRP layer. Carbon strips are placed in vertical grooves in the masonry which are filled with a ductile adhesive to bond the strips to the masonry (NSM FRP strips).

A polymer or cementitious base layer with an embedded polymer or carbon mesh is attached to one side of the masonry on the outer surface (EB FRP layer).

Both reinforcing measures increase stiffness, strength and ductility of the masonry. These three factors result in an increase in earthquake energy absorption and dissipation of the masonry. Which is important when reinforcing houses and buildings to prevent collapse due to earthquake loads.

In this project a FEM model is made based on a three point bend test (out-of-plane bending) performed on Quake-Shield reinforced masonry samples. The FEM model is used to develop knowledge about the effect of combining two existing independent seismic reinforcing measures as used in the Quake-Shield masonry reinforcing method.

The FEM model is a 3D model with a simplified micro-model approach for the masonry. The bricks are solid elements, the reinforcing materials are shell elements and the mortar and the ductile adhesive are interface elements.

The bond-slip behaviour of the ductile adhesive has a significant contribution in the behaviour of Quake-Shield reinforced masonry. The mechanical properties of the ductile adhesive determine mainly the pre and post peak behaviour of the reinforced masonry. Providing a gradual decline in load bearing capacity after the peak load. The EB FRP layer has a significant contribution to the reinforced masonry in the displacement range from the initiation of the first crack in the masonry till the onset of yielding of the EB FRP layer. In this range the EB FRP layer is the dominant reinforcing measure. After yielding of the EB FRP layer the NSM CFRP strip becomes the most dominant of the two. The EB FRP layer also provides cohesion between the individual bricks, keeping the masonry wall together after severe cracking has taken place.

The FEM model is also used for a configuration analysis to research different geometrical and material variations of the Quake-Shield masonry reinforcing method. The configuration analysis gives more insight in the behaviour of reinforced masonry.

For the configuration analysis two independent seismic reinforcing measures, NSM FRP strips and EB FRP layer, are applied separately to the FEM model. This is done to investigate its individual effect on the behaviour of reinforced masonry. Strip spacing has a significant effect on the load bearing capacity. If an epoxy is used as adhesive, which is much stronger and stiffer than the adhesive used by Quake-Shield, an increase in load bearing capacity is achieved but also sudden failure after the peak load is observed. This is an undesirable failure mode and reduces the total energy that the reinforced masonry can absorb.

Results of the different configurations used for the EB layer show that the polymer (PU) base layer has the most significant contribution of the used EB FRP layer materials when considering overall ductility and energy absorption of the reinforced masonry.



## Summary

Gas extraction from the soil causes induced earthquakes in the east part of Groningen. Houses and buildings in the Groningen region are not constructed to resist earthquake loads. The most vulnerable houses need to be reinforced to prevent collapse. The houses in Groningen are commonly built up out of single leaf masonry cavity walls. Royal Oosterhof Holman and SealteQ Group have designed a masonry reinforcing method that is called Quake-Shield. Quake-Shield is a unique reinforcing method and is a combination of two existing independent seismic reinforcing measures. Test results from small scale masonry samples ( $870 \times 550 \text{ mm}^2$ ), out-of-plane (OP) loaded, and full size masonry wall samples ( $4000 \times 2700 \text{ mm}^2$ ), in-plane (IP) loaded, reinforced with Quake-Shield show promising results.

This project focuses on the small scale OP loaded masonry samples. The samples are OP loaded with a three point bend test. A FEM model is made based on this test and used to get better insight in the combination of two existing independent seismic reinforcing measures used with the Quake-Shield method. A configuration analysis is done to see the effect on Quake-Shield reinforced masonry when different geometrical and material variations are applied.

OP loaded single leaf masonry is most critical when considering collapse of a house or building. The relatively thin wall can easily bend or buckle due to the OP load which results in a sudden loss of load bearing capacity. The failure mode of masonry depends on the aspect ratio, vertical load from roof or floor and how the wall is supported.

The basic principle of making single leaf unreinforced masonry (URM) earthquake resistant is to increase the amount of earthquake energy the masonry can absorb and dissipate. This can be done by increasing stiffness, strength and ductility of the masonry. Due to dynamic effects it is important to keep the mass of the reinforced masonry as low as possible.

Commonly applied reinforcing materials are fibre reinforced plastics (FRP) like Carbon (CFRP) or Glass (GFRP). These materials are applied in two commonly used methods: near surface mount (NSM) FRP strips and an external bound (EB) FRP layer. These two existing seismic reinforcing measures are combined in Quake-Shield. The EB FRP layer consists out of a polymer or cementitious base layer with an embedded polymer or carbon mesh. The NSM FRP strips are CFRP strips embedded in a groove in the masonry which is filled with ductile adhesive to bond the CFRP strip to the masonry.

In general, masonry has a large variation in mechanical properties due to its sensitivity to environmental conditions during manufacturing of the bricks and the construction of masonry itself. Material tests like compression tests are required to have good reference material properties for the development of the FEM model. In the case of modelling reinforced masonry also bond-slip behaviour of the NSM FRP strip in the adhesive is critical to achieve a good correlation between test results and FEM model results. Pull-out tests can provide such information. Material tests and pull-out tests are performed by the TU/e to get this information for Quake-Shield.

Different earthquake analysis methods can be used to determine if a house or building can resist a certain earthquake induced load. Lateral force analysis is the least complex method and non-linear

time-history analysis the most complex method. Latter one is used with FEM software. FEM software (DIANA 9.6) is also used for this project to model the reinforced masonry. Based on the literature study a 3D FEM model with a simplified micro-model approach is used. The mortar interfaces have a non-linear material model. Initially the combined cracking-shearing-crushing (CCSC) material model was selected. The NSM FRP strip is modelled with embedded reinforcing elements in combination with bond-slip behaviour. The combination of the CCSC (interface) material model and the embedded reinforcement elements with bond-slip behaviour could not be combined. Also the CCSC is assumed to be too complex for OP load situation and corresponding masonry failure modes. Therefore mortar interfaces are changed to a non-linear discrete cracking material model and the NSM CFRP is modelled discretely in the FEM model based on the Quake-Shield OP bend test. The shell elements used for the NSM CFRP strip are connected to the solid (brick) elements by interface elements that provide bond-slip behaviour.

A FEM model is made, based on the pull-out tests of the TU/e, to calibrate the bond-slip behaviour of the NSM CFRP strip in the Quake-Shield FEM model.

The significance of the ductility of the adhesive becomes more clear in a sensitivity study that was done during development of the Quake-Shield FEM model. This was done to develop knowledge about the effect of certain parameters on the behaviour of the model.

During two calibration steps the FEM model result was adjusted slightly to get a better correlation with the test result. The stiffness of the model is slightly overestimated by the EB FRP layer. The polyurea (PU) base layer and polypropylene (PP) mesh are homogenised into a single layer. The assumptions made for homogenising the layer result in a stiffness overestimation. The mechanical behaviour of a soft polymer is simplified by the material model used in the FEM model. Material properties involving this EB FRP layer are adjusted to reduce the overestimation of stiffness and onset of yielding of the EB FRP layer. Also the onset of compression failure in the bricks initiate at a too high displacement compared to the test results. Material properties of the bricks are adjusted slightly so onset of compression failure correlates better with the test results.

After calibration, the model shows a good fit with the test result but has still some deviations. The EB FRP layer is dominant from the initiation of the first crack in the masonry till the onset of yielding of the EB FRP layer. From this point the NSM CFRP strip becomes dominant for the behaviour of the reinforced masonry. Showing a distinct peak which is also the displacement at which the adhesive reaches its ultimate shear strength. In the test result the peak is less distinctive and could be considered as a wide plateau before a gradual decline in load bearing capacity sets in. The plateau could be caused by more severe compression failure compared to the FEM model which shows only compression failure in the bricks closest to the middle row of bricks. In the test sample the compression failure is more spread over the three middle rows of bricks. Also imperfection like premature debonding of the EB FRP layer or imperfection in the test setup could influence the mechanical properties of the reinforced masonry or displacement measurement, resulting in different peak load behaviour compared to the model.

The calibrated FEM model is used as a base model for the configuration analysis. In the configuration analysis multiple geometrical and material variations, based on Quake-Shield, are modelled to get better insight in the effect of the two combined existing reinforcing methods on the behaviour of reinforced masonry.



The first model variation is applying one of the two individual FRP reinforcement measures on the masonry in the model. The FEM results from these variations show the behaviour of the separate FRP reinforcement measures and show comparable behaviour to test results from a different test series (AG-series).

Changing the spacing between the NSM FRP strips has a significant effect on the load bearing capacity. Strip spacing could be expressed as number of strips per meter masonry. The base model has four strips per meter. Also one and two strips per meter masonry are modelled. Future model development and Quake-Shield method optimization could be done to find the minimum number of strips per meter masonry for a certain load condition. Optimization can also be done for the strip dimensions. The increased bonding area between adhesive, strip and masonry results in more ductility due to the ductile material properties of the adhesive used by Quake-Shield. The NSM CFRP strip width has also influence on the bending resistance due to the effect of increased area moment of inertia of the strip.

Using a stiff epoxy as adhesive to bond the NSM FRP strip to the masonry increases the stiffness and load bearing capacity of the reinforced masonry significantly. However a sudden loss of load bearing capacity after peak load takes place when using epoxy compared to the ductile adhesive used in Quake-Shield. Ductility after the peak load is an important factor for reinforced masonry which increases energy adsorption by the reinforced masonry. Comparing the energy absorption between these two variations, the ductile adhesive of Quake-Shield takes up more energy although the load bearing capacity is significantly lower.

For the EB FRP layer different combinations are compared involving a polymer and carbon mesh (PP-mesh and C-mesh) embedded in a polymer (PU) or cementitious base layer (AC). AC increases initial stiffness till the AC layer cracks. From this point on the AC losses its contribution to the behaviour of the reinforced masonry and functions only as bonding material for the mesh. A polymer has a contribution over a larger displacement range due to its elastic-plastic properties. From onset of yielding of the EB FRP layer its contribution to the behaviour of the reinforced masonry is reduced. C-mesh is stiffer than PP-mesh and therefore increases stiffness and reduces crack opening. This delay of crack opening and taking up load by the C-mesh reduces stress on the NSM CFRP strip and adhesive resulting in a higher load bearing capacity. Increasing stiffness and strength to the EB FRP layer at the bottom side of the masonry sample can result in an increased compression zone at the top side of the masonry sample. Masonry is in general already the weakest material in reinforced masonry and so shifting more stress to this material should be avoided.

Based on the results of the FEM models the following can be concluded about the reinforcing method of Quake-Shield. Both independent seismic reinforcing measure show improved stiffness, strength and ductility if applied separately. If both combined the EB FRP layer first is dominant, reducing the stress on the NSM FRP strip, and determines mainly the behaviour of the reinforced masonry. After the onset of yielding of the EB FRP layer the NSM FRP strip becomes dominant, determining the load bearing capacity and post peak behaviour of the reinforced masonry.

The bond-slip behaviour of the ductile adhesive to bond the NSM CFRP to the masonry determines mainly the pre and post peak behaviour of the reinforced masonry with a gradually decline in load bearing capacity after the peak load. The ultimate shear strength of the adhesive determines mainly

the peak load of the reinforced masonry. The EB FRP layer bonds the individual bricks and provides stiffness to the reinforced masonry from the first crack initiation till yielding of the EB FRP layer.

The FEM model and Quake-Shield masonry reinforcing method can be developed further and optimized in the future. Some recommendations for future research are the following.

Research into the adhesion and debonding of the NSM FRP strip adhesive and the EB FRP layer to the masonry. Improper adhesion or debonding could reduce the mechanical properties of the reinforced masonry significantly.

Use separate layers for the EB FRP layer in the FEM model. Using embedded grid reinforcement elements for mesh type materials appears to work properly.

Improve masonry behaviour of the model by improving non-linear behaviour of the masonry when compression loaded and implement more extensive shear effects in the mortar interfaces.

Perform the OP test in vertical position with an applied normal force to the reinforced masonry sample to get more realistic loading conditions. Also URM could be tested properly in this position which can then be used to compare results with Quake-Shield reinforced masonry.

## Acknowledgments

This thesis is written to complete my graduation project to obtain a Master's degree in Mechanical Engineering at the Delft University of Technology. Research is done on the behaviour of masonry that is reinforced with the Quake-Shield reinforcing method developed by Royal Oosterhof Holman and SealteQ Group. FEM modelling is used as a tool to get better insight and develop more knowledge about the Quake-Shield reinforced masonry when subjected to out-of-plane loading conditions.

During this graduation project guidance was provided by Delft University of Technology, TNO DIANA and Royal Oosterhof Holman. The graduation project was carried out between March 2015 and April 2016.

I would like to thank my graduation committee: Jan, Pierre, Ton, Marcel and Ömer, for guiding me during the process of this graduation project and a special thanks to Ab and Shen of TNO DIANA who offered their time to support me concerning DIANA related problems and development of my FEM model.

Furthermore I would like to thank my family, friends and colleagues from Royal Oosterhof Holman for their support.

## Acronyms

AC - Armo-crete  
AFRP - Aramid fibre reinforced plastic  
C-mesh - Carbon mesh  
CCSC - Combined cracking-shearing-crushing  
CFRP - Carbon fibre reinforced plastic  
DIANA - Displacement ANALyzer  
EB - External bond  
FEM - Finite element method  
FRP - Fibre reinforced plastic  
GFRP -Glass fibre reinforced plastic  
IP - In-plane  
KNMI - Koninklijk Nederlands Meteorologisch Instituut  
NSM - Near surface mounted  
OP - Out-of-plane  
PGA - Peak Ground Acceleration  
PP - Polypropylene  
PP-mesh - Polypropylene mesh  
PU - Polyurea  
TU/e - Technische universiteit Eindhoven  
URM - Unreinforced masonry  
VE - Vijf Eiken

## List of Symbols

$g$	Gravitational acceleration	$m/s^2$
$K_n$	Normal stiffness modulus	$N/mm^3$
$K_t$	Shear stiffness modulus	$N/mm^3$
$f_t$	Tensile strength	MPa
$f_c$	Compression strength	MPa
$f$	Force	N
$C$	Cohesion	MPa
$G_f I$	Fracture energy mode-I	N/mm
$G_f II$	Fracture energy mode-II	N/mm
$G_{fc}$	Compressive fracture energy	N/mm
$C_s$	Shear traction contribution	[-]
$K_p$	Peak Equiv. plastic relative displacement	mm
$G_c$	Compressive fracture energy of brick	N/mm
$f_c$	Compressive strength of brick	MPa
$E$	E-modulus	MPa
$E_{unit}$	E-modulus of brick	MPa
$E_{joint}$	E-modulus of mortar	MPa
$G_{unit}$	Shear modulus of brick	MPa
$G_{joint}$	Shear modulus of mortar	MPa
$h_{joint}$	Height of mortar joint	mm
$\nu_{unit}$	Poisson ratio of brick	[-]
$E_{eq}$	Equivalent E-modulus	MPa
$E_{pu}$	E-modulus of polyurea	MPa
$E_{pp}$	E-modulus of polypropylene	MPa
$A_{pu}$	Cross sectional area of polyurea	$mm^2$
$A_{pp}$	Cross sectional area of polypropylene	$mm^2$
$A_{tot}$	Cross sectional area of total PU+PP-mesh layer	$mm^2$
$E_{inp}$	Input energy	J
$E_{diss}$	Dissipated energy	J
$\Pi$	Induced potential energy	J
$\zeta_{hyst}$	Hysteretic damping	[-]
$m$	Mass	kg
$a$	Acceleration	$m/s^2$

# Contents

1	Introduction.....	1
2	Literature study .....	3
2.1	Earthquakes in Groningen .....	3
2.2	Masonry.....	8
2.3	Masonry reinforcing methods and materials.....	11
2.3.1	Commonly used masonry reinforcing methods and materials .....	11
2.3.2	Energy absorption & dissipation of URM and reinforced masonry .....	13
2.3.3	FRP masonry reinforcing methods .....	16
2.3.4	Depth of embedding NSM FRP strip.....	18
2.3.5	NSM FRP strip orientation and spacing .....	19
2.3.6	Optimal bonding of FRP to masonry .....	20
2.4	Testing unreinforced and reinforced masonry walls.....	22
2.4.1	Commonly used masonry test methods.....	22
2.4.2	Displacement limitation of reinforced masonry .....	25
2.5	Masonry FEM models.....	27
2.5.1	Construction analysis methods for earthquakes.....	27
2.5.2	FEM models from literature .....	30
2.5.3	Crack models for masonry.....	34
2.5.4	Modelling of reinforcement material combined with masonry.....	37
2.6	Literature study summary .....	38
3	Quake-Shield samples and test results .....	40
3.1	Quake-Shield sample geometry and materials .....	40
3.2	Quake-Shield sample preparation.....	43
3.3	Test setup .....	44
3.4	Quake-Shield test results.....	45
3.5	Imperfection of testing and samples.....	47
4	Reinforced masonry FEM model .....	48
4.1	Quake-Shield FEM model .....	48
4.1.1	FEM model Geometry .....	48
4.1.2	Load and boundary conditions .....	52
4.1.3	FEM model material properties .....	54

4.2	Pull-out of NSM CFRP strip .....	59
4.2.1	Pull-out test results .....	59
4.2.2	Pull-out FEM model .....	61
4.3	FEM model sensitivity study.....	63
5	FEM model calibration & results .....	68
5.1	FEM model calibration .....	68
5.2	FEM Base model results .....	73
5.3	Discussion of FEM Base model results .....	77
6	Quake-Shield configuration analysis .....	78
6.1	URM, without NSM CFRP strip, without EB FRP layer.....	78
6.2	Geometrical variations .....	81
6.2.1	Spacing of NSM CFRP strips.....	81
6.2.2	Dimensions of the CFRP strips.....	83
6.3	Material variations .....	85
6.3.1	Different types of NSM FRP reinforcing materials .....	85
6.3.2	Different types of adhesive .....	87
6.3.3	Different types of EB layer.....	92
6.4	Discussion of configuration analysis results.....	97
7	Conclusions & Recommendations.....	99
	Bibliography.....	102
	Appendix A .....	105
	Appendix B .....	113





# 1 Introduction

In the last few years research on earthquakes in the Netherlands is increased. Gas extraction from the soil in Groningen induces earthquakes that damage buildings and potentially could result in building collapse. Buildings in the Netherlands are not designed to withstand earthquake loads and are commonly build out of single leaf masonry cavity walls. To prevent these buildings from collapsing, reinforcing methods have to be applied to strengthen the masonry walls.

Quake-Shield, a method designed by Royal Oosterhof Holman and SealteQ Group, is a reinforcing method to strengthen masonry walls. Oosterhof Holman and SealteQ performed small scale out-of-plane (OP) and large scale in-plane (IP) tests on Quake-Shield reinforced masonry. The results are promising and the first building in Usquert (Groningen) is reinforced with the Quake-Shield reinforcing method [1].

The reinforcing method is unique because it combines two in literature common fibre reinforced plastic (FRP) reinforcing methods. These two reinforcing methods are near surface mounted (NSM) FRP strips and external bond (EB) FRP layer. Future development and optimization of the Quake-Shield reinforcing method is possible if knowledge and insight about the behaviour of reinforced masonry is increased. Finite element method (FEM) modelling can be very useful to research reinforced masonry behaviour and investigate the combination of two independent reinforcing methods like Quake-Shield. Conclusions and recommendations found in this thesis could be used for optimization and further development of the Quake-Shield reinforcing method.

A configuration analysis is used to investigate different variations of reinforced masonry. During the development of the FEM base model and the results from the configuration analysis, more insight in the behaviour of Quake-Shield reinforced masonry is obtained. For the configuration analysis a FEM base model of the Quake-Shield reinforcing method is required. Test results of Quake-Shield reinforced masonry is used to validate the FEM base model. Due to the difficulties involved in validating masonry FEM models and the limited time of the graduation project, only a FEM model based on the OP tests is made. The FEM model is made with use of DIANA 9.6. The model is 3D and consists out of solid, interface and shell elements. The OP test is a three point bend test in which the load is applied monotonic.

## Goals

- Develop knowledge about the effect of combining two existing independent seismic reinforcing measures used in the Quake-Shield masonry reinforcing method and how this can be modelled with FEM software (DIANA 9.6)
  - FEM model validation by using experimental tests results of Quake-Shield reinforced masonry
  - Applying the two existing independent seismic reinforcing methods to the model separately to research its contribution to Quake-Shield
- Get more insight in the behaviour of reinforced masonry when different geometrical and material variations are used for the Quake-Shield masonry reinforcing method
  - Comparing model variation results to the validated FEM Base model

**Main research question**

What are the effects of combining two independent seismic reinforcing methods and how does this change the behaviour of a masonry wall?

***Thesis outline***

Chapter 1 gives an introduction of the thesis describing the subject, goals and main research question of the project. Chapter 2 contains the literature study. The literature study provides information about earthquakes in general and the earthquake problems in Groningen. How unreinforced and reinforced masonry behave during an earthquake. Reinforcing methods used in other researches and how unreinforced and reinforced masonry is modelled in FEM.

Chapter 3 describes the Quake-Shield samples, test setup and test results.

The Quake-Shield FEM model is described in Chapter 4.

Chapter 5 contains the calibration and results of the Quake-Shield FEM Base model. The calibrated FEM Base model is used for the configuration analysis. The configuration analysis is described in Chapter 6. The configuration analysis contains variations in model geometry and material properties. Results from these Chapters are used to come to conclusions and recommendations that can be found in Chapter 7.

## 2 Literature study

This chapter covers the literature study. The literature study is used to gain basic knowledge about: masonry in seismic active areas, how masonry can be reinforced to withstand earthquake loads and experimental tests that can be used to test reinforced masonry. Eventually a FEM model is made based on Quake-Shield reinforced masonry. The literature study is used to find out how unreinforced and reinforced masonry is modelled with FEM by other researchers. The literature study is based on the Quake-Shield reinforced masonry method, therefore the information mainly relates to the techniques used in Quake-Shield. Quake-Shield is applied to single leaf masonry walls made out of clay brick masonry. If from now on masonry is mentioned only clay brick is considered unless otherwise stated.

First part of the literature study is about earthquakes in Groningen, masonry in general and reinforcing methods for masonry. The middle part is about tests performed on masonry found in literature. The last part is literature on FEM models and how masonry is modelled in FEM.

### 2.1 Earthquakes in Groningen

Earthquakes in the Groningen region are different compared to most earthquakes worldwide because the earthquakes are induced by gas extraction from the soil and not by a natural phenomenon like sliding of fault lines [2]. In Groningen the gas volume in the soil is reduced by extraction of gas. A large area at the east of Groningen sinks slightly due to this volume change. This sinking does not happen very smoothly but in increments which release large amounts of energy which is translated to vibrations in the soil. These vibrations are the earthquakes that took place in Groningen for the last decades.

The first earthquake in Groningen that was noticed due to gas extraction was in 1986 [2]. Last decade the earthquakes are not getting significantly larger in magnitude but the frequency is increasing. There are clear indications that there is a correlation between the amount of gas extraction and the frequency of the earthquakes. Figure 1 shows the number of earthquake in each year from 1995 till 2013 with a magnitude of 1,5 or higher on Richter scale.

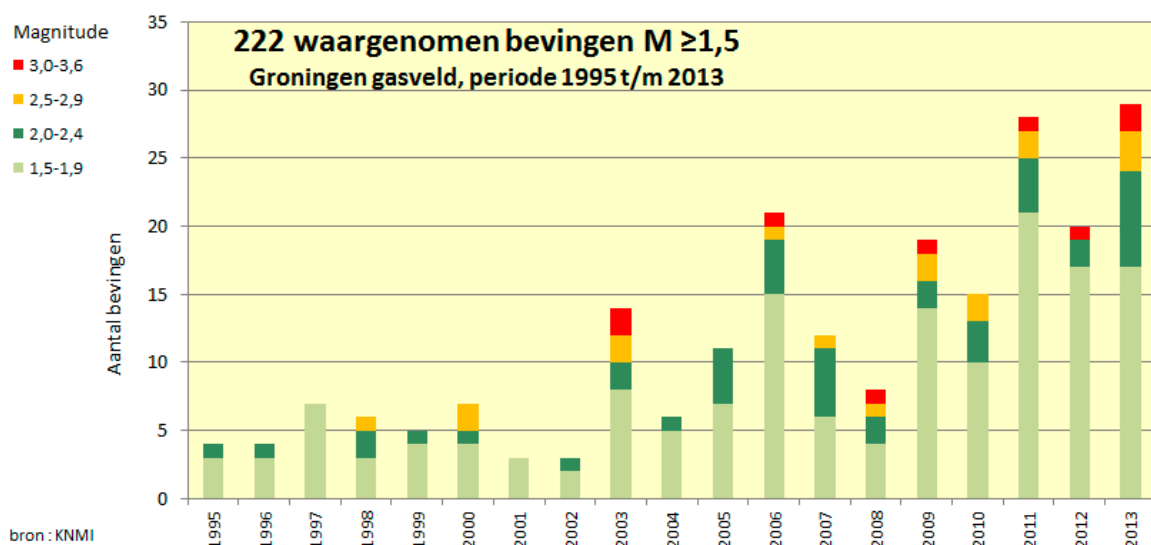


Figure 1: Measured earthquakes above 1,5 on Richter scale in Groningen from 1995 till 2013 [3]

Figure 2 shows a map of Groningen where all the earthquakes until 2013 took place in the Groningen region.

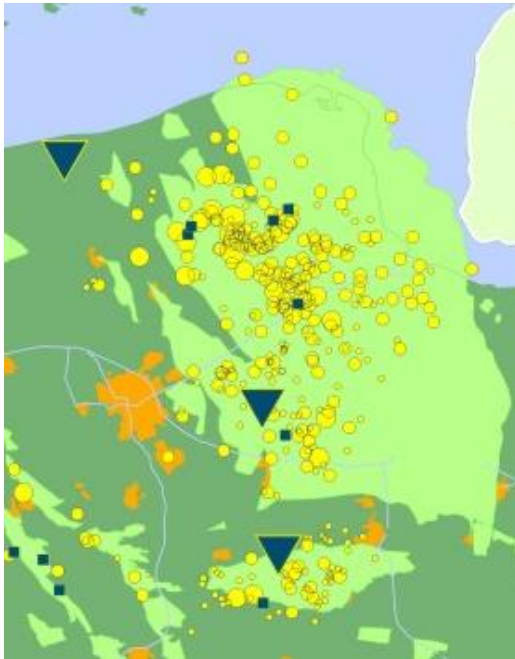


Figure 2: Map of east side of the city of Groningen with earthquake locations (yellow dots). The light green indicates the gas field [4].

The earthquake vibration frequency and magnitude are dependent on the type of soil and depth of the hypocentre (location in the earth where the earthquake energy is released). The hypocentre is very shallow at Groningen because the gas is also very shallow located in the soil. The soil is soft clay, which transmits the vibration better compared to a rocky soil. These two factors in combination with the fact that the earthquakes are induced by gas extraction make the situation of Groningen unique and therefore a challenge for the scientists and engineers to come up with solutions to either reduce the earthquakes or make the buildings earthquake resistant. Research on earthquakes and seismic resistant building design done in other countries cannot always be used in Groningen because of its unique situation.

Most houses in the east of Groningen are located in villages. The load bearing walls of these houses are usually made out of single leaf masonry cavity walls and are only designed to withstand wind loads. The houses in Groningen are not build according to earthquake design standards and therefore are not designed to withstand earthquakes of large magnitude (about 5 on Richter scale).

Usually the magnitude of an earthquake is expressed on Richter scale. An earthquake is a vibration in which not only the amplitude of the vibration but also the frequency plays a significant role. In the case of Groningen peak ground acceleration (PGA) gives a better indication of the earthquake intensity and the relating earthquake loads on the buildings. Analytical and numerical models can be used to calculate what forces are acting on a structure when a certain ground acceleration is induced by an earthquake. More information about modelling can be found in paragraph 2.5.

Research and measurements done by the KNMI provides a contour plot of peak ground acceleration (PGA) of the Groningen area [5]. The maximum value in this contour plot is 0,42g with a return period of 475 year (Figure 3).

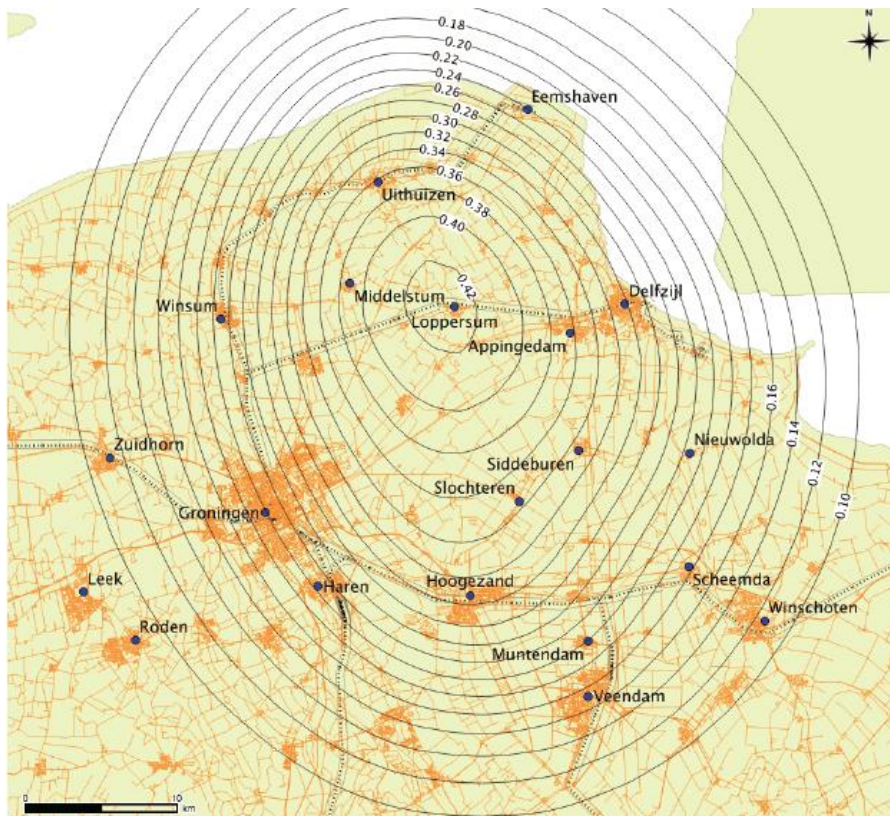


Figure 3: Contour plot peak ground acceleration (PGA) in [g] with return period of 475 year [5]

Between 1970-1980 a building company called Jarino built a lot of terraced houses in the east of Groningen [6]. Recent inspection showed the quality of these houses are lower than expected due to poor construction execution by Jarino. Therefore the 'Jarino houses' are vulnerable for earthquakes and should be reinforced before an earthquake occurs with a larger magnitude until now have taken place. Arup investigated in 2013 many houses in the east part of Groningen [7]. Most of the houses in this area are built after 1960. Figure 5 gives an overview of the type of house in Groningen put in categories by Arup. After 1960 the floors are usually concrete which has a lot more mass compared to wood.

Based on the PGA contour plot of the KNMI (Figure 3) and the house assessment by Arup it is possible to determine to what level a house needs to be reinforced. These reinforcing levels are divided in seven 'intervention levels' [7].

**Permanent upgrading measures – intervention levels:**

- **Level 1:** Mitigation measures for higher risk building elements (potential falling hazards);
- **Level 2:** Tying of floors and walls;
- **Level 3:** Stiffening of flexible diaphragms;
- **Level 4:** Strengthening of existing walls;
- **Level 5:** Replacement and addition of walls;
- **Level 6:** Foundation strengthening; and
- **Level 7:** Demolition.

Figure 4: Seven intervention levels [7]

For example Level 2 'tying of floors and walls' is done to connect walls and floors to create a stiffer construction so earthquake loads can be transferred through the connections. Concrete and masonry have different coefficient of heat expansion. Due to this difference in heat expansion it could be



assumed that the walls and floor are not connected if only mortar is used to connect the walls with the floor. Lateral loads are in this case only transferred between wall and floor by dry friction. Quake-Shield reinforcing method is a level 4 reinforcing measure. It is only applied to strengthen existing masonry walls.









Nr	Type	Image	Floor	Note
1	T1 Terraced house		Concrete	80% of the terraced houses built after 1960. Concrete was introduced as a building material for regular houses around 1953. Therefore it is assumed that primarily concrete floors are used for terraced houses.
2	T2a Semi-detached		Wood	
3	T2b Semi-detached		Concrete	65% of the semidetached houses built after 1960. Therefore it is assumed that primarily concrete floors are used for semi-detached houses.
4	T3a Detached		Wood	50% of the detached houses built after 1960. At least 40% of all detached houses will have wooden floors only. The other 60% may contain wooden floors, concrete floors or both.
5	T3b Detached		Concrete	
6	T4 Labourers cottage		Wood	Typical building found in rural areas in the neighbourhood of farms
7	T5 Mansion		Wood	Typical square building found in towns and villages in the region
8	T6 Large masonry villa		Wood	Large masonry residence containing a ground level and at least 2 stories. Richly decorated with ornaments and generally well maintained.

Figure 5: Type of houses in Groningen divided in 6 categories by ARUP [7]

Investigation done by Adviesbureau Hageman suggests the critical houses as described above cannot withstand more than 0,1g to 0,14g depending on the vertical load on the wall [8]. In this investigation a non-linear pushover analyses is performed on a single leaf masonry wall OP loaded. Until 2016 no buildings have collapsed or casualties have taken place suggesting the 0,1g-0,14g values have likely not been exceeded until now. But the contour plot of the KNMI (Figure 3) indicates values above 0,14g are likely to happen in the future. To prevent building collapse, with likely casualties, it is necessary to improve the earthquake resistance of the current buildings in that area which do not comply to the earthquake design building standard stated in the European codes and 'Nederlandse Praktijkrichtlijn' [5].

Arup made a risk assessment based on the combination of the research of the KNMI (contour plot) with the house inspections done by Arup. Arup gives an example of an earthquake with magnitude of 5 on Richter scale. In this case: "expected that 8,000 to 9,000 buildings will be slightly or moderately damaged, 1,300 to 3,200 buildings extensively to completely damaged and approximately 370 to 1200 buildings will collapse. It is estimated that 470 to over a 1000 people could be injured with 45

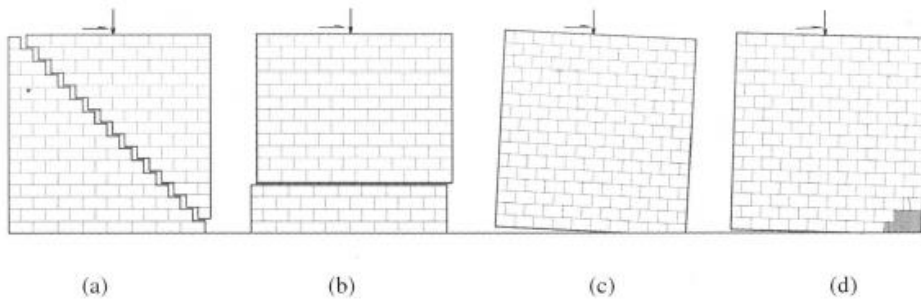
to over 100 life threatening injuries or direct fatalities” [7]. It should be noted that these values are based on the contour plot shown in Figure 3 and at the moment of writing the KNMI and other institutes are still investigating possible improvements of this contour plot. The PGA values could become higher or lower. Assuming that this plot is generated with a conservative approach, it is more likely that improvements of this plot result in lower PGA values instead of higher PGA values. The possible lower PGA values on the contour plot will also influence the risk assessment in a positive way.

## 2.2 Masonry

All over the world masonry is used for the construction of buildings [9]. It is one of the oldest techniques to construct buildings. Studies have proven severe building damage and most casualties during earthquake take place in seismic areas where masonry is used in buildings [10]. Masonry is used as construction material because it is relatively easy to manufacture, low cost and due to its good properties to withstand compressive loads [9]. Load bearing masonry walls are mainly loaded in vertical direction because of the weight of other floors or roof on top of the walls.

During an earthquake the soil will vibrate in longitudinal, lateral and vertical direction. The longitudinal and lateral directions will introduce horizontal loads in the masonry walls. This results in bend, shear and tensile loads in the masonry which is not the preferred way to load masonry. The mortar-brick interface is usually a weak link when these types of loads are applied. The interface quality between mortar and brick can be of large influence for the total load capacity of the masonry. Factors that can influence this interface quality are: type of brick, type of mortar, mortar mix ratio and environmental conditions like for example moisture and temperature [11].

The bend, shear and tensile loads could result in failure modes that are often seen in masonry during or after an earthquake [12]. The In-plane (IP) failure modes are: shear diagonal failure, shear sliding failure, rocking failure and toe crushing (Figure 6).



In-plane failure modes of a laterally loaded URM wall: (a) shear failure; (b) sliding failure; (c) rocking failure; and (d) toe crushing

Figure 6: Masonry failure modes when the wall is loaded in-plane [12]



The out-of-plane (OP) failure modes of a masonry wall are: bending failure, buckling failure, flexural and sliding shear failure [13] (Figure 7).

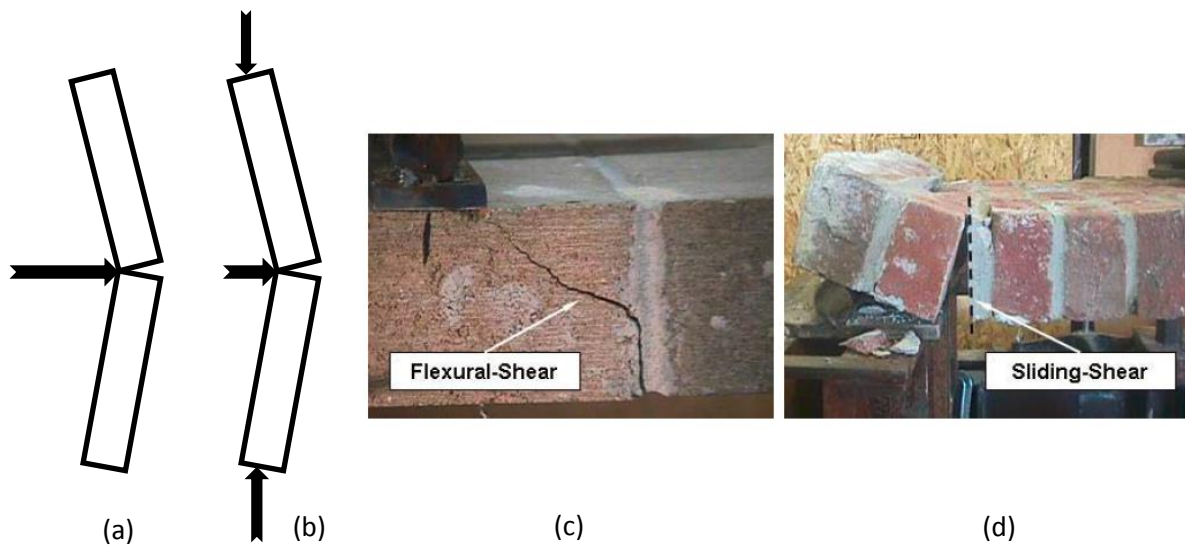


Figure 7: Out-of-plane failure modes: (a) bending, (b) buckling, (c) flexural-shear, (d) sliding-shear [13]

The type of failure mode for IP and OP which will occur in a wall depends on how the wall is supported along the edges, the aspect ratio and vertical load applied to the wall [9]. With OP bending the wall support especially determines how the wall will bend and what type of cracks are likely to form (Figure 8) [14]. Also windows and door frames can function as supports and will affect the failure mode of the masonry wall.

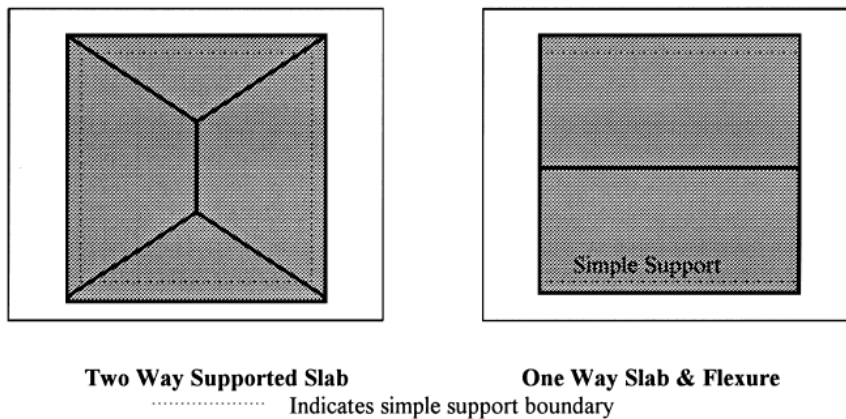


Figure 8: Effect of different types of support for OP bending of a masonry wall [14]

The aspect ratio is defined as the height of the wall divided by the length of the wall (Figure 9).

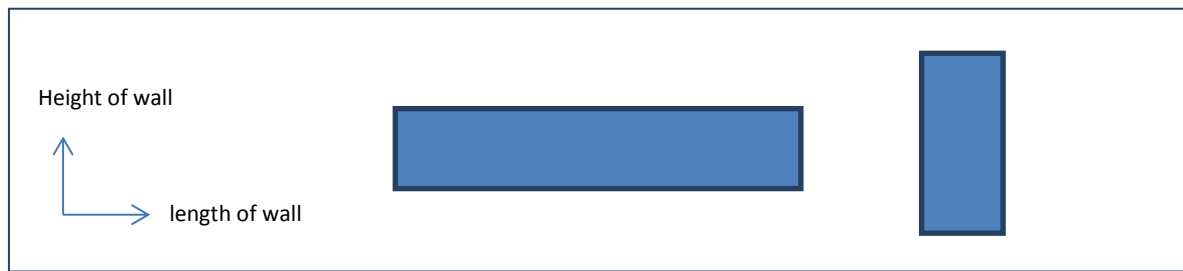


Figure 9: Examples of aspect ratio. Left: low aspect ratio (<1), Right: high aspect ratio (>1)

The possible combinations and the resulting failure modes are shown in Table 1. For example a low aspect ratio (<1) and a high vertical load will result in diagonal cracks. Increasing vertical load will increase shear and bending capacity until the compressive strength of the mortar and bricks will be reached [15]. For shear the increase in capacity with increased vertical load is due to increased friction. Friction depends on the friction coefficient of the material multiplied with the normal force (in this case the vertical load). For the bending capacity the vertical load compresses the masonry. This will prevent the bricks from rotating individually. The slightly rotating of the bricks is possible due to the spacing between the bricks because of the mortar layer. When the OP displacement gets too large and a high vertical load is applied, the wall is likely to fail due to buckling.

Table 1: Effect of vertical load and aspect ratio on the failure mode in IP and OP loading [9]

IP loaded	Lower vertical load	Higher vertical load
<b>Lower aspect ratio (&lt;1)</b>	Sliding failure mode	Diagonal tension failure mode
<b>Higher aspect ratio (&gt;1)</b>	Rocking failure mode	Toe crushing failure mode

OP loaded	Lower vertical load	Higher vertical load
<b>Lower aspect ratio (&lt;1)</b>	Bending/tilting failure mode	Buckling/compression failure mode
<b>Higher aspect ratio (&gt;1)</b>	Bending/sliding/tilting failure mode	Flexural shear/ Buckling/compression failure mode

Out-of-plane failure is in most cases critical to prevent the building from collapsing [16] [17] [18]. With the IP failure modes the masonry could be severely damaged, usually visible by large cracks or crushed masonry, but could still have a certain amount of load carrying capacity which prevents the building to collapse. With OP failure there is a significant chance the wall will bend or buckle and therefore immediately loses all its load carrying capacity which could result in building collapse if the considered wall is a load bearing wall.

Nowadays constructions are still build with masonry but need to comply with European design standards for earthquake resistance design which are documented in Eurocodes [19]. In these codes seismic loading is taken into account and design criteria like: wall aspect-ratio, type of bricks/mortar, wall thickness and connection between wall and other construction elements.

## 2.3 Masonry reinforcing methods and materials

### 2.3.1 Commonly used masonry reinforcing methods and materials

First papers about seismic loaded masonry were published around 1960-1970. With the gained knowledge of these researches many scientist and engineers started to develop and experiment on reinforcing methods for unreinforced masonry (URM). The key to make URM earthquake resistant is by increasing the capability of the URM to absorb and dissipate seismic energy which will be explained more elaborate in paragraph 2.3.2. Increasing energy absorption and dissipation can be achieved by increasing ductility, strength and stiffness of masonry because the area under the force-displacement curve is the energy that the wall can absorb. Figure 10 shows an example of a force-displacement curve that is observed if URM is compared to reinforced masonry in general. Due to the increase in stiffness, ductility and strength it is visible the area under the curve of reinforced masonry is significantly increased compared to URM.

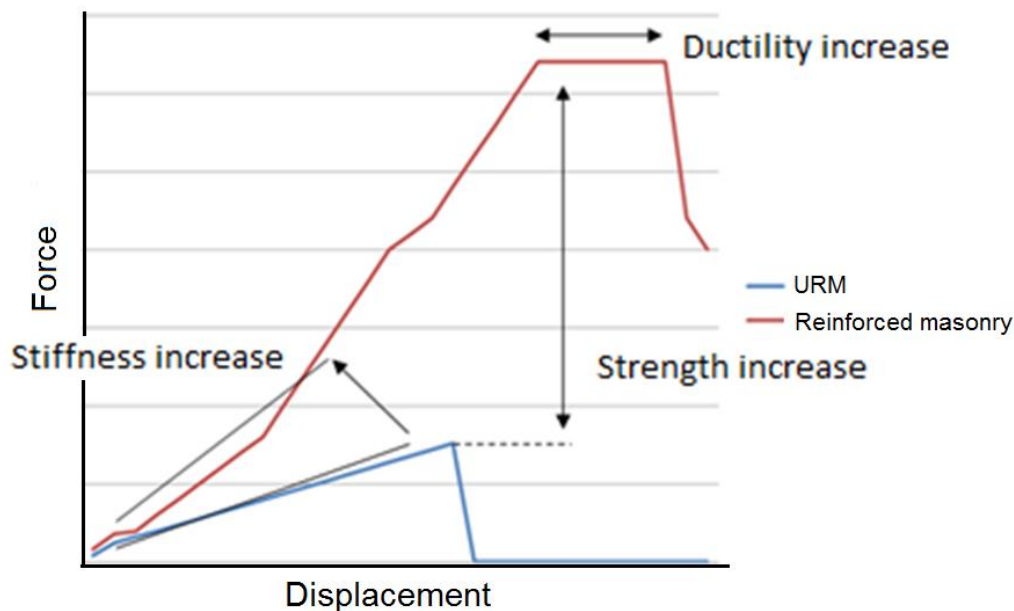


Figure 10: Force-displacement curve that is usually observed if URM and reinforced masonry is compared (only for illustrative purpose, not based on real data)

The natural frequency of the wall determines its response to a seismic vibration [20]. The natural frequency of the wall is determined by its mass and stiffness. It is favourable to have a natural frequency of the structure that is not the same or close to the frequency of the earthquake. This will result in resonance and triggers a heavy response of the construction to the earthquake causing usually more damage (Figure 11).

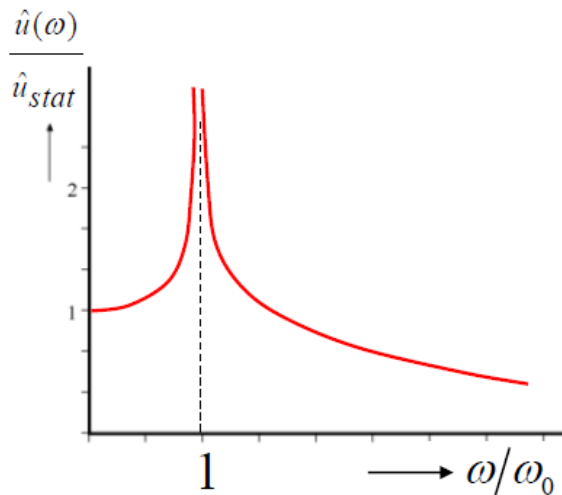


Figure 11: Resonance response spectrum for undamped situation with  $\omega$ =frequency,  $\omega_0$ =natural frequency, vertical axis is displacement divided by static displacement [20]

It is not desired to increase the mass of the construction to change the natural frequency because this will increase also the horizontal force which needs to be dealt with by the construction. This effect can be derived from Newton's second law ( $F=m \cdot a$ ). At a certain acceleration induced by the earthquake and with an increased mass also the force acting on the construction increases. So when applying reinforcing materials to an URM wall the added mass should be minimized.

Composite materials like FRP such as glass (GFRP), carbon (CFRP) and aramid (AFRP) can be used as masonry reinforcing materials. These materials provide relatively high strength and high stiffness with low mass i.e. these types of materials have a high specific strength and high specific stiffness.

### ***Biomaterials as reinforcement material***

Besides the common glass, carbon and aramid fibres for FRP also biomaterials can be used as fibre material. Some examples of these fibre biomaterials are: flax, jute and hemp [21]. If one of these natural fibres is combined with a matrix like a polymer, it is called a green composite. Usually the mechanical properties are lower compared to the FRP that contains the traditional synthetic fibres. The problem with using these synthetic fibres like carbon and glass is that they cannot be reused or recycled properly. The current increase in using FRP materials for all kinds of products has a large impact on the environment when these FRP products are disposed. The natural fibres have less impact on the environment or could be reused in other products. Current development on green composites is trying to find a biodegradable matrix material which can substitute the polymer matrix without lowering the mechanical properties of the FRP.

Although FRP is a good reinforcing material for masonry because of its low mass and good mechanical properties, it should be considered to use other materials like green composites in the near future. Green composites have usually good thermal and acoustic insulation properties which is an advantage when using these kind of materials in a building.

### 2.3.2 Energy absorption & dissipation of URM and reinforced masonry

At paragraph 2.3.1 it is stated that to make masonry more earthquake resistant the energy absorption and dissipation of the masonry needs to be increased. This can be achieved by changing the ductility, strength and stiffness of the masonry. Some conventional techniques to reinforce masonry to increase these parameters are: surface treatments with ferrocement, shotcrete, reinforced plaster, injection with epoxy and grout, confining masonry with reinforced concrete, mesh, frame or place steel bars and strips in the masonry [9]. An advantage of using steel reinforcement is the ability of steel to plastically deform. Plastic deformation of a material requires energy. This energy is introduced by the earthquake and is dissipated by the plastic deformation of steel. A disadvantage is the large increase in mass if steel or other metals are applied to a construction. Adding mass results in larger forces acting on the construction during an earthquake. FRP does not plastically deform and therefore cannot dissipate energy but has a low mass and provides stiffness and strength to the system as a whole. In combination with the brittle masonry this results in ductile behaviour of the total masonry wall. Other materials like mortar, bricks and adhesive need to provide energy dissipation and can do so by crack forming, crushing, plastic deformation and sliding (friction).

In the case of masonry, the material fractures usually in mode 1 or mode 2. Mode 1 is due to tensile failure of the material and mode 2 due to shear failure of the material (Figure 12)

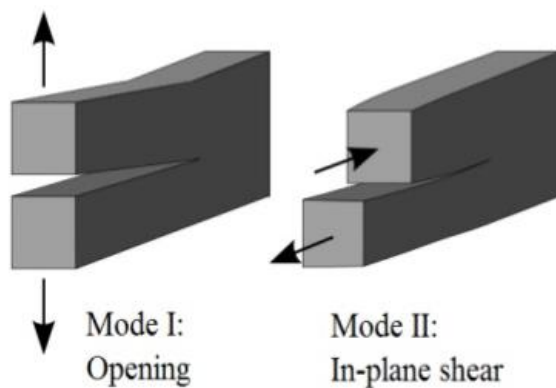


Figure 12: Fracture modes [22]

During crack forming in a material the surface of that material is increased. Creating surfaces in a material requires energy. This energy is stored in the material as surface energy and therefore dissipates the earthquake energy. Crushing also dissipates energy because micro cracks are formed due to boundary sliding of grains in the material. Movement of the grains relative to each other also will take up energy. This is the same principle as in sliding of two surfaces where friction will result in energy dissipation.

During testing of URM or reinforced masonry the dissipated energy can be calculated with use of the force-displacement curve [23]. The Area under the force-displacement curve is the energy that is introduced into the wall. When the OP or IP load is removed the curve will show a certain permanent displacement of the wall. The area that is now enclosed by the axis and the curve is the dissipated energy due to the deformation, cracking and sliding of the wall. For IP loaded walls usually a static-cyclic loading pattern is used. The force-displacement curve will become a hysteresis loop due to the

tension and compression cycle on the masonry. Figure 13 shows an example of a hysteresis curve (one cycle) with the marked areas under the curve indicating the input energy ( $E_{inp}$ ) and the dissipated energy ( $E_{diss}$ ). The energy dissipation can also be expressed as the hysteretic damping ( $\zeta_{hyst}$ ) and is a measure of how well a masonry wall can dissipate energy. Hysteretic damping ( $\zeta_{hyst}$ ) is the dissipated energy ( $\Delta E_{diss}$ ) divide by the induced potential energy ( $\Pi$ ) times  $2\pi$  (Equation 1) [23].

$$\zeta_{hyst} = \frac{\Delta E_{diss}}{2 \cdot \pi \cdot \Pi} \quad (1)$$

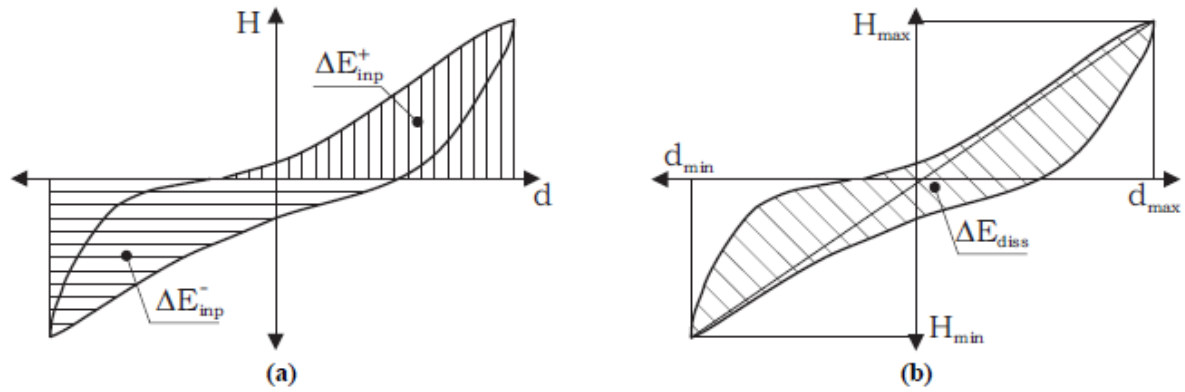


Figure 13: (a) Input energy by the cyclic loading (b) Dissipated energy in the masonry wall [23]

By adding FRP to the masonry the total wall behaviour changes. Using adhesives to bond the FRP also provides some elastic behaviour. If an external reinforcing layer like a mesh is applied than the mesh will create cohesion between the brick units and keeps the masonry wall together to some extent. During bending tests on the Quake-Shield samples, which will be discussed in more detail in Chapter 3, this effect was noticed. Spring back of the masonry wall was visible when the load was removed from the sample (Figure 14).

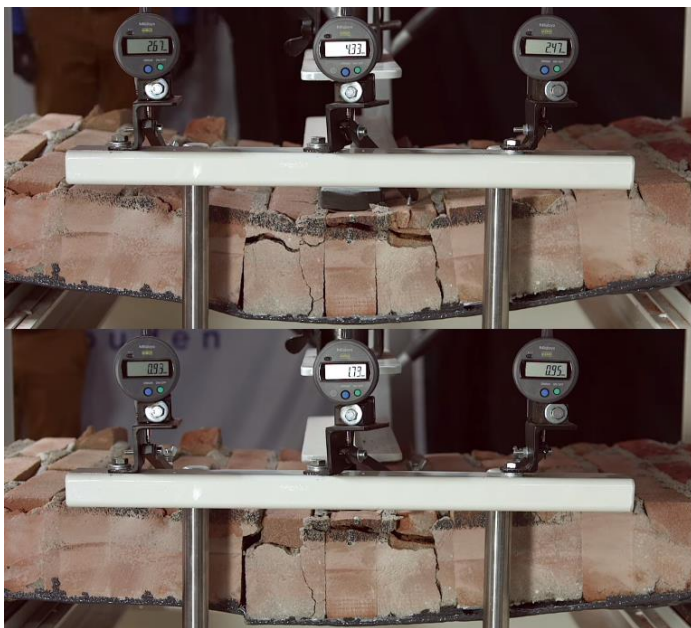


Figure 14: Spring back effect after load is removed from sample (centre displacement: top 4,33mm bottom 1,73mm) (test performed at SealteQ Group Stadskanaal)

Spring back is the release of stored elastic energy in the sample. The energy is transferred to other parts of the construction. This should be kept in mind when masonry walls in a building are reinforced that it is possible that other components in the building could become critical due to the extra elastic energy that is transferred from the reinforced masonry to that certain components.

### 2.3.3 FRP masonry reinforcing methods

FRP masonry reinforcing materials are applied in different ways. Most commonly found method in literature is the external bond (EB) FRP because it is easy to apply to constructions. EB FRP is also a method used for reinforced concrete retrofitting.

A sheet, mesh or strip of FRP is fixed with an adhesive to one or two of the masonry faces. Research has shown that the combination of the FRP, adhesive and masonry results in a transition of brittle failure of masonry to a more ductile failure behaviour. This is for example visible in the force-displacement curve in Figure 10 (paragraph 2.3.1). The sharp decline in the URM curve could indicate brittle failure. The plateau forming in the reinforced masonry curve shows ductile behaviour.

Cracks are easily formed in mortar when masonry is OP loaded and due to bending a part of the mortar will have stresses in tension. Bricks become separated from each other because of cracks in mortar and cohesion of the masonry wall is lost. The EB FRP connects the brick units and takes over tensile loads so the cohesion and tensile strength of a reinforced masonry wall is higher compared to URM.

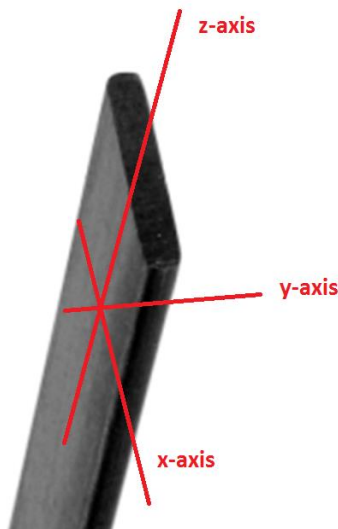


Figure 15: Axis orientation of carbon strip [25] (figure is modified by the author of this thesis)

Another method to apply FRP to masonry is by embedding FRP strips or bars into the masonry [24]. This is usually done by making a groove in the masonry wall varying from 10mm to 40mm depth. The groove is then filled with an adhesive and a FRP strip or bar is placed into this adhesive. This method is called near surface mount (NSM). If OP bending of the masonry wall is taken into consideration the NSM FRP strips provide much more bending stiffness about the y-axis compared to the x-axis indicated in Figure 15. Bending about the x-axis happens when the wall is subjected to an IP load. Although the NSM strips are more effective in OP bending than in IP shearing it still contributes to an increase in the shear capacity (Figure 16) [24]. This is because the strips provide some dowel action so shear sliding along the bed joint is partly prevented. If shear sliding occurs the strips will be tension loaded and as a result the bed joint will be loaded in compression. This compression force increases friction and therefore also the shear capacity of the wall. This effect has a much larger contribution in the increase in shear capacity compared to the dowel action.

During diagonal cracking the strips will be loaded in tension and take up a part of the IP load [24]. The strips also reduce crack growth because the strips keep both free edges of a formed crack



together to a certain extent. The ductility of the adhesive where the NSM strips are embedded in will provide some strain and therefore cracks will form but are less coarse compared to cracks in URM.

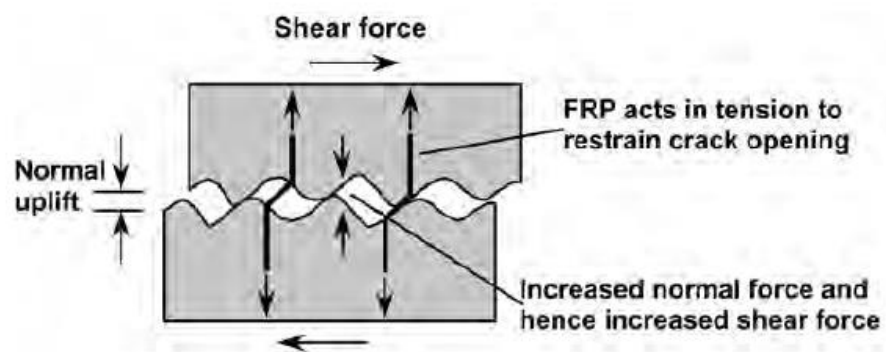


Figure 16: Effect of NSM strips on shear sliding of masonry [24]

### 2.3.4 Depth of embedding NSM FRP strip

Due to the orientation of the strips, the NSM FRP strip reinforcing method is more effective for OP than IP loading. The depth at which the NSM FRP strips are placed is limited and has an effect on the mechanical properties of the reinforced masonry. In this paragraph the limitations and effects are described based on research done by D. Dizhur et al. [26]. Results of this research show that the groove depth is limited to 25%-30% of the brick width. At 30% the test prism split in half because the groove was too deep into the brick to keep sufficient brick strength. Taking a nominal brick width of about 100mm, this gives a maximum strip width of 25-30 mm. Different groove depths and relating strip widths were tested. Table 2 shows the effect of strip width to the increase in pull-out force.

**Table 2: Effect of using different width for the NSM CFRP strips [26]**

Strip width (from -> to) [mm]	Strip width increase [%]	Increase of ultimate pull-out force [%]
10 -> 15	50	60
15 -> 20	33	13
20 -> 25	25	4
25 -> 30	20	-10

Also the width of the groove has influence on the pull-out behaviour of the strip. However the ultimate axial pull-out force does not change if the groove width is changed.

The groove width tested are 2,5 / 5 / 7,5 and 10 times the thickness of the strips. The strip thickness is the same in each test. A wider groove results in more slippage of the bonding material, in this case an epoxy. Slippage of the bonding material is ductile behaviour which is favourable compared to brittle fracture. Based on the research results a NSM CRFP strip with a width of 20% to 25% of the wall thickness gives an optimum ultimate axial pull-out strength. By designing a certain groove width based on the thickness of the NSM CFRP strip the ductile pull-out behaviour can be controlled in certain extent. In this research only a pull-out test is done (shown in Figure 17). It could be interesting to also investigate the bonding strength of the strip to the masonry when the wall is loaded in OP i.e. a pull-out test while the masonry prism is bend OP.

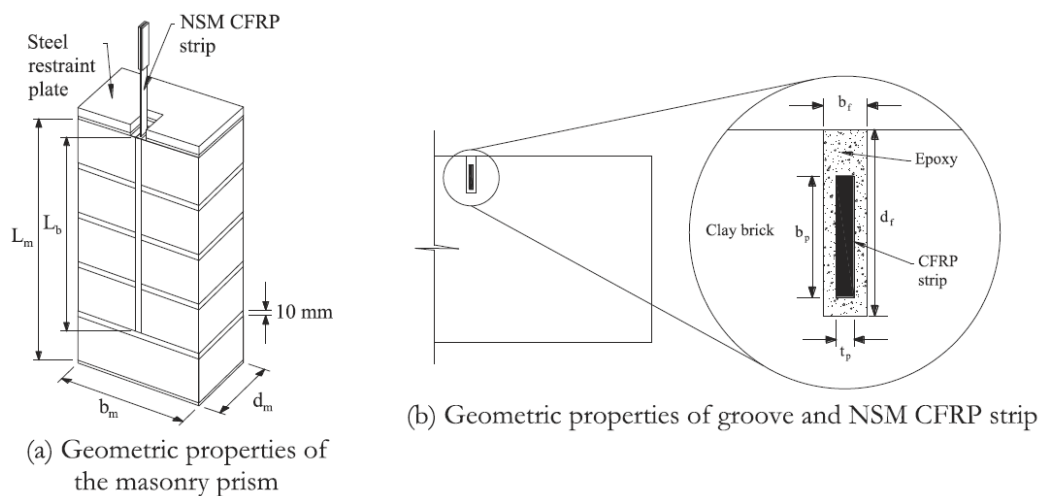


**Figure 17: (a): Test masonry prism to determine the ultimate pull-out strength of NSM CFRP strip in masonry. (b): Location and geometry of NSM CFRP strip in a brick of the masonry prism. [26]**

### 2.3.5 NSM FRP strip orientation and spacing

NSM strips are used only in vertical direction because in this orientation the NSM strips can increase the OP bending capacity and also partly the IP shear capacity [24]. If the NSM strips are placed horizontally they will reduce wall diagonal shear failure but do not contribute to an increase in shear sliding and OP bending. In the PHD research of Petersen [24] multiple URM and masonry walls with NSM strips in vertical and horizontal direction are tested with a diagonal tension test. The research has proven that vertical NSM strips have a higher load carrying capacity increase compared to horizontal NSM strips. The load increase difference is about 30% (average of multiple samples). The load increase is the difference in load at first crack and ultimate load. Also the maximum IP displacement is higher for the vertical NSM strips which is about 22 mm compared to 6,5 mm. So if NSM FRP strips are used as reinforcement measurement it is recommended to place the strips in vertical direction.

The spacing between the NSM strips is also of importance to the load bearing capacity and the total behaviour of the reinforced masonry wall. Research was done by Michael C. Griffith, Jaya Kashyap and M.S. Mohamed Ali on the effect of the number of NSM FRP strips, strip spacing and the amount of reinforcing material on the behaviour of a masonry wall OP loaded [16]. The samples have a constant amount of reinforcing material for the different number of strips and strip spacing tests. The wall samples are 1070mmx2312mm. Figure 18 shows a clear difference in strength increase (114%) and displacement increase (60%) when three strips are used instead of one.

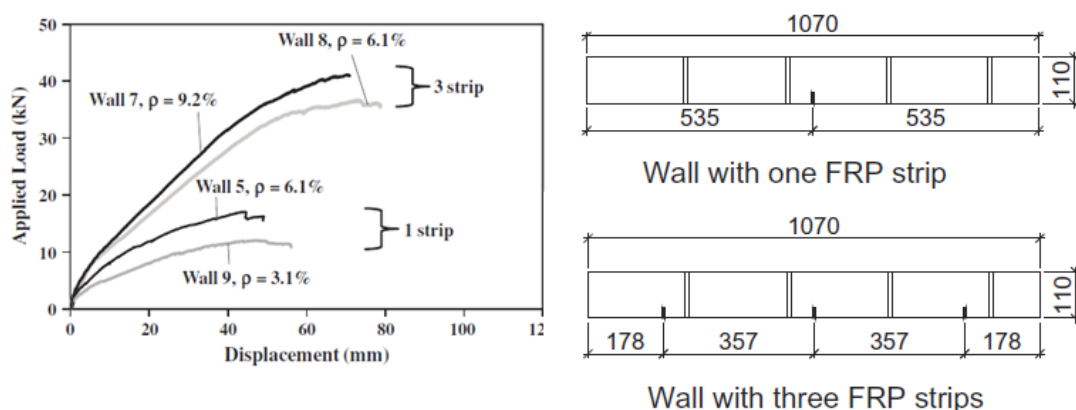


Figure 18: Influence of number of strips and reinforcement ratio (results from a masonry wall OP test) [16]

In Figure 18 also the influence of reinforcement ratio ( $\rho$ ) is indicated, i.e. the amount of reinforcing material applied. The reinforcement ratio is defined as the surface area of the masonry wall sample divided by the surface area of the total combined NSM FRP strips applied expressed in percentages. Also here increase in strength is visible. Due to the increase in the amount of stiffer FRP material the ductility of the total masonry wall is reduced which can be seen by the reduced maximum displacement in the graph in Figure 18 (wall 5 & 7). More strips per unit wall area gives a smaller effective width which results in a smaller compressive zone and more load taken up by the FRP strips. From this research it is concluded that the bonded surface area of the FRP strip has greater influence on the wall behaviour compared to the reinforcement ratio. The same accounts if strip spacing is compared to reinforcement ratio. Thus applying NSM FRP strips of certain dimensions and at optimal locations is more relevant than the amount of FRP that is applied to the wall for the total behaviour of the masonry wall.

### 2.3.6 Optimal bonding of FRP to masonry

Properly bonding the FRP reinforcing material to the masonry is critical for: maximum increase in load capacity, prevent undesired failure modes and total behaviour of the masonry wall. Proper surface treatment and using materials designed for bonding to masonry and FRP materials is important. Surface treatment include sanding, dusting, activating surface energy and if necessary applying a primer [27]. Sanding is done to increase surface area and remove unwanted materials on the substrate surface that will lower surface energy. Surface energy can increase even more by dusting and extra cleaning of the substrate. Masonry like materials absorb moisture but also solvents from adhesives when they are still uncured. A primer can be applied to the substrate to prevent this effect and create a better adhesion between adhesive and substrate. The primer will be absorbed partly by the masonry but this also increase adhesion due to mechanical interlocking (Figure 19). The FRP is surface treated in similar way as the masonry substrate (grinding, cleaning, etc.).

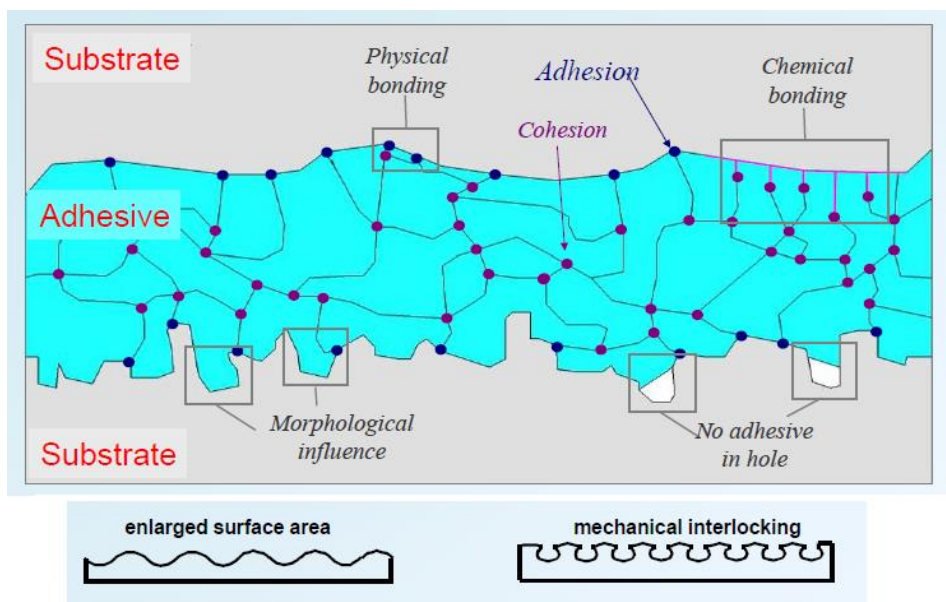


Figure 19: Adhesive layer between two substrates. Bonding mechanisms of the adhesive layer [27]

Research was done on bonding NSM FRP strips to masonry compared to EB FRP strips [28]. From experimental pull test it is concluded that NSM FRP strips have better bonding properties due to their larger surface area and confinement. The mean peak shear stress is more than double for NSM FRP strips compared to EB FRP strips. Surface preparation is a little less critical due to the adhesive and strip confinement in the groove. The NSM FRP strip is also shielded by the adhesive for environmental influences like UV and moisture. From this it can be concluded that when using FRP strips it is more efficient to use the NSM technique instead of the EB.

If bonding is optimal and therefore assuming not to be the weakest link anymore the FRP can be used more efficient. Although the bonding is important, the mechanical properties of the adhesive and other bonding materials should also be considered. Ductility of the adhesive influences the failure mechanism of FRP debonding. With a more ductile adhesive, slip between the FRP and masonry is possible. This failure mode will dissipate some energy and makes the failure behaviour of the masonry more controlled compared to sudden debonding of the adhesive [29].

Energy dissipation will primarily be accommodated by the masonry if FRP reinforcing measures are used. By selecting reinforcing materials, FRP and adhesive, with certain mechanical properties a desired, more ductile, overall failure mode can be designed for. But the long term effect of material degradation over time should also be taken into account for selecting the proper reinforcement materials.

## 2.4 Testing unreinforced and reinforced masonry walls

### 2.4.1 Commonly used masonry test methods

#### *Out-of-plane testing of masonry*

In literature two main types of masonry testing are used to determine load bearing capacity of masonry. These two types of tests are loading masonry in OP and IP. An example of a norm for a four point bend test for small scale masonry samples is NEN-EN 1052-2 [30]. Also OP loading of masonry using a three point bend test can be used to determine the bending capacity of the masonry. The difference between a three point and a four point bend test is with a four point bend test pure bending is achieved with stress distributed over a larger area. In a three point bend test the stresses are concentrated around the middle section of the sample.

The test samples are usually relatively small when using a three of four point bend test, ranging from a masonry prism (single stack of multiple bricks) (Figure 20) to a small size wall of 1,3x1,3m [18] [14]. In the commonly used three of four point bend test setup the sample is placed horizontally. This is not the orientation in which a masonry wall is applied in a construction. In horizontal position the URM wall test samples are already close to their maximum bending capacity due to their own weight. With reinforced masonry the bending capacity is significantly increased so the walls can be tested horizontally but it should be kept in mind that the own weight of the masonry plays a different role when the masonry is orientated horizontally instead of vertically. In vertical position the own weight of masonry will compressive the masonry which is beneficial when testing bending capacity of masonry.

On large scale masonry walls the OP bending tests is usually done in vertical position and the OP load is applied with an airbag to create a uniform distributed load (Figure 21) [18]. Also a vertical load is applied to simulate the weight of a roof or second floor [18]. The airbag is placed on one side of the wall and air pressure is increased until the wall fails in OP direction. Also a semi-cyclic pressure could be applied by inflating and deflating the airbag to simulate cyclic loading. This method could also be used if on both sides of the wall airbags are placed so the wall can be OP loaded in both directions. The cyclic method showed larger maximum displacement of the wall compared to monotonic loading although the flexural strength of the wall was the same in both cases [18]. The large lateral displacement could be caused by the fact that cracks are opened and closed in the cyclic method which influences crack growth compared to continuously opening of the cracks when monotonically OP loading is applied.

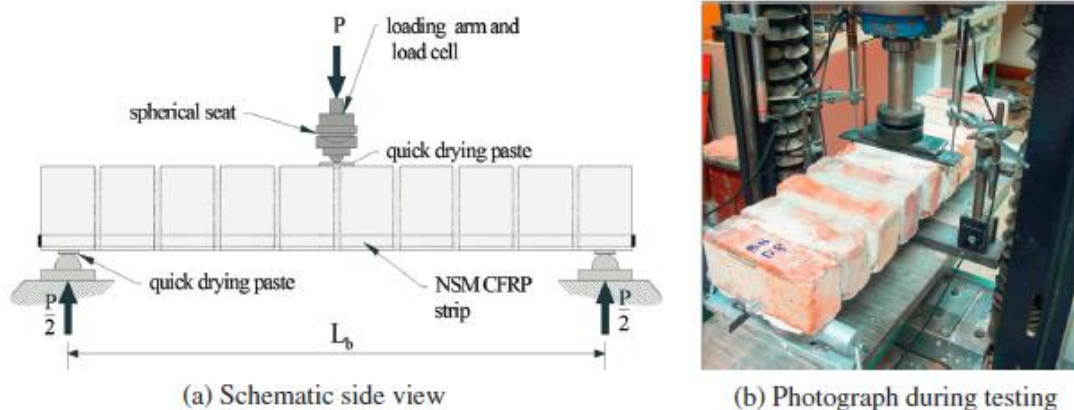
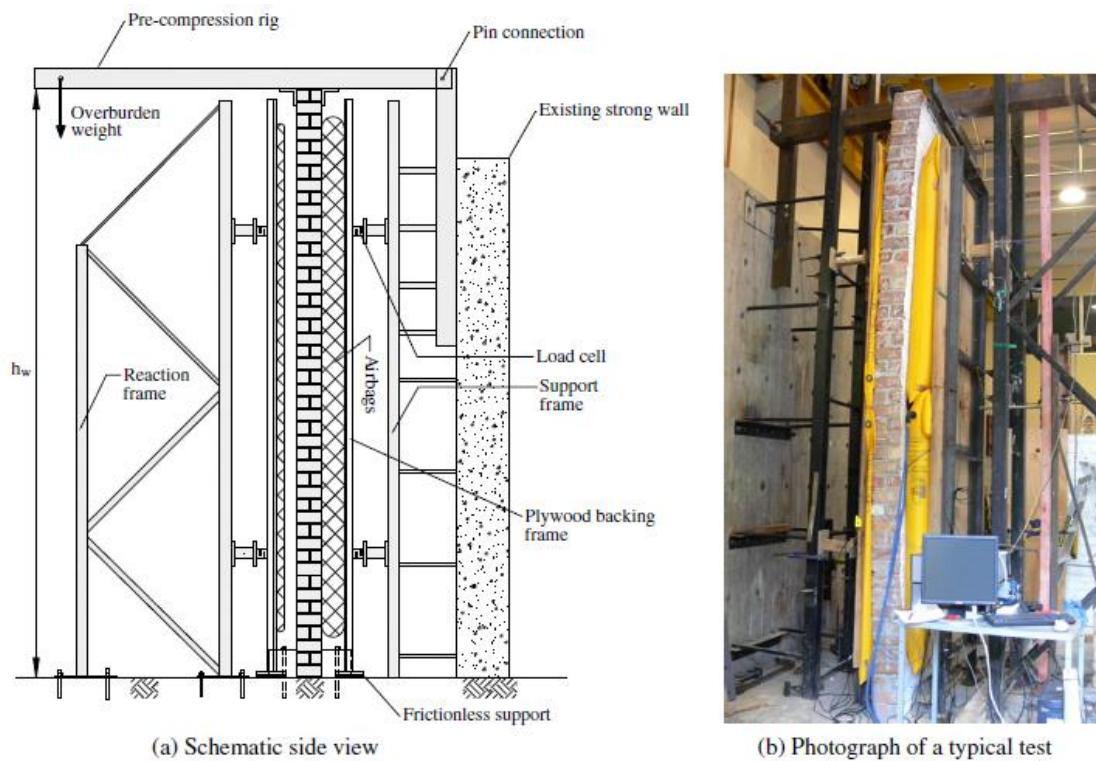


Figure 20: three point bending test on masonry prism [18]



**Figure 21: Testing of large scale wall sample with OP loading induced by airbags [18]**

The measurements are usually done using load cells and Linear Variable Displacement Transducers (LVDTs). If FRP strips are applied to reinforce the masonry also strain gauge can be used to measure the strain in the FRP strips. FRP strips have a maximum strain at tensile failure. With the strain gauges it can be measured if the FRP strips are close their maximum strain during the tests [18].

### **Material testing**

Material properties are one of the important input parameters in a FEM model. If these parameters are not correct it is unlikely to get results that are close to the test results. Material properties for masonry materials like compressive strength, tensile strength, shear strength and E-modulus can be found with some basic material tests which are described in test standards, for example: NEN-EN 1052-1 for compressive strength and NEN-EN 1052-3 for shear strength.

FRP has a linear elastic behaviour until failure occurs at ultimate strain. This information is usually available on the datasheets provided by the manufacturer. Many different adhesive types can be used to bond the FRP to the masonry. Basic material properties like density, ultimate tensile strength and maximum elongation are given on the datasheet but not information about bond-slip behaviour. This is important information when making a model of NSM FRP reinforced masonry and is explained in more detail in the next paragraph.

### **Pull-out test and behaviour of FRP bonded to masonry**

One of the critical properties of NSM FRP strip embedded in adhesive is the bond-slip behaviour. This behaviour shows the interaction of the interfaces between NSM FRP strip, adhesive and masonry. The bond-slip behaviour can be implemented in interfaces in the FEM models. The bond-slip behaviour along with material properties like bond strength and critical bond length can be found



with a pull-out test [31]. In the pull-out test a NSM FRP strip is embedded in a prism of bricks and is pulled out by a tensile load in the direction of the strip, as shown in Figure 22.

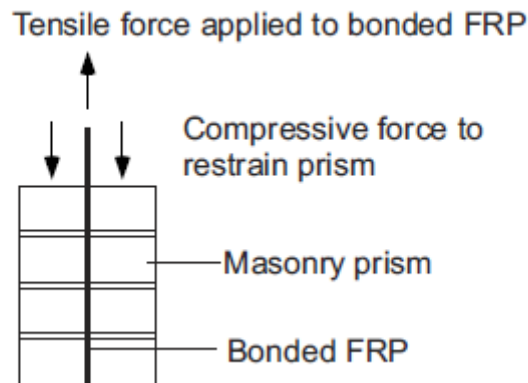


Figure 22: Typical pull-out test [31]

In the research of Robert B. Petersen, Mark J. Masia and Rudolf Seracino 18 masonry prisms with NSM FRP strips were tested [31]. One of the results from the tests is shown in Figure 23. At multiple locations along the length of the NSM FRP strip strain gauges were located to measure the strain at these locations at a certain load. Relating the strains to shear stress and combining these values with the measured displacement during the pull-out test gives the bond-slip curve. The curves from different locations along the strip can be transformed into a bi-linear curve which can be used for the FEM model to describe the bond-slip behaviour.

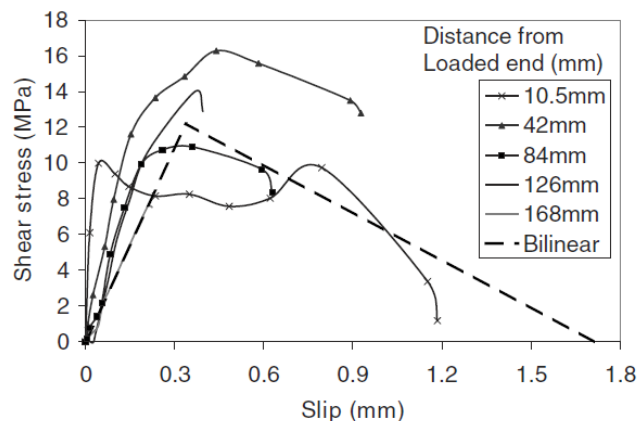


Figure 23: Bond-slip behaviour of NSM FRP strip in masonry prism test [31]

Some prisms from the test had a through thickness crack in line with the direction of the NSM FRP strip [31]. The research recommends to minimize the groove depth to prevent this type of crack from occurring. A through thickness crack can create a plane of weakness in the wall and could possibly create problems in the total behaviour of the wall. It is also recommended not to place the NSM FRP strips in the head joints. Mortar has usually lower mechanical properties and could therefore potentially reduce the bond strength of the total NSM FRP strip in the masonry wall [28].



### 2.4.2 Displacement limitation of reinforced masonry

The main reason for reinforcing masonry is to prevent wall collapse. OP bending of the wall is the main failure mode which causes wall collapse. Research found in literature shows that masonry one-sided reinforced with NSM FRP strips can cope with 4% drift before wall collapse [18] (Figure 25). Drift is defined as two times mid-plane displacement divided by the wall height (Figure 24).

For a 2,7 m tall wall this gives a displacement of 54mm (4% drift).

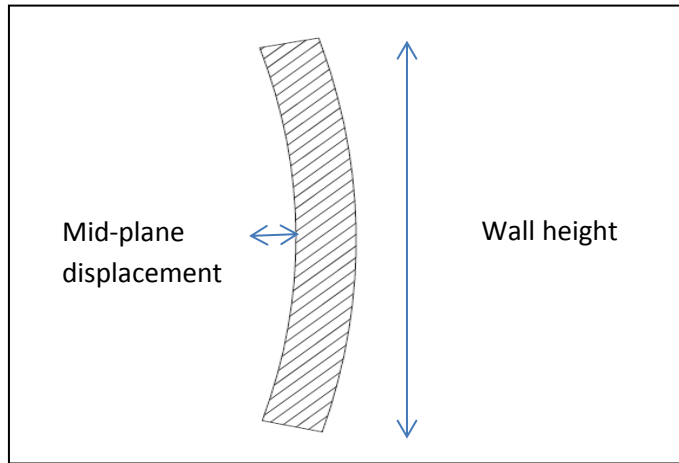


Figure 24: Illustration of OP bending of a wall

Translating this to the three point bending tests performed on Quake-Shield (discussed in Chapter 3), theoretically 14 mm could be achieved based on this 4% drift. Comparing the research of D. Dizhur et al. [18] to the three point bending test performed by Quake-Shield, the following should be considered, in the research: double leaf walls, airbag reversed cyclic loading is applied and the walls were vertical tested. When also a vertical load is applied drift increase to about 8% and the maximum lateral force also increases (Figure 26).

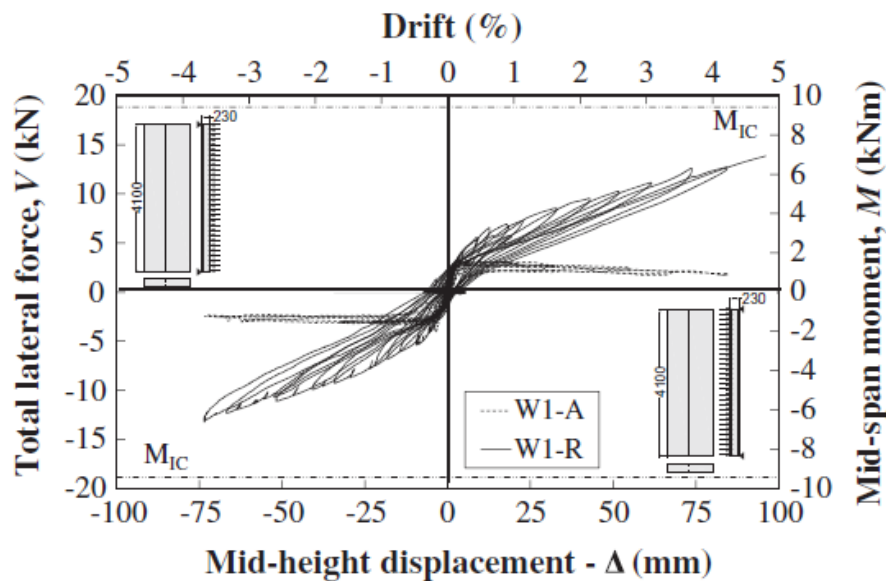


Figure 25: Test wall reversed cyclic load with airbags without vertical load, shows drift up to 4%-5% is possible before collapse (W1-A = wall 1 as-built URM, W1-R = wall 1 reinforced masonry) [18]

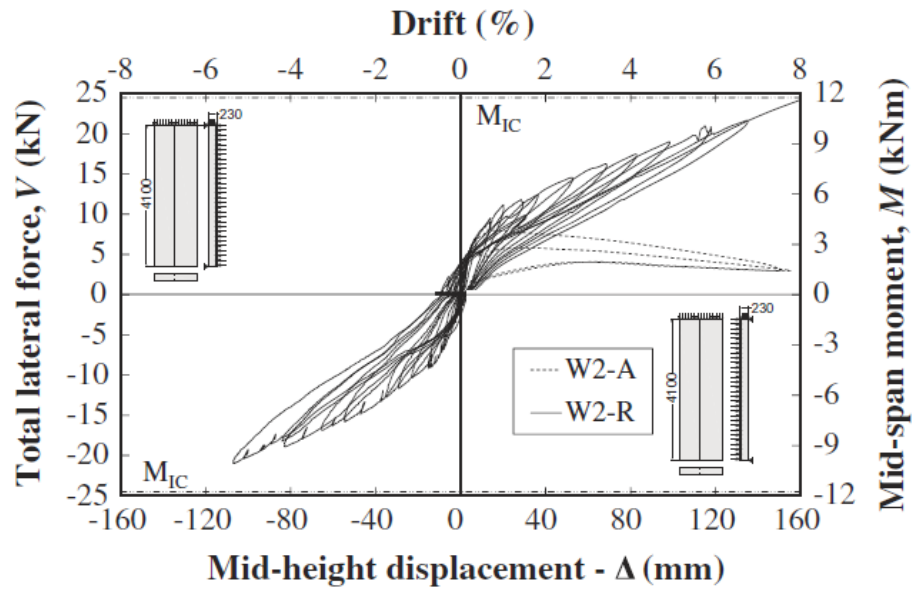


Figure 26: Test wall reversed cyclic load with airbags and with a vertical load of 100kPa, shows drift up to 6%-8% is possible before collapse (W2-A = wall 2 as-built URM, W2-R = wall 2 reinforced masonry) [18]

## 2.5 Masonry FEM models

### 2.5.1 Construction analysis methods for earthquakes

Building construction materials and particular masonry behave non-linear during loading conditions like an earthquake. In the past and also still nowadays analytical methods are used to determine how a building reacts when an earthquake load is introduced onto the construction. The construction is simplified in a spring-damper system to be able to calculate the response of the building to the earthquake vibrations.

There are four methods described in Eurocode 8 [32]. Lateral Force Analysis (Figure 27) which uses a lateral force, determined by the ground acceleration, dead weight and natural frequency of the construction, to calculate if the construction can withstand the introduced earthquake load.

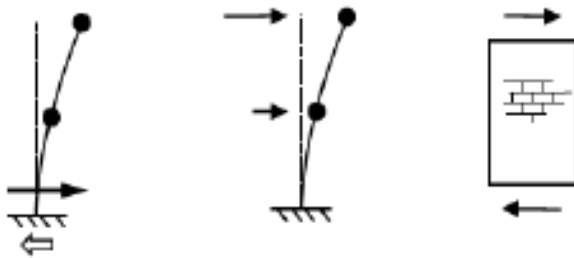


Figure 27: Lateral Force Analysis [32]

Second method is Modal Response Spectrum Analysis which is the same principle as the Lateral Force Analysis but also takes the dynamic response of the construction into account. This means the input is not a lateral force but a vibration and therefore the construction has a dynamic response.

The third method is the Non-linear static (pushover) analysis (Figure 28) which also takes into account the non-linear behaviour of the construction.

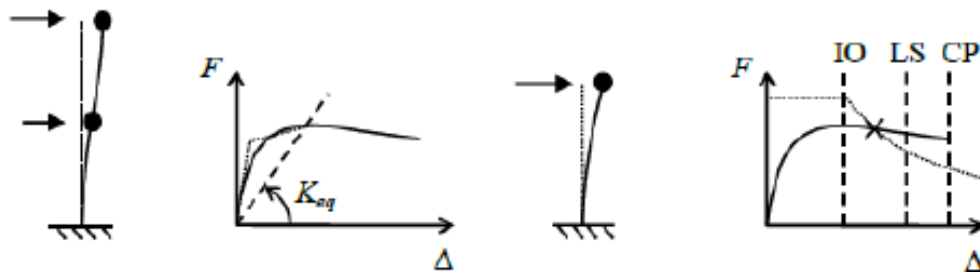


Figure 28: Non-linear static (pushover) analysis [32]

A fourth method is construction analysis by using FEM software and is called Non-linear time-history analysis (Figure 29). This method is most detailed and simulates construction response to earthquakes more realistically compared to the other methods. Although the other methods are more simplified they are also more conservative. If with FEM modelling a mistake is made the model could lead to an unsafe situation due to the less conservative method and smaller margin of error. Other disadvantages of this method are that it is time consuming and costly. First a model to a certain level of detail has to be made where decisions have to be taken how to build up the FEM model, like which type of: elements, damage models and material models will be used. The choices in the FEM model development determine also the calculation time that is needed to analyse the model. This processing time is also depending on the computer processing power. Computer processing power has increased exponentially in the last decade and will continue to improve which

makes FEM models more suitable for this kind of earthquake analysis. The previous mentioned analytical methods become too much work or too much simplified if the construction that needs to be analysed is getting too large or has too complex geometries.

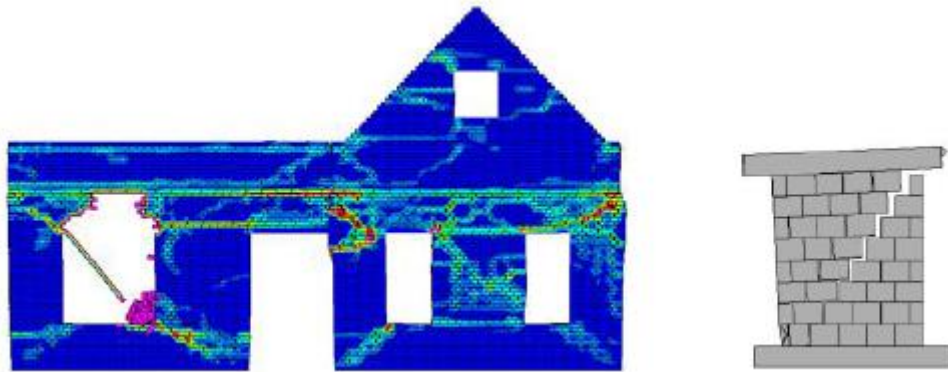
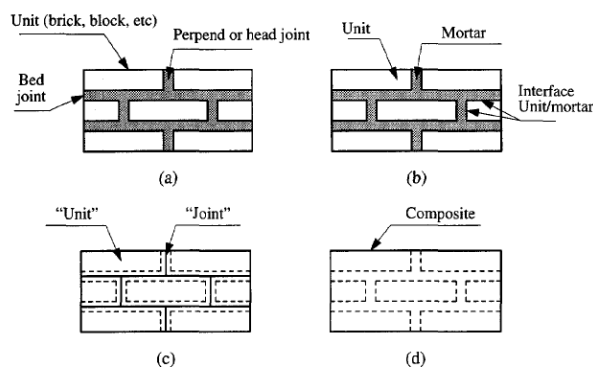


Figure 29: Non-linear time-history analysis [32]

Different approaches to FEM model masonry are researched in the past [33]. For large constructions the macro model is favoured. In this approach the masonry is considered as homogeneous anisotropic continuum, i.e. a composite material. The brick unit and mortar are modelled as one unit of material. For large constructions it is more interesting how the construction as a whole response to earthquakes and not the individual brick-mortar connections. For this model it is assumed that the stresses are relatively uniform over a large area of masonry. This method of masonry modelling saves a lot of calculation time for large constructions.

If the behaviour of masonry and the brick-mortar interaction is more interesting to investigate in a small part of a building, than the micro model is more appropriate. In the micro model the brick unit and mortar are modelled as continuum elements and the brick-mortar interface as discontinuous elements. The interfaces can provide shear and crack behaviour of the masonry. The brick units and the mortar can simulate the inelastic properties of masonry. Also a simplified micro-model can be used to reduce the level of detail of the model and thus the calculation time. In this model the brick units and mortar are combined to provide inelastic behaviour of these materials and the interfaces still simulate the shear and crack behaviour of the unit connections. Figure 30 shows an overview of the different masonry models that are described.



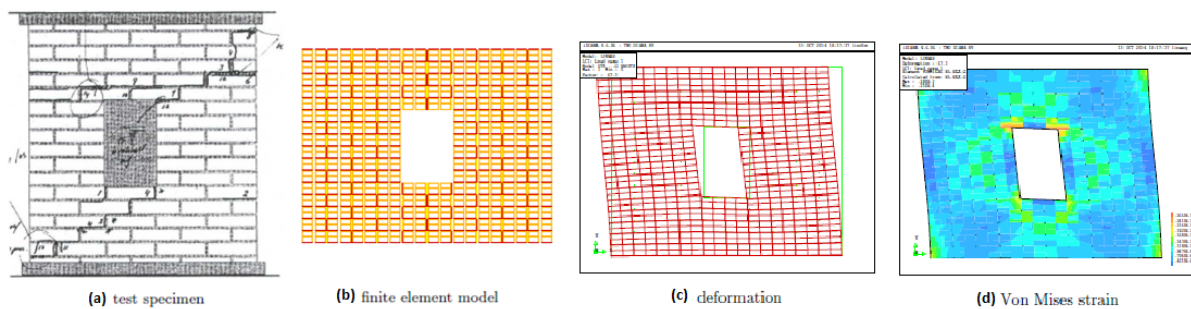
Modeling strategies for masonry structures: (a) masonry sample; (b) detailed micro-modeling; (c) simplified micro-modeling; (d) macro-modeling.

Figure 30: Different methods to model masonry [33]

Research by Lourenço shows that the simplified micro-model in most cases results in relatively accurate masonry model behaviour compared to experimental tests [33]. The research also indicates that brick units should be divided by interface elements to accommodate for the potential vertical crack formation in the brick unit caused by vertical loads. This way the cracks formed in the head joints can continue through the brick unit which was also observed by Lourenço during experimental testing of masonry. The research of Lourenço is based on IP loading of masonry walls.

### 2.5.2 FEM models from literature

TNO DIANA provides an example of discrete modelling of masonry in the DIANA manual [34]. The wall is build up out of half bricks divided in a 2x2 mesh of continuum plane stress linear 4-node elements. The vertical potential crack in the brick unit and the joints will be modelled with use of linear interface elements. The brick unit and the vertical potential crack have linear elastic properties. The joint interface has linear stiffness and non-linear properties. This half brick is copied to create a wall of the desired size. An opening is cut out of the model which simulates a window opening. Boundary conditions are set and the wall is loaded monotonically in-plane with displacement control. This model is also described in the book of 'Structural Masonry' [15] and shows good correlation with experimental test results. The displacement controlled load used in this model is not self-evident for load control in FEM modelling. The model is compared to results plotted in force-displacement graph. An increment in displacement in the model results in a reaction force which can also be plotted in a force-displacement graph. In FEM modelling it is often hard to get stable model results post peak when force controlled loading is applied. With a displacement controlled load the chance of converged results post peak is much higher.



**Figure 31: Masonry model example TNO Diana [34], (a) based on tests, (b) model before analysis, (c) deformed masonry model, (d) Von Mises strains in masonry**

The TU Delft provided Oosterhof Holman with a preliminary analysis of Quake-Shield by making a simplified 2D FEM model [35]. The model is made with DIANA 9.6 and consists out of three layers of shell elements. The three layers represent the masonry, NSM FRP strips and the EB FRP layer. For the purpose of this project this type of model is considered to be too much simplified.

Another FEM model found in literature on masonry modelling is made by H.O. Köksal, O. Jafarov & B. Doran and C. Karakoç [36]. The research also includes the modelling of reinforced masonry with GFRP sheets on one-side of the URM which is the EB FRP layer reinforcing method. The FEM model is made with LUSAS and consists of 3D solid eight-nodded hexahedral elements for the bricks and mortar. Thick shell four-nodded elements are used for the EB GFRP layer. The walls in this research are IP loaded. The FEM models are verified with experimental tests. Figure 32 shows the effect of reinforcing the URM with GFRP. The maximum strain in the lower area of the wall and the sliding along the bed joint change to diagonal cracking. In Figure 32 the aspect ratio of both walls are the same only the scale of the wall figure is different.

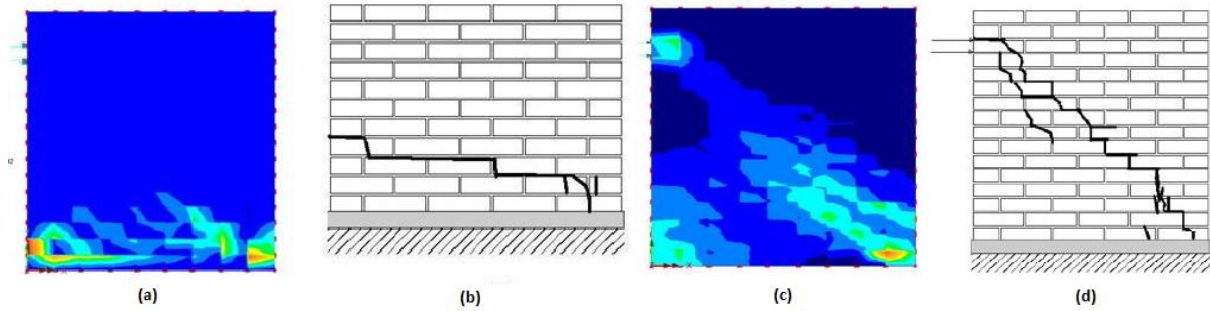


Figure 32 (a) maximum strain in URM (b) crack pattern experimental testing URM (c) maximum strain GFRP reinforced masonry (d) crack pattern experimental testing GFRP reinforced masonry [36]

The resemblance between the model and the experimental tests is also visible in Figure 33 where the load-displacement curves are plotted.

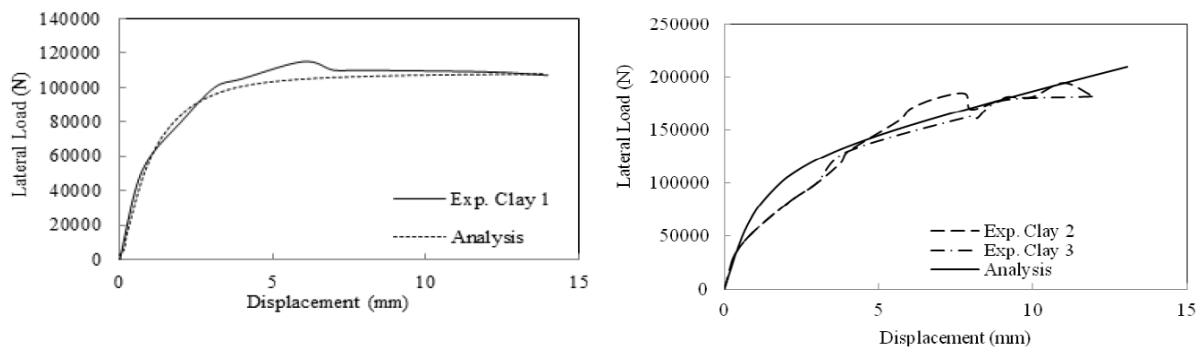


Figure 33: load-displacement curves comparison between model and experimental tests for URM and GFRP reinforced masonry [36]

With a 3D solid element model both the IP and OP load can be applied. The 3D solids will give a good indication of the masonry wall behaviour under these kind of loads. Experimental tests are done in separate IP and OP loading but with a 3D model it should be possible to see the effect of the combined loads on a masonry wall.

A FEM model of 3D continuum solid elements and 2D interface elements is made by L. Macorini and B.A. Izzuddin (Figure 34) [37]. ADAPTIC FEM software is used to make the model. In the research the model is compared to experimental tests based on IP loaded URM and OP loaded URM.

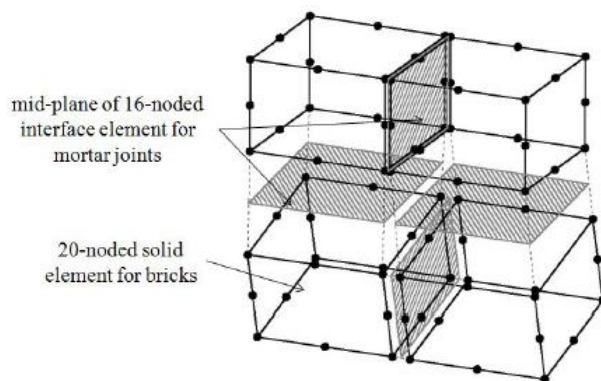


Figure 34: 3D and 2D elements to model masonry with the micro-model method [37]

The FEM model results are compared with experimental results and a 2D shell FEM model proposed by Lourenço & Rots (1997) (Figure 35). The 3D model shows proper post peak behaviour when comparing results from the model with the experimental results.



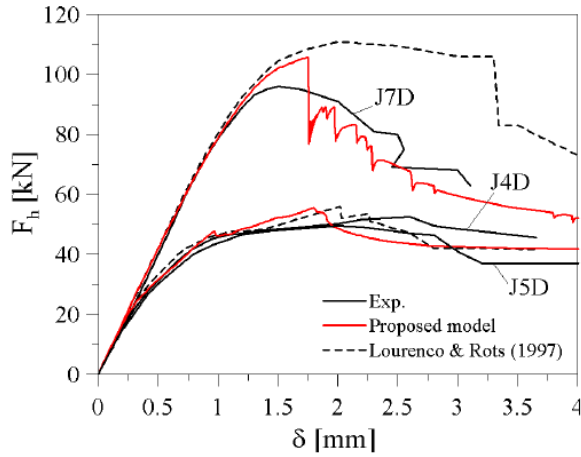


Figure 35: FEM model comparison with experimental results and the 2D shell model of Lourenço & Rots (1997) of different type of URM walls IP loaded [37]

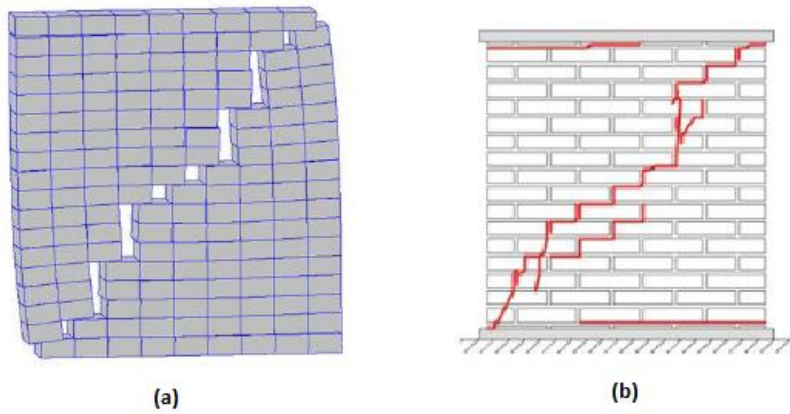


Figure 36: (a) Deformed shape of IP loaded masonry wall result with FEM model, (b) Crack pattern observed during experimental tests [37]

The force-displacement curves show good resemblance between the model and the experimental tests and also the crack patterns are well simulated in the model as can be seen in Figure 36. The same is visible in the OP loaded masonry wall model (Figure 37). Similar crack patterns are simulated in the FEM model as was visible in the experimental results.

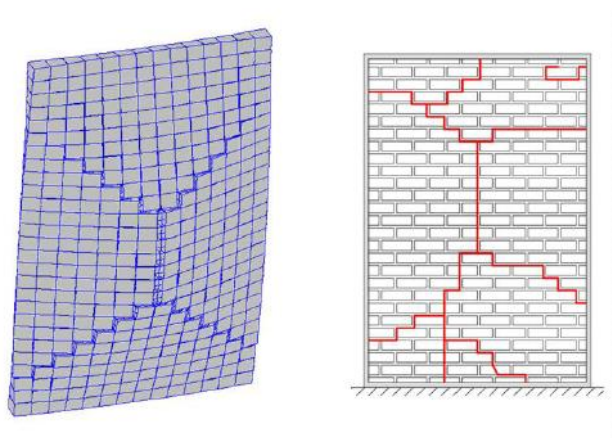


Figure 37: Left: crack pattern simulated in FEM model, right: crack pattern visible in experimental tests [37]



For the FEM model of this project the simplified micro-modelling method is used and so during literature research into existing masonry FEM models the focus is in the next paragraphs only on the simplified micro-modelling masonry models. Masonry FEM models with the simplified micro-model show in general good correlation with experimental test results for both IP and OP loading conditions.

### 2.5.3 Crack models for masonry

DIANA has different crack models for different materials and construction types [38]. The crack models available for masonry are discrete crack models like Brittle cracking, (Non)Linear Tension softening, shear retention and Combined cracking-shearing-crushing. These models can be used for interface elements in the brick-mortar joint.

#### *Combined cracking-shearing-crushing model Diana*

When making a FEM model the possible failure modes of the construction should be known to select a proper damage or in this case crack model that can be used for the FEM model. In case of masonry the combined cracking-shearing-crushing (CCSC) model is an appropriate selection for the brick-mortar joint [38]. The brick and mortar are simulated as a linear elastic continuum element and the brick-mortar joints as interface elements with the CCSC model because of its non-linear behaviour. Masonry is considered as a quasi-brittle material with softening properties. This occurs in tension, compression and shear. The softening effect occurs because of micro crack forming and eventually will lead to macro cracks [15]. Figure 38 shows a graph of the quasi-brittle behaviour of masonry.

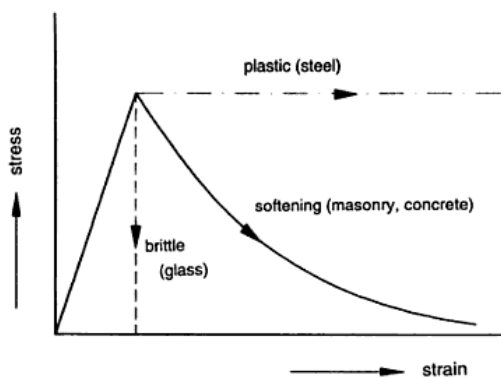


Figure 38: Stress-deformation behaviour of certain materials [15]

This softening behaviour is also taken into account within the CCSC model. Other physical properties included in the CCSC model are: shear slipping, dilatancy, tension cut-off and compression cap [38]. Some of these properties interact with each other when stresses are applied which is made visible in the graph shown in Figure 39. Shear slipping is described in the model by the Coulomb friction criterion. Tension cut-off accommodates the tension softening in the brick-mortar interface due to formation of micro cracks [33]. During fracture of the joint in tensile direction energy is dissipated. The energy that is necessary to fracture the joint in tensile direction is called the mode I fracture energy. For the Coulomb friction criterion the fracture mode II energy is used in the model. Both fracture modes are illustrated in Figure 40.

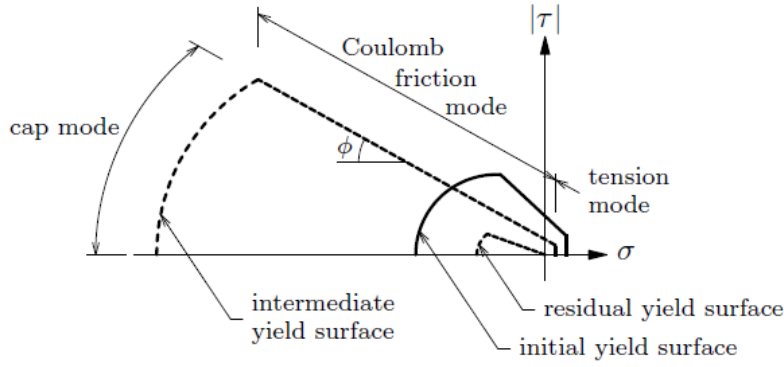


Figure 39: Two-dimensional interface model for the CCSC model [38]

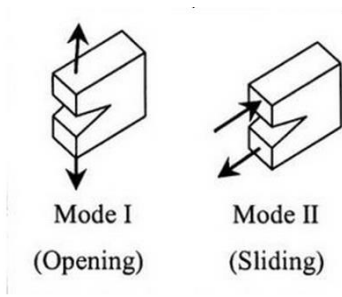


Figure 40: Fracture modes [39]

Dilatancy is also incorporated in the CCSC material model. A dilatant is a material of which the viscosity changes due to shear strain. It is also called a shear thickening fluid because when shear strain is introduced also the volume will change (expand). If expansion due to volume change is restricted the normal force is increased causing for a different shear strength and behaviour [15].

The compression cap is introduced to cope with the effect of hardening-softening in the material. Compression loading of the material increases the compressive strength of the material due to hardening. At a certain point the peak strength is reached and micro cracks start to form resulting into softening as described before and is illustrated in Figure 41.

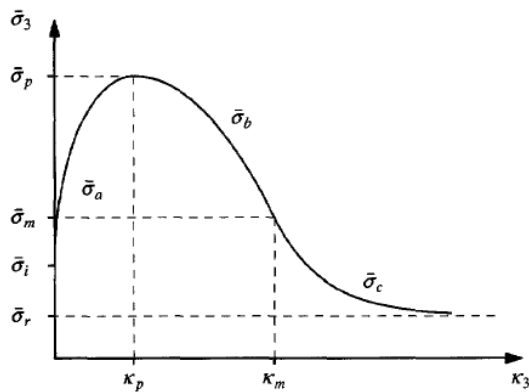


Figure 41: Hardening and softening behaviour of quasi-brittle material under compression load [33]

### *Total strain crack model*

For the brick units a total strain crack model can be used [38]. The total strain crack model could be a better option opposed to a linear elastic material model for the brick units if the brick units are build up out of 3D solid elements and need to have compression failure abilities.

For masonry the coaxial rotating crack concept as part of the total strain crack model gives good results [40]. With the rotating crack model the effect of stress-locking should considered because of the geometrical discontinuities in masonry. This problem does not occur when discrete crack modelling is used.

In the coaxial rotating crack model the stress is evaluated in the crack directions [38]. The strain transformation matrix is depended on the strain vector direction. This model allows, for example in case of bending a concrete beam, rotation in the geometry of the model. This new position of the model geometry gives a new situation to evaluate how the crack growths further into the material. The model also takes, degradation and other material property changes due to the cracking into consideration.

#### 2.5.4 Modelling of reinforcement material combined with masonry

The FRP material is build up out of small filaments that are bundled together with a resin. The FRP strips used in Quake-Shield are unidirectional carbon strips. When modelling a composite product in general the structural properties of the composite determine what kind of failure modes the product will have. Delamination between carbon layers or filaments is one of the key failure modes in this case. To model this failure mode the layers, filaments and resin need to be modelled as separate materials. In the case of reinforcing masonry with FRP, the masonry structure itself or interfaces like adhesive bonded to masonry are the weak links. Therefore delamination in the FRP itself is not likely to happen. Therefore it could be assumed that homogenizing the carbon fibres, resin and adhesive as one material for the FEM model is possible.

DIANA has the ability to model embedded reinforcement elements in solid elements. This is usually used for steel bars in reinforcing concrete but with the proper material parameters input for FRP, it is possible to use these reinforcement elements for modelling the NSM FRP strips. The bond-slip behaviour of the FRP strip in the adhesive can also be implemented in the embedded reinforcement model.

The EB FRP layer could be modelled with shell elements which are connected to the solid elements or with 2D interface elements if slip or debonding between this EB FRP layer and masonry is required. The values for the different material properties which are also used for the FEM model are described in Chapter 3 & 4.

## 2.6 Literature study summary

Masonry walls in houses in the Groningen region are not designed for earthquake loads and should be reinforced to prevent building collapse during, for Groningen standards, a severe earthquake. The soil in Groningen in combination with the gas extraction induced earthquakes are unique in the world. This means earthquake knowledge from other countries cannot always be applied for the Groningen region. Engineers and scientist in the Netherlands are challenged to find solutions for the unique earthquake situation in Groningen.

Single leaf load carrying masonry walls loaded in OP direction are most critical when collapse of the building is considered during an earthquake. The main focus in making constructions earthquake resistant is energy absorption and dissipation which can be increased by applying reinforcing measures to the construction. Reinforcing URM with FRP appears to be a good measure to increase strength, stiffness, ductility and cohesion of the masonry wall without adding too much mass to the building. Shear and bending capacity can be increased significantly with reinforcing methods like NSM FRP and EB FRP.

Quake-Shield is based on the combination of these two types of reinforcing measures. This makes Quake-Shield unique because in literature the combination of NSM FRP strips and an EB FRP layer could not be found. From the test results of Quake-Shield the combination of two existing independent reinforcing measures looks promising.

More conventional methods to adsorb and dissipate earthquake energy is by applying a steel frame to a house. Steel has the ability to plastically deform and dissipate energy but adds much mass to the house or building compared to FRP reinforcing materials. FRP itself does not plastically deform and thus cannot dissipate energy while other materials like adhesives and masonry can. Bond-slip behaviour between FRP, adhesive and masonry and crack forming in masonry can dissipate energy when FRP reinforcements are applied. Combining masonry with FRP reinforcing materials result in a reinforced masonry wall that has an increased stiffness, strength and ductility which gives an increased energy absorption and dissipation. The amount of energy absorption and dissipation can be extracted from a force-displacement curve by taking the area under the curve.

For OP loaded masonry walls the NSM FRP strips are most effective to increase bending capacity. For IP loaded masonry an EB FRP sheet or mesh is most effective. In an earthquake most of the walls will be loaded in multiple directions, i.e. in OP and IP direction combined.

Research is done on the influence of the amount of applied NSM FRP strips and different strip spacing. The location of the strips and spacing has more influence on the behaviour of the masonry wall compared to the amount of FRP applied. Also the depth and width of the grooves for the NSM FRP strips are investigated. The depth of the groove should be minimized to a maximum of 30% of the wall thickness to prevent through thickness cracking.

In literature two main types of masonry tests are used to determine load bearing capacity of masonry. These two types of tests are loading masonry in OP and IP. For OP loading of masonry a three point bending test can be used to determine the bending capacity of the masonry. But large masonry walls tested in vertical direction loaded with airbags give better insight in the behaviour of

the wall when it is OP loaded. Research on a full scale half brick, static cyclic OP loaded, NSM FRP strips reinforced masonry wall, shows a maximum drift of 4% to 8% is possible. Drift is defined as two times mid-plane displacement divided by the wall height.

In the case of NSM FRP strips the bond-slip behaviour is a critical parameter for the overall behaviour of the reinforced masonry wall. A small scale pull-out test can give this bond-slip behaviour which is also critical for implementing in a FEM model to have a proper correlation with the test results.

Based on the literature study the FEM models for this graduation project are in 3D. The masonry walls that are modelled are relatively small and from the geometrical point of view not complex. It is assumed that making a more detailed reinforced masonry model gives better understanding of the behaviour of the reinforced masonry without making the model too complex. The size of the model is relatively small and therefore calculation times will be not too long. After the model is verified with the experimental test results a configuration analysis is done. Variants on the calibrated FEM base model are used to give better insight in the model behaviour. Some of the variations are: spacing and width of the FRP strips and types of reinforcing materials.

Studies show that a simplified micro-model of masonry gives accurate results compared to experimental test results performed in other researches. L. Macorini and B.A. Izzuddin [37] made a model for IP and OP loaded URM. The FEM model is based on this model of L. Macorini and B.A. Izzuddin. The brick-mortar units are 3D continuum linear elastic solid elements with 2D non-linear interface elements for the brick-mortar joints. The non-linear interface elements for the brick-mortar joints use a CCSC model to provide crack, shear and crushing behaviour of the masonry.

The NSM FRP strips are modelled with 1D embedded reinforcement elements. The EB FRP layer is homogenised into a single layer and is modelled with 2D shell elements. This choice is based on the research of H.O. Köksal, O. Jafarov & B. Doran and C. Karakoç [36]. In this research EB glass FRP is modelled as thick-shell elements which give proper results compared to the strains and crack patterns observed during experimental testing. For the FEM model the length and width of the sheet is large compared to the thickness. It can be assumed no shear stresses are present over the thickness of the sheet. Therefore not thick-shell but normal shell elements are used. More details about the FEM models can be found in Chapter 4.

### 3 Quake-Shield samples and test results

This chapter describes the reinforced masonry samples used for the Quake-Shield OP bend test. Sample geometry, material properties and the test setup are explained. The test results of the Quake-Shield OP bend test are described and analysed. Possible imperfection found in the samples and test setup that are also described in this chapter

#### 3.1 Quake-Shield sample geometry and materials

To make a proper functioning model that correlates with experimental test results key parameters and accurate material properties need to be implemented in the model. Table 3 gives a list of used materials and products for the test samples with the corresponding values for the material properties. The material properties are found in datasheets and literature. Most manufactures of the materials provide limited material properties or only general material properties. For the FEM model also FEM specific parameters are required like normal stiffness modulus (Kn) and shear stiffness modulus (Kt). These values are taken from literature or calculated with equations found in literature. Details about these kind of specific FEM parameters are discussed in Chapter 4.

Table 3: Material properties from datasheets and literature. Source: datasheet manufacturer, Structural masonry [15], Petersen research [24], Performance Composites [41], Constitutive Modeling and Experiments on Polyurea [42].

Material properties of:	Brick	Mortar	carbon strip	adhesive	C-mesh	PP-mesh	Armo-crete	PU
Density [kg/m <sup>3</sup> ]	1566	2990	1600	1550	1790	920	2090	1110
Young's modulus [GPa]	6,05	0,7	165	7,5*	160	1,2	26	0,013
Tensile strength [MPa]		1,16	2800	2,5	650	30	6,5	23
Compressive strength [MPa]	20	>12,5- <32,5				38	45,5	
Poisson's ratio [-]	0,14		0,3	0,495**	0,3	0,45		0,486
max Elongation tensile [%strain]			1,5-2,0	60	1,5-2,0	600		330

\* Calculated with use of given stress at certain strain in datasheet, assuming it is in the elastic range.

\*\* Not known, but is very rubber like so Poisson's ratio will be close to 0,5.

\*\*\* The bricks are from Steenindustrie Strating b.v. type Vuilwerk Waalformaat. The mortar is from Dyckerhoff type metselcement MC12,5 KAA.



The empty cells in Table 3 mean the values for these material properties are unknown and are not relevant for the development of the FEM model.

The dimensions of the materials used for the Quake-Shield test samples are listed in Table 4. Two types of EB FRP layers are used for the Quake-Shield samples that are considered in this project. A polyurea (PU) base layer with an embedded mesh of polypropylene (PP-mesh) which is also the variant used for FEM Base model. The other variant is a cementitious base layer called Armo-Crete (AC) with an embedded carbon mesh (C-mesh). This latter variant will be modelled in the Quake-Shield configuration analyse (Chapter 6).

**Table 4:** l=length, w=width, h=height, d=diameter, t=thickness. \* and \*\* see Figure 42 for clarification of dimensions of the pp-mesh and c-mesh. \*\*\* 5±1mm layer of material, mesh plus 5 to 10mm of material on top of mesh.

	Dimensions [mm ]
Brick	209x100x50 (lxwxh)
Mortar joint	100x15 (wxh)
CFRP strip	15x2,5 (wxt)
Cut for strip	12,5x20 (wxd)
PP-mesh (polypropylene)	10x10 D=2±1 *
C-mesh (carbon)	20x20 / 3x0,044 (wxt)**
Armo-crete (AC)	5±1+5-10 (t)***
PU (polyurea)	5±1+5-10 (t)***

Before the masonry wall samples were tested the outer dimensions were measured and the total mass of the sample was calculated. These values can be found in Table 5.

**Table 5:** Quake-Shield sample dimensions used for the three point bend test

	Dimensions [mm]	Mass [kg]
URM	870x550x100 (lxwxh)	75
AC + C-mesh	870x550x110 (lxwxh)	98
PU + PP-mesh	870x550x110 (lxwxh)	76

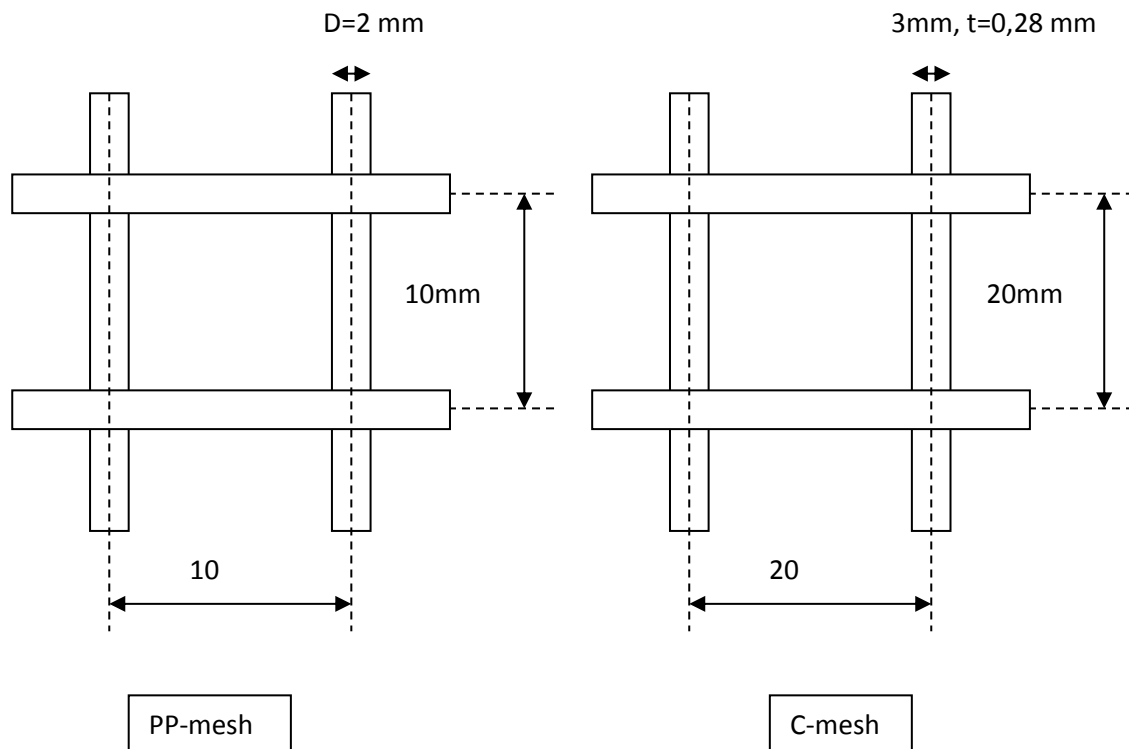


Figure 42: PP-mesh and C-mesh dimensions

Figure 42 gives an impression of the dimensions and geometries of the two types of meshes that are used for the EB FRP layer. The PP-mesh consist out of round threads with a diameter of 2 mm and the C-mesh are flat woven carbon filaments with a thickness of about 0,28 mm.

The meshes are embedded in a base layer. PU is used as a polymer base layer to bond the PP-mesh to the masonry. The mesh is fully covered and therefore this layer could be considered as a composite FRP layer. For the C-mesh the base materials is AC. This material is designed by the manufacturer to be used in combination with reinforcing materials like the C-mesh.

### 3.2 Quake-Shield sample preparation

All masonry wall samples are constructed by the same masons and with the same type of brick and mortar (Table 3). After a minimum of 28 days of curing the samples are reinforced with the Quake-Shield reinforcing method. First two grooves are cut with a depth of about 20 mm and 12,5 mm width. The grooves are located 125 mm from the centreline of the sample and are never cut in one of the head joints. The grooves and carbon strips are cleaned. A primer, adhesive and the carbon strips are placed in the grooves so the grooves are filled up. A primer is applied to create proper adhesion between the masonry and the adhesive. After the adhesive has cured sufficiently the face of the sample is cleaned and a 5 mm layer of PU or AC is applied, depending on the type of sample. PP-mesh for PU and C-mesh for AC is placed on the still wet PU or AC layer. Then a second layer (5-10mm) of PU or AC is applied to embed the mesh. Details about the sample construction are shown in Figure 43 and Figure 44. The figures are only illustrative, the scale is adjusted to make the build up of the reinforcing layers on the masonry more clear. In reality the layer thickness is in total about 10 to 15 mm where the brick is 100 mm in thickness.

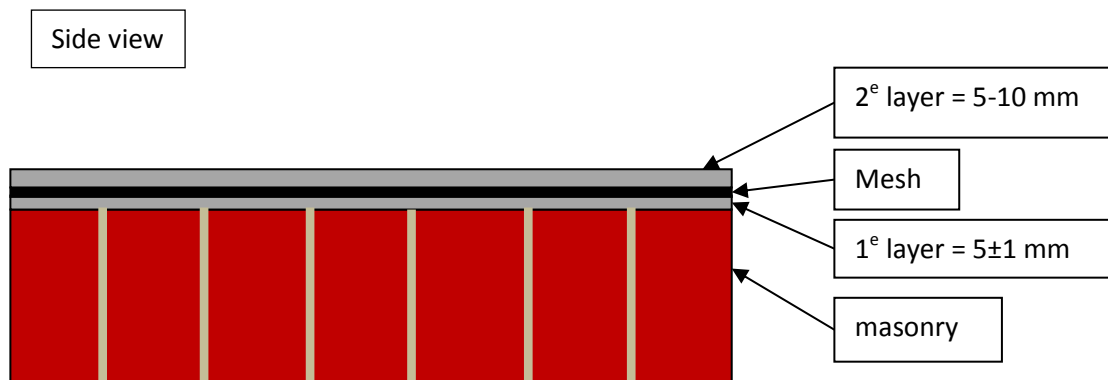


Figure 43: Side view of reinforced masonry wall sample (scale adjusted for illustrative purpose)

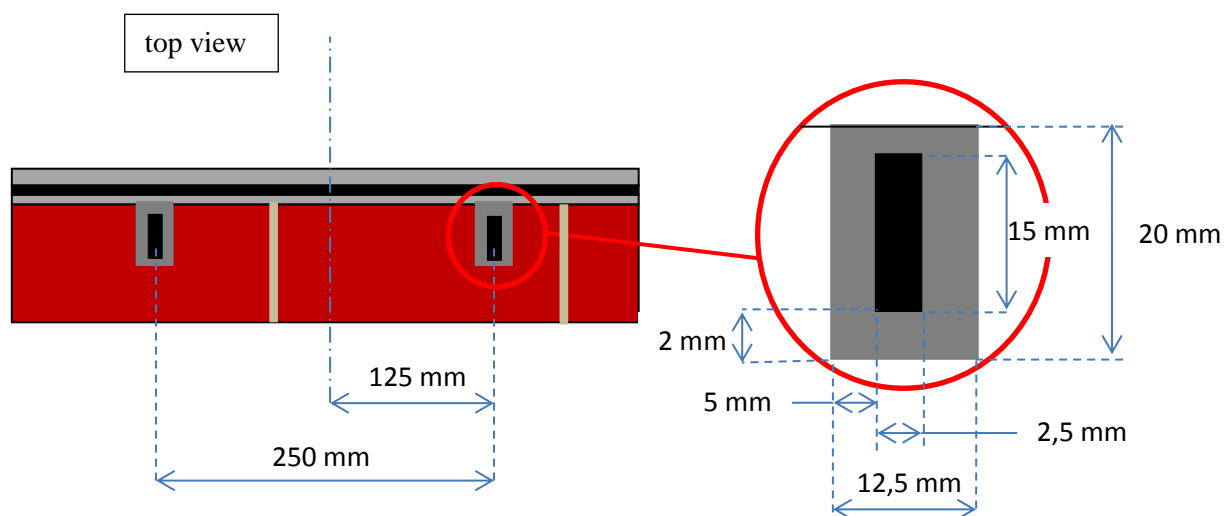


Figure 44: Top view of masonry wall sample (scale adjusted for illustrative purpose)

### 3.3 Test setup

The test setup for the OP bending test is located at SealteQ Group (Stadskanaal) (Figure 45). It is a simple three point bending test where the load is applied with use of a hand pump. Three displacement measuring devices are placed on the sample to measure the relative displacement at a certain applied load.



Figure 45: Test setup used for the OP bending test (screenshot taken from a Youtube movie of the Quake-Shield Youtube channel [43])

The samples are horizontally tested during the three point OP bend test with the reinforcing side of the sample on the bottom side. Figure 46 shows how the sample is supported and loaded during the three point bend test.

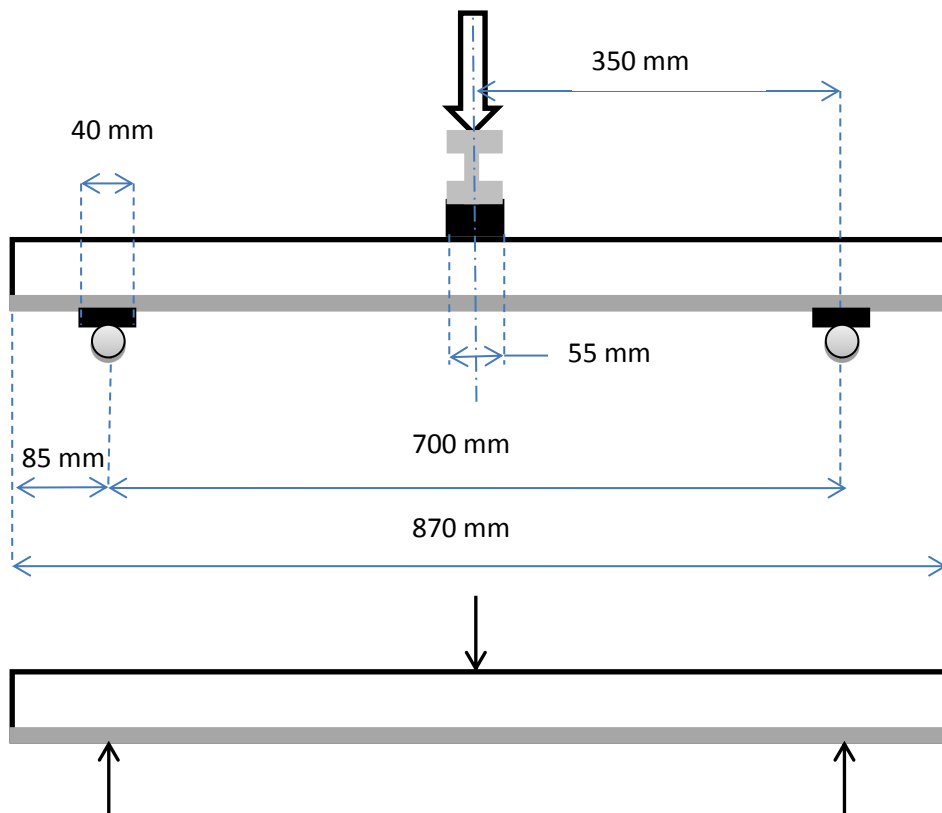


Figure 46: Support and loading locations of test setup and simplified support and load for FEM model

### 3.4 Quake-Shield test results

The sample with PU+PP-mesh EB FRP layer and NSM CFRP strips (BG1 series) is used for the FEM model which acts as a base model for the configuration analysis. In the configuration analysis the sample with AC + C-mesh EB FRP layer is one of the variations on the base model.

Figure 47 shows the test results of three samples of the BG1 series. Video material is available from the BG1-1 test [43]. During the build up of the model the BG1-1 will act as the reference sample. The test results shown in Figure 47 also show the large variation involved in masonry and in this case reinforced masonry. Many factors could influence the test results but material properties have a large contribution to this. Not only the large variation that is usually found in masonry during material testing but also in the way the reinforced materials are applied. Proper bonding of the FRP to the masonry has also an influence in the behaviour of the reinforced masonry.

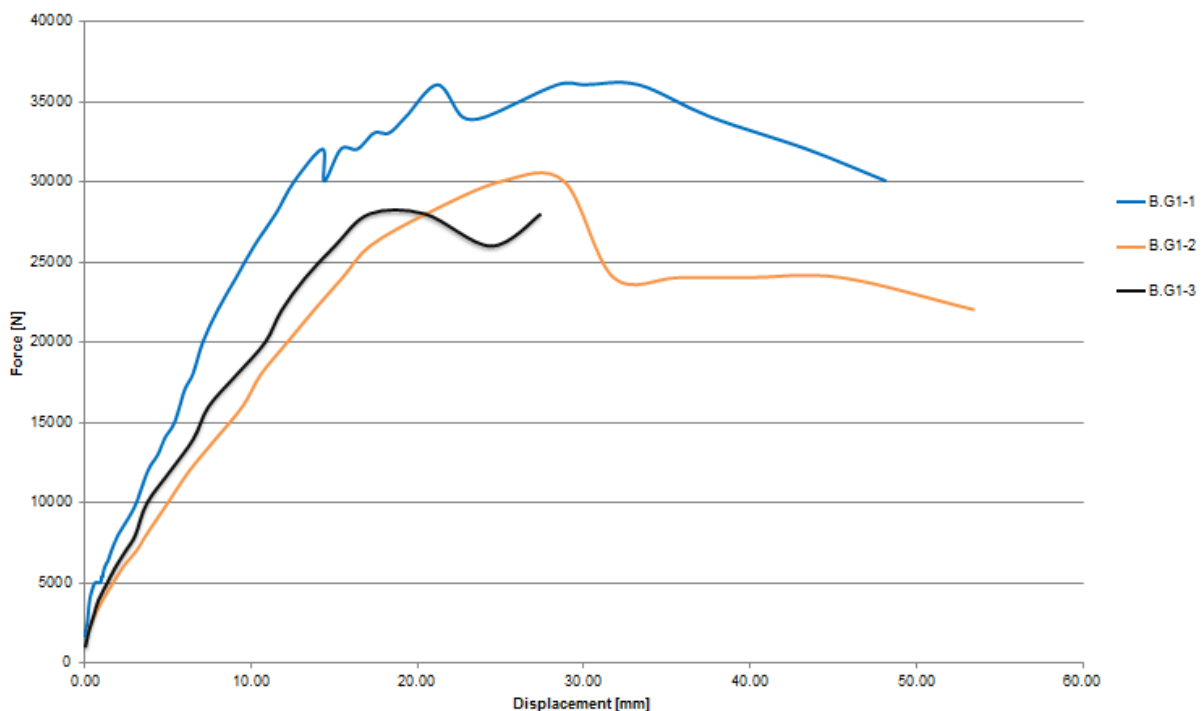


Figure 47: Test results of samples of the BG1 series

Correlating the test results from BG1-1 to the video of the BG1-1 test, some noticeable effect can be indicated in the test results. It should be noticed that the video is taken from a side view angle so for instance crack forming is only visible at one of the side edges of the sample.

Figure 48 shows the test result of BG1-1 with numbered vertical lines that indicate the following:

1. Probably first crack initiation at 0,6 mm displacement at 5 kN. The crack has opened enough to be visible on the video at 1,6 mm displacement. Second crack follows quickly in the other mortar interface closest to the centre row of bricks in the sample. Here the relative displacement is the highest and therefore the stresses are also the highest in the mortar interface.
2. Around 5 mm displacement cracks initiate in the mortar interfaces at the left and right side of the cracks from the previous step.

3. At about 15 mm displacement the first local peak appears in the test results. In the video the initiation of the first horizontal crack in top of the bricks is visible. Here the stresses in compression zone are reaching values that exceed ultimate compression strength of the masonry.
4. A second peak appears in the test results but nothing noticeable is visible in the video. Cracks keep propagating and opening up more. Also a larger area of the masonry in the compression zone is affected by compression failure.
5. A plateau is reached. Compression failure continues and significant plastic deformation of the polymer layer is visible at the location of the cracks at the bottom side of the sample.
6. Plastic deformation rate of the EB FRP layer increases and eventually partly tensile failure is visible. The NSM CFRP strips are embedded so it is difficult to see in the video what is happening with the strips. The measuring device at the mid-plane of the sample reaches its maximum measuring range at about 48 mm so testing is stopped at this point.

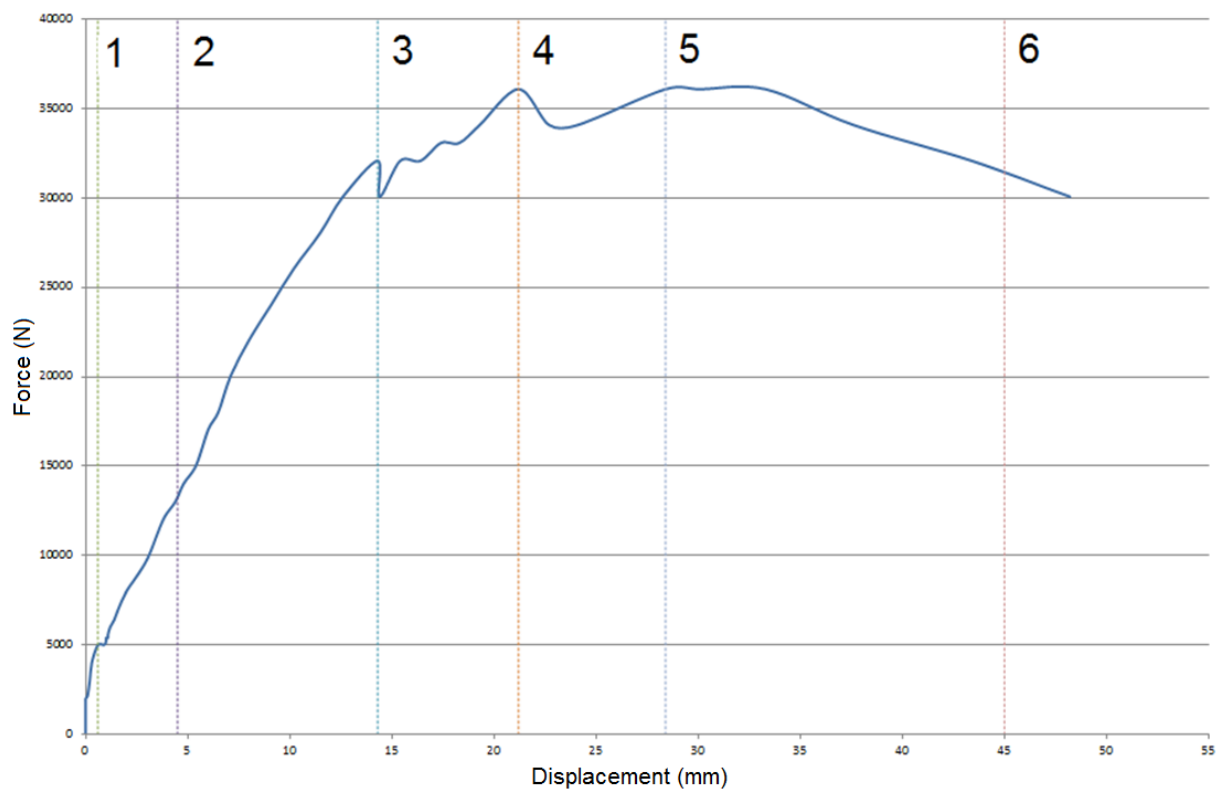


Figure 48: Noticeable effects observed during test and visible in force-displacement curve of sample BG1-1

### 3.5 Imperfection of testing and samples

Observing the sample and test setup some imperfections are noticed. These imperfections can influence the test results but are also useful to know when comparing the test results to the results from the FEM model. The remarks for the test sample and test setup are listed below:

- Samples are tested horizontally. Masonry walls are normally used in vertical position so a normal load due to self-weight and dead weight of other floors compresses the masonry increasing its load carrying capacity. The effect of self-weight of the sample in horizontal position was also visible with URM samples that were tested. Two out of three collapsed just by their self-weight when putting them horizontally on the supports of the test setup.
- The samples are build up in vertical position and then transferred into horizontal position for the test setup. This movement could induce unwanted damage to the sample.
- Masonry is very sensitive to manufacturing conditions. The condition in which the bricks, mortar and eventually the build up of the masonry itself is made influences the mechanical properties of the masonry sample. This introduces large variations in mechanical properties for masonry.
- In the video of the BG1-1 test it is visible that likely the EB FRP layer is not fully bonded to the masonry from the start of the test.
- It is hard to make perfectly straight masonry samples so if for instance the sample is torqued a little, this will introduce extra stresses in the masonry that are not wanted in a three point bend test.
- Rubber strips at the support are used to compensate for the geometry imperfections but also influence the displacement measurement because of the indenting of the rubber.
- The location of the sample in the test setup is determined with the naked eye. The pressure beam is located on one of the middle brick rows. The exact location is not measured every time a new sample is tested.
- The measuring devices are digital clocks that are controlled by levers that are placed on the sample. The lever moves down in an arc and not straight down.
- Load is applied to the sample with an hydraulic hand pump which introduce stepwise load increments instead of more smooth continues like load increase when using a computer controlled hydraulic pump.
- Pressure of the hand pump is displayed with an analog pressure gauge. Test data is observed by a person and logged on paper. This could introduce some reading errors when logging the test data.

## 4 Reinforced masonry FEM model

In this Chapter it is explained how the FEM model for Quake-Shield reinforced masonry is made. The development of this model is a process in which changes are made in the model during model development. The start point for the development of the Quake-Shield reinforced masonry model are the findings from the literature study (paragraph 2.5). These findings are first checked with a more simple FEM model based on a research by Dmytro Dizhur, et al. [18]. In this research a three point bend test on a NSM CFRP reinforced masonry prism (stack of 10 bricks) is described. More details about this FEM model can be found in Appendix A.

The results of the FEM model based on this experimental test of Dmytro Dizhur, et al., showed modelling problems when using embedded reinforcing elements with bond-slip properties in combination with interface elements for the mortar. For the FEM model of Quake-Shield reinforced masonry, the NSM CFRP strip is modelled discretely to resolve this modelling problem. The NSM CFRP strip is connected to the masonry with interface elements that provide bond-slip behaviour. Details about the Quake-Shield reinforced masonry FEM model is described in this Chapter.

### 4.1 Quake-Shield FEM model

#### 4.1.1 FEM model Geometry

Figure 49 shows a top view of a schematic representation of a Quake-Shield reinforced masonry sample as described in Chapter 3. Symmetry is used to reduce the model size resulting in less elements and thus faster calculation time. Figure 49 shows how the reinforced masonry sample can be divided into smaller quarter 'symmetry sections' by mirroring the model about the two symmetry planes. This gives the model overall dimensions of  $400 \times 278 \times 100 \text{ mm}^3$ , which is actually a representation of 1,25 bricks in width and 6,5 bricks in length. The sample has a total of 14 bricks in length but one row of bricks is removed from the model because this row is outside the span of the test setup, so does not contribute to the bending capacity. In the test sample the NSM CFRP strips are placed at 250 mm from each other so the strip is located in the symmetry section at 125 mm from the symmetry plane.

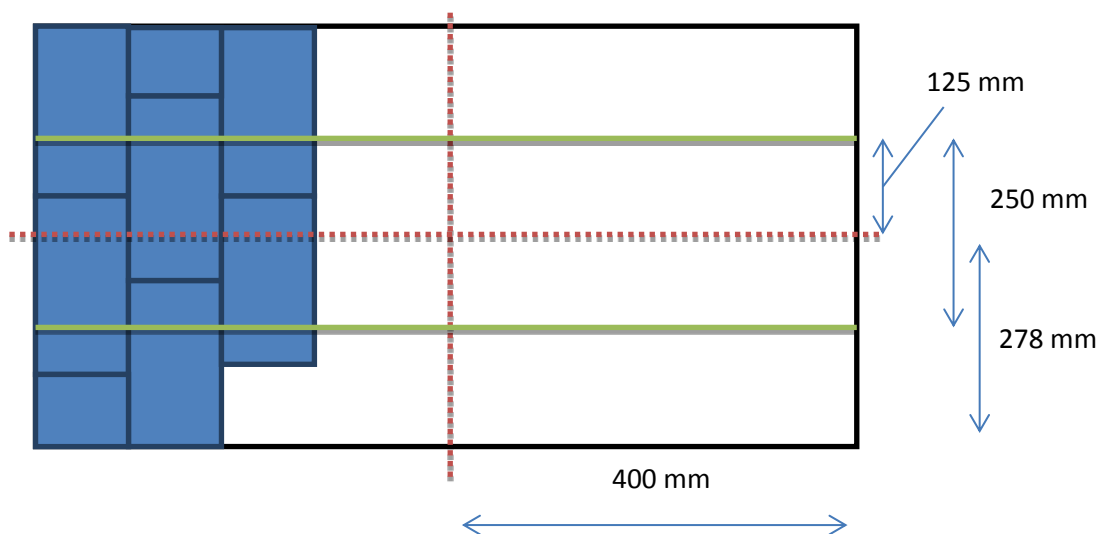


Figure 49: Top view of reinforced masonry test sample. Red dotted line = mirror planes of quarter symmetry model, green line is location of NSM FRP strips



Figure 50 shows the FEM model of the reinforced masonry test sample and is thus only a quarter of the full scale masonry test sample. DIANA has a function to easily mirror results so in Chapter 5 the results are presented as the full scale reinforced masonry test sample. Figure 51 shows the bottom side of the FEM model where the EB FRP layer is located. Figure 52 shows a cross-section of the FEM model to make the NSM CFRP strip better visible

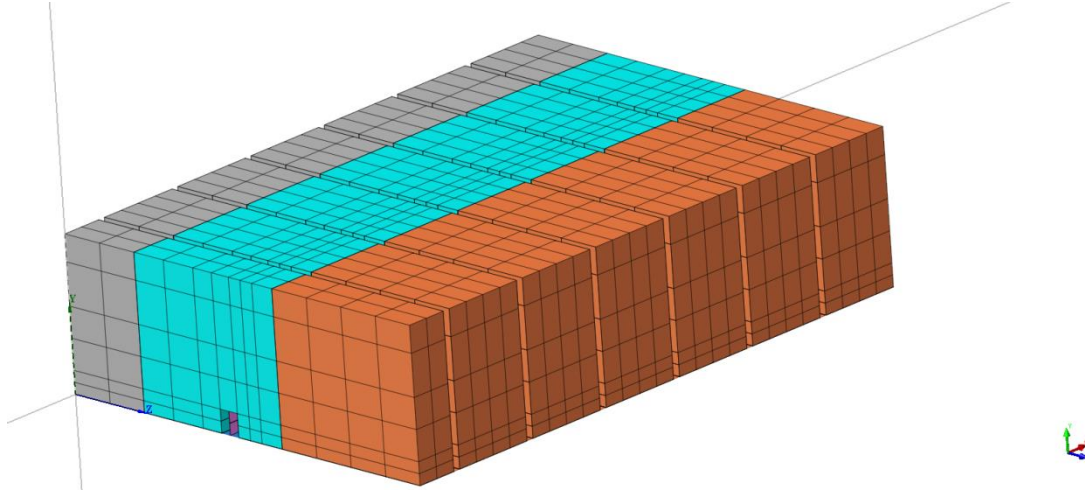


Figure 50: Geometry of FEM model (quarter symmetry model). Light blue and orange section is half a brick width. Grey section is a quarter brick width.

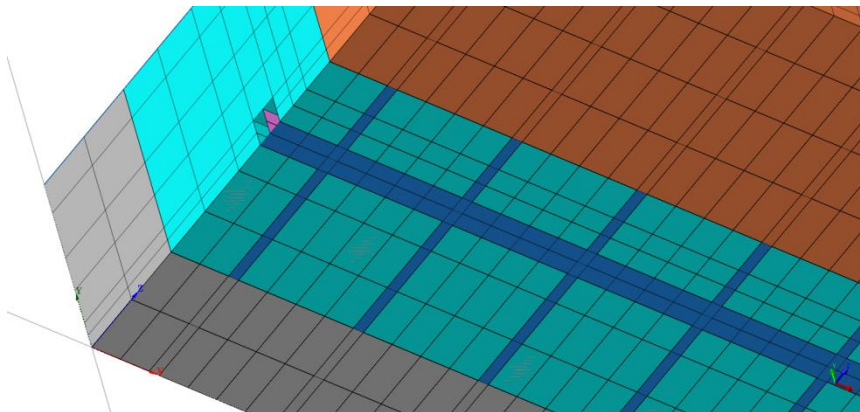


Figure 51: Section of FEM model, bottom view. The EB FRP layer is visible in dark blue. The EB FRP layer is covering the whole bottom side area of the model.

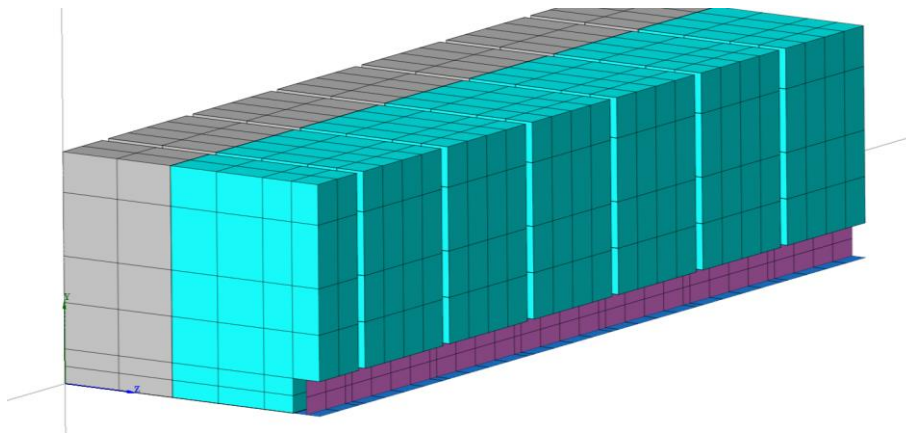


Figure 52: Cross-section of model along the length of the model with the NSM CFRP Strip visible

Table 6 gives more details about the dimensions of the FEM model. The width of half a brick in the model is chosen by taking the width of a brick plus the thickness of the mortar layer divided by two. Because the quarter symmetry section is 1,25 bricks wide plus some extra to compensate for the mortar in the head joints. The model does not contain interfaces at the head joints because these have not a significant contribution to the overall bending behaviour of masonry compared to the bed joints.

The mortar joint was given a non-zero-thickness to avoid problems with CFRP strip elements at the intersection with the mortar interfaces. The mortar interface elements have a thickness of 5 mm determined by the aspect ratio of the elements of the CFRP strip. If the thickness of the mortar interface was smaller the aspect ratio would become too low.

The height of the groove for the CFRP strips is determined according to the CFRP strip dimensions. The width is chosen as the off-centre distance of the FRP strip. So later for the configuration analysis an easy shift can be made to put the CFRP strip in the centre of the model. Different strip spacings are investigated in the configuration analysis which is easier if the strip is in the centre of the model.

**Table 6: Dimensions used for FEM model, half brick, mortar joint, CFRP strip and EB FRP layer**

	<b>Dimensions [mm ]</b>
<b>quarter sym. section</b>	400x278x100 (lxwxh)
<b>half brick</b>	111,25x100x57,5 (lxwxh)
<b>mortar joint of half brick</b>	111,25x100x5 (lxwxh)
<b>groove for strip</b>	400x13,75x15 (lxwxh)
<b>CFRP strip</b>	15x2,5 (wxt)
<b>EB FRP layer</b>	400x278x10 (lxwxh)

Different types of elements are used to model the different materials. All elements in this model are quadratic. The bricks are twenty-node isoparametric solid elements (CHX60) with a default 3x3x3 Gauss integration scheme [44]. The mortar joints are interface elements (CQ48I) with a default 3x3 Newton-cotes integration scheme. The CFRP strip consists out of curved shell elements (CQ40S) with a default 2x2 Gauss integration scheme. A cut is made into the bricks (solid elements) to place the NSM CFRP strip in the bricks. The strip and bricks are connected with interface elements (CQ48I) only on the two largest surface area of the strip. The top and bottom of the strip surface area are small (2,5mm thickness vs 15mm width) and therefore the contribution of these areas connected to the adhesive can be neglected. The EB FRP layer at the bottom side consists out of curved shell elements (CQ40S) connected to the solid (brick) elements

The adhesive interface elements have a non-linear material model used to model the bond-slip behaviour of the NSM FRP strip. Bond-slip behaviour is implemented with the TAUDIS function of DIANA. The material model for the mortar interfaces is non-linear discrete cracking. During bending of masonry mainly tensile strength and normal stiffness modulus of the mortar affect the behaviour of crack initiation and propagation if the wall is loaded like in the Quake-Shield OP bend test. The CCSC material model, as suggested in the literature study and used in the more simple FEM model based on Dmytro Dizhur, et al research, contains a lot of parameters that do not play a significant role in a bending load case. A more simple material model like non-linear discrete cracking is sufficient to simulate crack opening and gives a more stable FEM model.

During the three point bend test the top part of the sample is compression loaded and reaches eventually compression failure. The material model for the solid brick elements describes non-linear elastic behaviour.

The EB FRP layer has non-linear elastic material properties and the PP-mesh and PU base layer are homogenised into a single layer which will be explained in more detail in paragraph 4.1.3.

#### 4.1.2 Load and boundary conditions

Boundary conditions are applied at the location where in the test setup the supports are located on the sample. The boundary condition of the support is in the model a single row of nodes constrained in the Y and Z direction located at left edge of the most right brick (Figure 53). Due to the use of symmetry in the model also constrains have to be applied at the X-Z and X-Y mirror planes. For the X-Z mirror plane a constrain to all nodes on the X-Z mirror plane is applied in the X-direction. For the X-Y mirror plane the constrain is applied to all nodes at the X-Y mirror plane in the Z-direction (Figure 53 & Figure 54). With these constrains applied a simply supported beam is created.

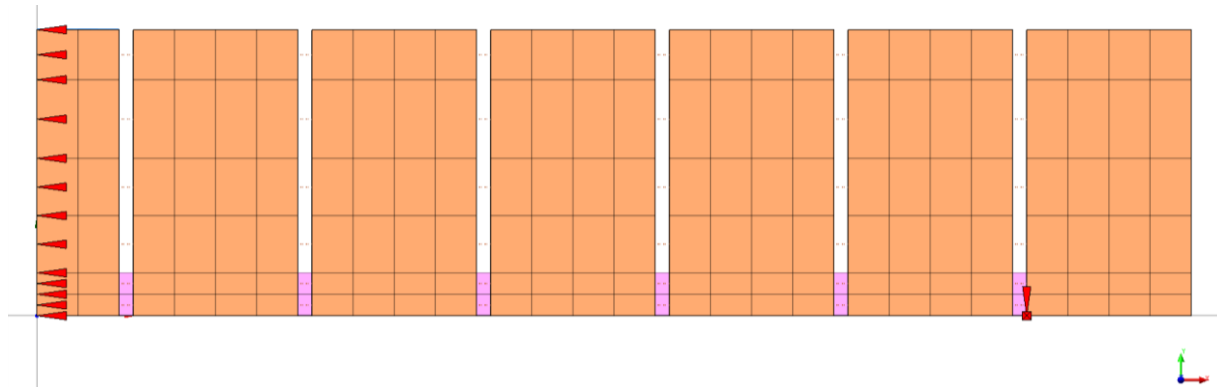


Figure 53: Side view of model with boundary conditions indicated with the red arrows (translation constrain)

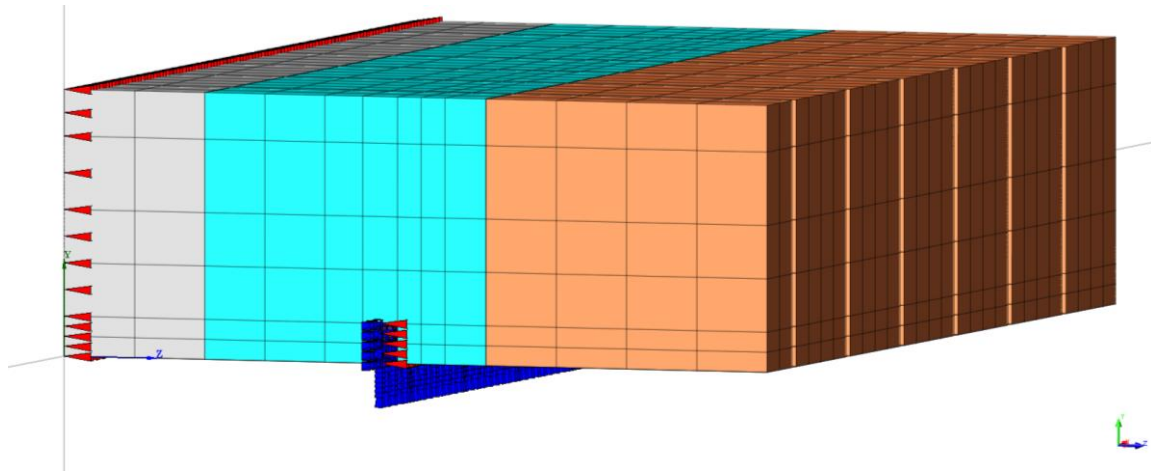


Figure 54: Front view of model with boundary conditions indicated with red (translation constrain) and blue arrows (rotation constrain)

The NSM CFRP strip also has extra constrains because in the sample it is confined by the adhesive. Bond-slip behaviour takes place in the X-Y plane and therefore the other directions are constrained (Figure 54).

The load is applied to one node indicated by the arrow at the corner of the model (on Y-axis) (Figure 55). Multiple nodes are linked to this single loaded node to create a distributed load over a certain area in the model. The linked nodes are indicated with the blue lines shown in Figure 55.

In the test setup the load is applied as a distributed load induced by a beam. This beam has a length of 430mm so it does not cover the whole width of the sample. This is visible in Figure 55 where the linked nodes to the loaded node do not cover the whole width of the model.

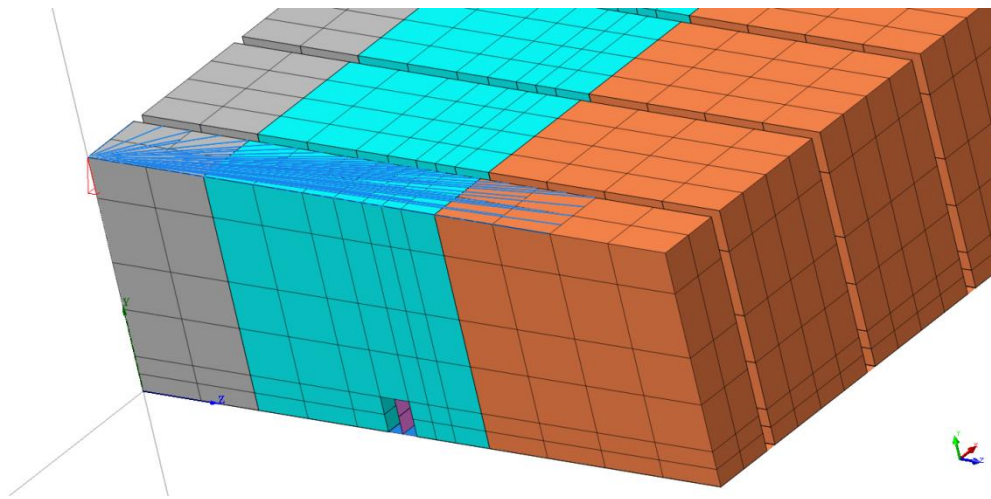


Figure 55: Top view of model with load indicated with red arrow (left corner) and linked nodes to load indicated with blue lines

#### 4.1.3 FEM model material properties

In the model the mortar is partly lumped into the solid brick elements and partly in the interface elements. Therefore the compressive behaviour of the bricks in the model could be considered as the compressive behaviour of masonry. Some of the material properties of the bricks and mortar are unavailable. However the TU/e performed material tests on small masonry samples made with the same materials and by the same mason as with the Quake-Shield OP bend test. The material properties found for the masonry samples can be found in Table 7 and are used for the brick elements in the model.

Table 7: Material properties of brick [45]

Material properties of:	Young's modulus (E-modulus)	Poisson's ratio	Density	Compressive strength	Compressive fracture energy	Compression curve
Brick 1 (solid)	7886 MPa	0,08	1786 kg/m <sup>3</sup>	14 MPa	20 N/mm	Parabolic
Brick 2 (solid)	7886 MPa	0,08	1786 kg/m <sup>3</sup>	14 MPa	24,2 N/mm	Parabolic

The compressive fracture energy is not available from the test performed by the TU/e and is calculated based on the compressive strength with equation ( 2 ) from the Petersen research [24].

$$G_c = 15 + 0,43 \cdot f_c - 0,0036 \cdot f_c^2 \quad (2)$$

$G_c$  = Compressive fracture energy of brick

$f_c$  = Compressive strength of brick

Two types of brick materials are used, brick 1 and brick 2 (Table 7). The only difference is the compressive fracture energy. This is due to the fact that compressive energy is influenced by the element size. The half brick containing the CFRP strip has on average 1,78 times smaller elements in volume. By taking the cube root of this values gives a factor of 1,21 that need to be applied to compressive fracture energy of the larger solid elements to give all the solid elements in the model the same compression behaviour.

Table 8: Material properties of mortar (non-linear) [15] [45]

Material properties of:	Normal stiffness modulus (Kn)	Shear stiffness modulus (Kt)	Tensile strength (ft)	Softening criterion
Mortar non-linear (interface)	141 N/mm <sup>3</sup>	64 N/mm <sup>3</sup>	0,2 MPa	Hordijk et al.
	Fracture energy	Mode-I unloading	Mode-II shear after crack	Shear modulus after crack
	0,006 N/mm	Secant	constant	0 N/mm <sup>3</sup>

Equation ( 5 ) and ( 6 ) are used to calculate  $K_n$  and  $K_t$  for the mortar interface and can be found in Appendix A. The E-modulus of mortar and brick separately are not known. Based on literature the E-modulus of masonry is usually somewhere in the middle between the E-modulus of the bricks and mortar so an estimate guess is made for calculating  $K_n$  and  $K_t$  values (Table 8).

The E-modulus of mortar found during a compression test can be as much as four times higher compared to E-modulus of the mortar found in a tensile test [15]. This is an indication that the calculated  $K_n$  and  $K_t$  values are potentially too high and in this case needs to be corrected in the calibration phase of the model.

Fracture energy for the mortar interface is estimated from values from the book Structural Masonry by comparing mortars with about the same tensile strength [15].

**Table 9: Material properties of adhesive (non-linear)**

Material properties of:	Normal stiffness modulus ( $K_n$ )	Shear stiffness modulus ( $K_t$ )	Diagram Normal direction	Diagram Shear direction
Adhesive non-linear (interface)	1000 N/mm <sup>3</sup>	0,345 N/mm <sup>3</sup>	SIGDIS function See Figure 56	TAUDIS function see Figure 57

$K_n$  and  $K_t$  values for the adhesive are coupled to the SIGDIS and TAUDIS diagram. The linear gradient in SIGDIS is  $K_n$  and for TAUDIS this is  $K_t$ . For the bond-slip behaviour of the NSM CFRP strip only TAUDIS is used. SIGDIS values are large enough to prevent the FRP strip to displace in the normal direction. The TAUDIS curve is determined with calibration of a pull-out model based on the pull-out test performed by the TU/e [46]. This pull-out test model and calibration is described in more detail in paragraph 4.2.

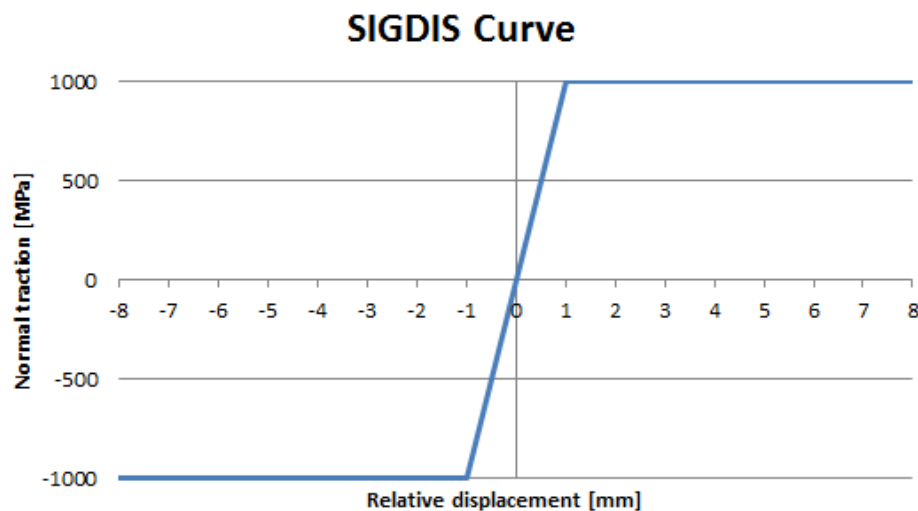


**Figure 56: SIGDIS curve**

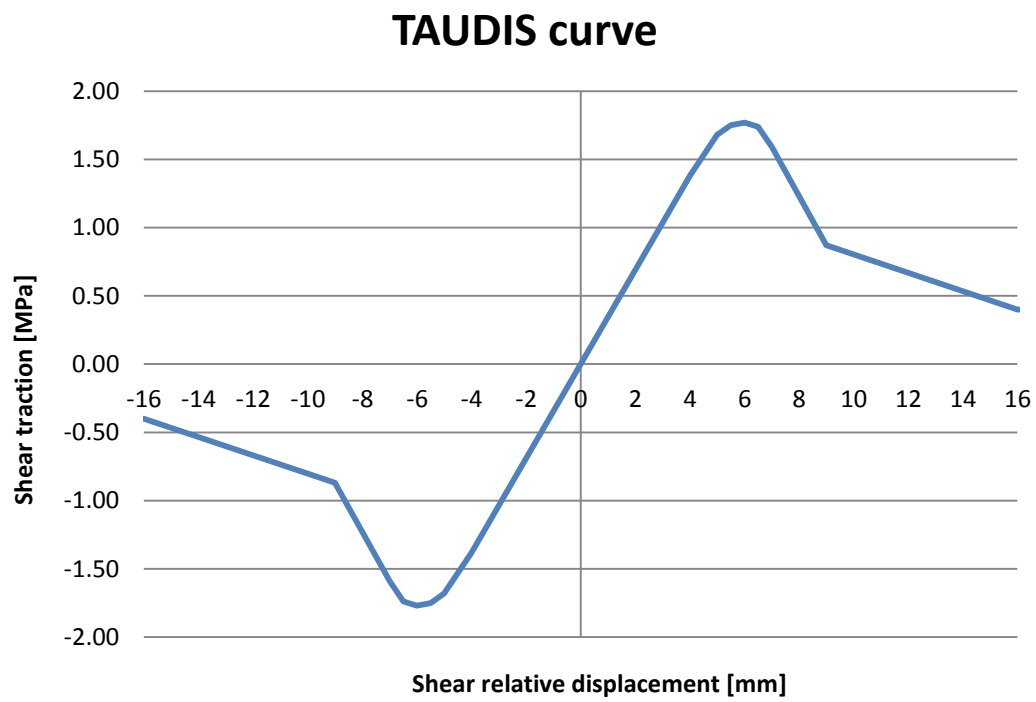


Figure 57: TAUDIS curve



Table 10: Material properties of NSM CFRP strip and EB FRP layer

Material properties of:	Young's modulus (E-modulus)	Poisson's ratio	Density	Yield stress
NSM CFRP strip	165000 MPa	0,3	1600 kg/m <sup>3</sup>	-
EB FRP layer	58 MPa	0,486	1000 kg/m <sup>3</sup>	11 MPa

Material properties values for the CFRP strip are from the datasheet and general values found for CFRP strips in literature [41]. Same accounts for the EB FRP layer (PU+PP-mesh) [42]. The PP-mesh and PU could be considered as a composite material. For the model these two materials are homogenised into one layer. The E-modulus of PP is 1200 MPa and for PU estimated at 22 MPa. By smearing out the PP-mesh over a uniform layer an equivalent E-modulus can be calculated for the homogenised layer using equation ( 3 ) [47]. For this equation it is assumed that there is an iso-strain state during loading and only PP threads in longitudinal direction are loaded.

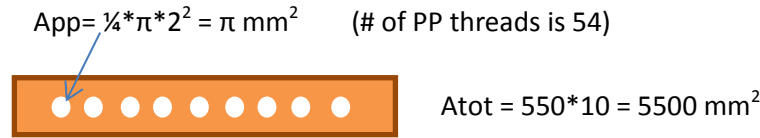


Figure 58: Schematic side view of PU+PP-mesh layer

$$E_{eq} = E_{PU} \frac{A_{PU}}{A_{tot}} + E_{PP} \frac{A_{PP}}{A_{tot}} \quad (3)$$

$$E_{eq} = 22 \frac{550 * 10 - 54\pi}{550 * 10} + 1200 \frac{54\pi}{550 * 10} = 58 \text{ MPa} \quad (4)$$

- $E_{eq}$  = Equivalent E-modulus
- $E_{pu}$  = E-modulus of polyurea
- $E_{pp}$  = E-modulus of polypropylene
- $A_{pu}$  = Cross sectional area of polyurea
- $A_{pp}$  = Cross sectional area of polypropylene
- $A_{tot}$  = Cross sectional area of total PU+PP-mesh layer

The same principle can be used to calculate an equivalent yield stress for the homogenised layer. With PP and PU having a yield stress of respectively 21 MPa and 11 MPa. The equivalent yield stress is about 11 MPa. It is so close to the yield stress of PU because only about 3% of the homogenised layer is PP. For the E-modulus this effect is larger because the difference between the E-modulus for PP and PU are relatively large. It should be noticed that these material properties have not been found by material tests and are only available from datasheets and literature. Therefore there is uncertainty in these values and so these values are taken into consideration in the calibration phase.

### *Bond-slip*

From the Quake-Shield tests and literature study (paragraph 2.4.1) it is clear that the adhesive that bonds the FRP to the masonry plays an important role in the behaviour of the masonry wall [24]. Material tests are conducted by the TU Eindhoven (TU/e) on the adhesive (NSM FRP strip to masonry) that is used for Quake-Shield. TU/e used a pull-out test to determine the bond-slip behaviour of the embedded NSM CFRP strip. The manufacturer of the adhesive has limited material properties available so these types of tests are required to get proper material properties for the FEM models.

Slip as in bond-slip has different meaning compared to slip as in material science. In material science slip is the movement of atoms along each other in a certain plane (slip-plane) [47]. This type of slip is permanent deformation or could be considered plastic deformation. In the bond-slip curve the first linear part could still be in the elastic zone of the adhesive, especially if it is a ductile adhesive. So when slip is mentioned in this thesis it is about the bond-slip behaviour and slip is thus considered as a relative displacement between two materials (in this case masonry and FRP strip).

## 4.2 Pull-out of NSM CFRP strip

### 4.2.1 Pull-out test results

Six samples with different bond-length were tested during the first series of the pull-out tests by the TU/e. Figure 59 shows a sample with a bond length of three rows of bricks. Also full bond length (230mm) (four rows) and two rows bonded were tested [46].



Figure 59: A sample from the pull-out tests performed by the TU/e [46]

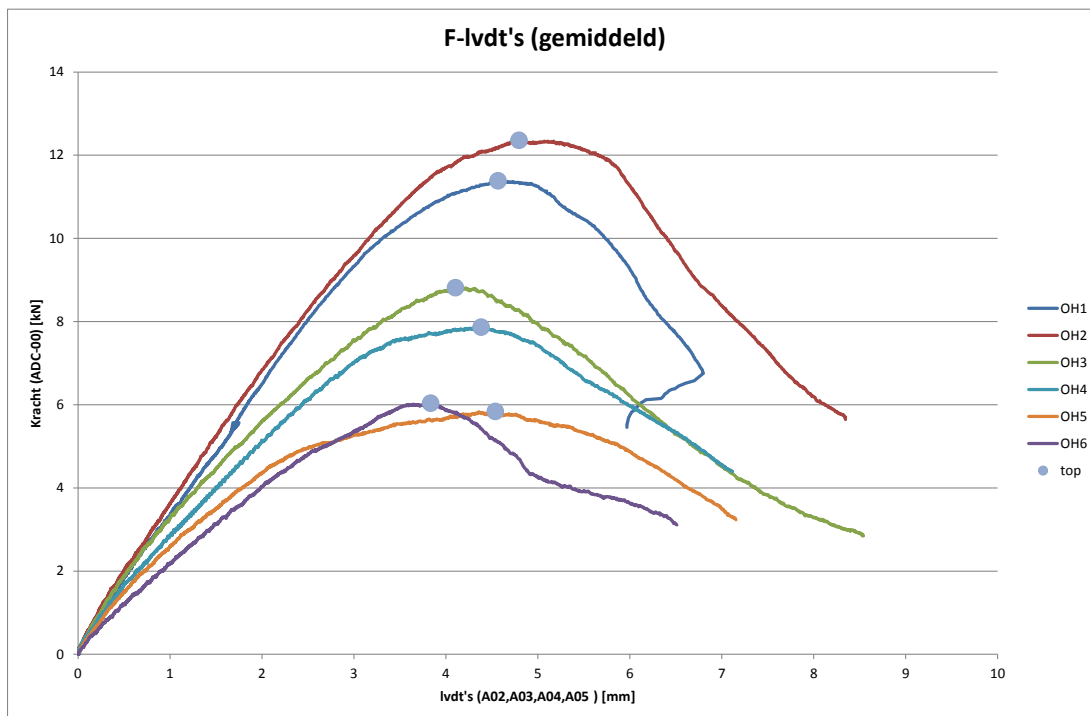


Figure 60: Pull-out test results from 6 samples with 3 different bond lengths [46]. Bond length: OH1/2= 230mm, OH3/4= 175mm, OH5/6= 115mm [46].

The results show a linear correlation between the bond-length and pull-out force. The ratio is 50,36 between the force (in kN) and bond-length (in m).

The adhesive used with Quake-Shield is rather ductile (rubber like). Therefore it is assumed the shear stress distribution along the length of the CFRP strip could be considered uniform. During the first

series of pull-out tests by the TU/e no strain gauges were used so this assumption could not be confirmed with this test.

In literature usually a much stiffer epoxy is used to bond the NSM FRP strips to the masonry. Strain gauges are necessary in this case to translate the pull-out test results to a bond-slip diagram which is required in the FEM model [24]. Figure 61 shows an example of the pull-out test results where strain gauges were used in combination with an epoxy adhesive. It is clearly visible that there is no uniform shear stress distribution along the CFRP strip because at a certain load the shear stresses are not the same at every location along the strip.

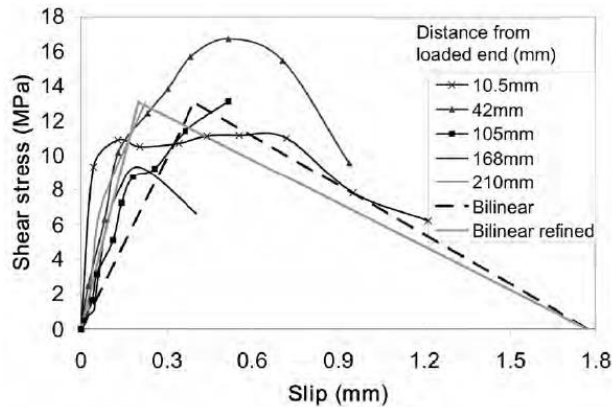


Figure 61: Example of bond-slip curves fitted with a bi-linear curve to be implemented in a FEM model [24]

With the uniform shear stress distribution as assumed with the Quake-Shield adhesive a simple translation (force divide by CFRP strip bond area) from the force-displacement curve to a shear-displacement (slip) curve can be made. The slope of the initial linear part of the latter curve is also the value for  $K_t$ .

#### 4.2.2 Pull-out FEM model

A FEM model based on the pull-out test is used to calibrate the bond-slip behaviour of the NSM CFRP strip. The properties that are calibrated with this model are  $K_t$  and the values for the TAUDIS diagram (curve). The height of the prism is 230 mm (four bricks) by 111,25 mm (half a brick) by 100 mm. The mortar interface elements are removed because in this load case these interfaces will not contribute to the bond-slip behaviour of the CFRP strip in the adhesive (recommended by Petersen [24]). Material properties from Table 7, Table 9 and Table 10 are used for or derived from the pull-out test model.

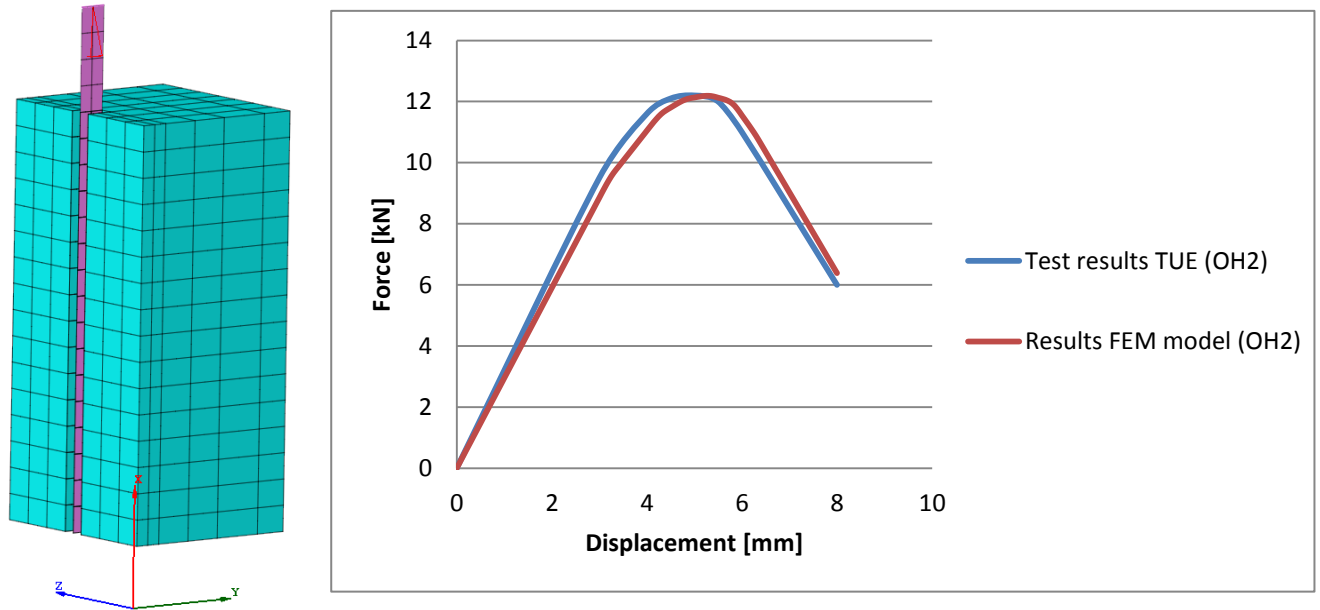


Figure 62: Pull-out test FEM model geometry (left). Test results OH2 compared to FEM model results (right).

First it was tried to find values for a bi-linear bond-slip curve for the TAUDIS diagram to simulate the pull-out test results of the TU/e. It appeared that due to the low  $K_t$  value there is a uniform shear distribution along the length of the NSM CFRP strip. This results in that the shape of the force-displacement curve (result of FEM model) is the same shape as the shape of the TAUDIS curve.

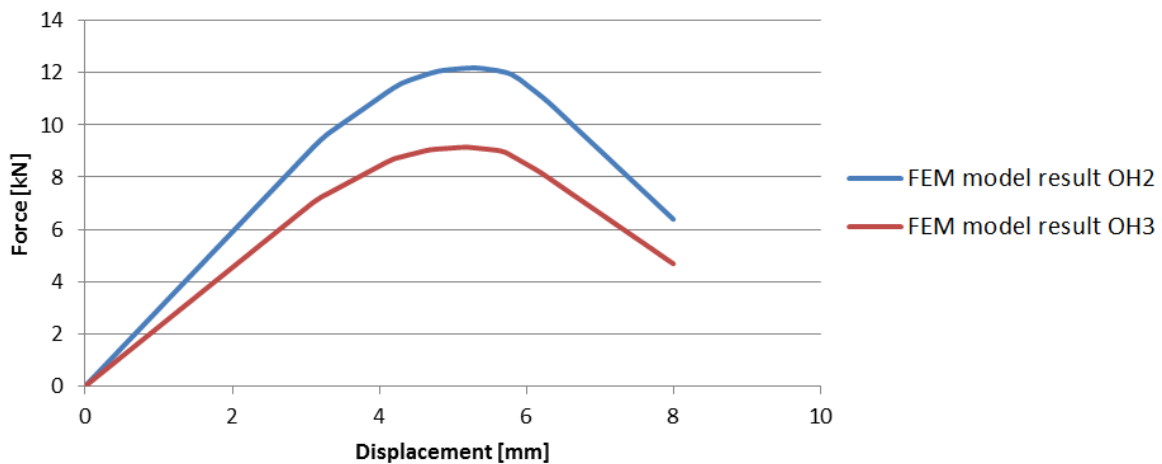


Figure 63: Comparison FEM model results with different bond-length (OH2=230mm, OH3=172,5mm)

Test sample OH3 has a 57,5 mm shorter bond length compared to OH2 (172,5 mm vs 230 mm). The FEM model is verified by changing the model to the geometry of the OH3 test sample bond-length. The result of the OH3 FEM model is compared to OH2 FEM model in Figure 63. The peak load is about 9 kN which is also the case for the test results of OH3 (Figure 60). The peak force of OH3 in the test results is at about 4 mm displacement (Figure 60). In the FEM model results of OH3 the peak is not shifted to the left and is around 5 mm displacement.

In the pull-out test results (Figure 60) it is visible there is a shift in displacement at peak load if the bond length increases. Taking a linear trend line through the peaks of the six test samples it can be assumed that with a bond length of about 800mm (length of OP bend Quake-Shield samples) the peak force is at 43 kN (linear correlation found in the test results) and with a displacement of about 8mm.

Scaling up the Pull-out test model to a length of 800mm it appeared that the peak of the TAUDIS curve had to be shifted 1 mm to the right. This automatically also changes the slope of the TAUDIS curve and thus also the Kt value. The Pull-out test FEM model results show now a displacement of 8 mm at a peak load of 41kN (Figure 64).

The pull-out tests were stopped at 8 mm displacement and not tested until complete failure. How the pull-out test curve continues after 8 mm (10 mm in the calibrated pull test model in Figure 64) is therefore unknown at this point. The TAUDIS curve needs an extension to work properly so it is estimated, based on how the curves of the test results were developing, to take a gradually decreasing linear slope after 10 mm displacement. The TAUDIS curve (Figure 57) calibrated with this model is used for the FEM model based on the Quake-Shield OP bend tests.

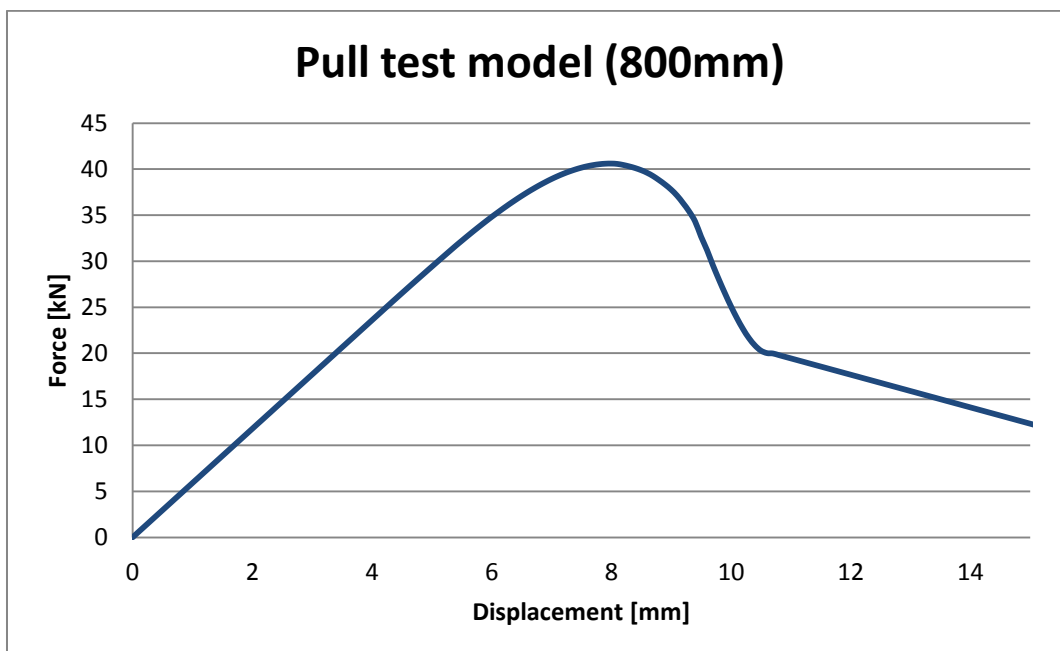


Figure 64: Results from FEM model with a bond length of 800mm and a shift in the TAUDIS curve of 1 mm for displacement

### 4.3 FEM model sensitivity study

A sensitivity study is done to get a better understanding of the effect of certain parameters on the behaviour of the model. From literature and experience it is assumed that the following parameters have a significant effect on the behaviour of the model: Kt of the adhesive and the corresponding TAUDIS curve, E-modulus of the NSM FRP strip, E-modulus of the brick and of the EB FRP layer, tensile strength and Kn Kt values of the mortar interface.

It should be noticed that the sensitivity study was performed to develop knowledge about the behaviour of the model by changing certain parameters. The model has improved in certain ways during the project. The model version used for this sensitivity study did not yet include non-linear behaviour for the bricks, EB FRP layer and the TAUDIS curve shift from the 800 mm pull-out test model. Therefore Kt of the adhesive in this model is  $0,46 \text{ N/mm}^3$ . The sensitivity study is still useful for the purpose of developing knowledge about the model and find out which parameters are sensitive by comparing different values for a certain parameter.

#### *Effect Kn Kt value & TAUDIS curve adhesive and E-modulus of NSM FRP strip*

Figure 65 shows the effect of Kt and corresponding TAUDIS curve on the behaviour of the model. Kt is the slope of the first linear part in the TAUDIS curve and so these parameters are connected.

Results Kt65 ( $K_t=65 \text{ N/mm}^3$ ) and 'E-mod FRP' in Figure 65 are based on the bond-slip curve from the research of Petersen [24]. This is a stiff epoxy that gives a sharp drop in force-displacement curve when the NSM CFRP strip debonds. The rising curve after the drop is caused by the linear elastic modelled EB FRP layer. Kt0,46 ( $K_t=0,46 \text{ N/mm}^3$ ) results are TAUDIS values based on the pull-out tests of the TU/e. The more ductile adhesive gives an overall stiffness reduction. This is visible for the displacement which increases 167% compared to the stiffer epoxy used in the Petersen research. The peak load drops 16% and less sudden debonding of the NSM CFRP strip is observed. The result of 'E-mod FRP' is the effect of reducing the E-modulus from 165000 MPa to 66000 MPa (2,5 times). This results in a 50% displacement increase.

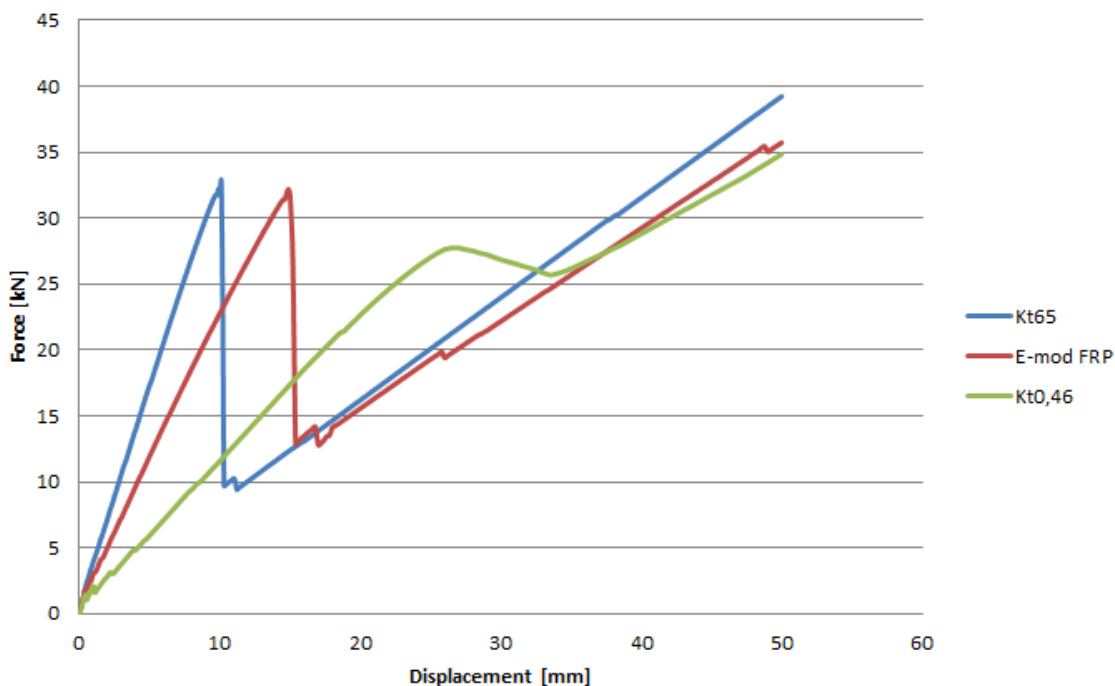


Figure 65: Model behaviour comparison, effect of Kt & TAUDIS curve, effect of E-modulus of CFRP strip

### Effect E-modulus of brick and EB FRP layer

The sample contains 14 bricks in the length direction of the masonry sample. It is assumed that the E-modulus of the bricks will have effect on the overall stiffness of the model. FEM model result of 'E-mod brick' in Figure 66 is the effect of two times higher E-modulus compared to the results of the model 'Kt0,46'. The peak load is increased by 13%.

Increasing the E-modulus of the EB FRP layer two times gives a significant increase in overall strength and stiffness but also reduces the effect of the bond-slip of the CFRP strip (E-mod EB FRP, Figure 66) . The EB FRP layer becomes in an earlier stage the primary load carrying reinforcing material and so the drop at the peak is no longer present. The peak load cannot be determined like in the other curves. If the peak load is estimated around 40 kN this will result in a 44% strength increase due to a two times higher E-modulus of the EB FRP layer.

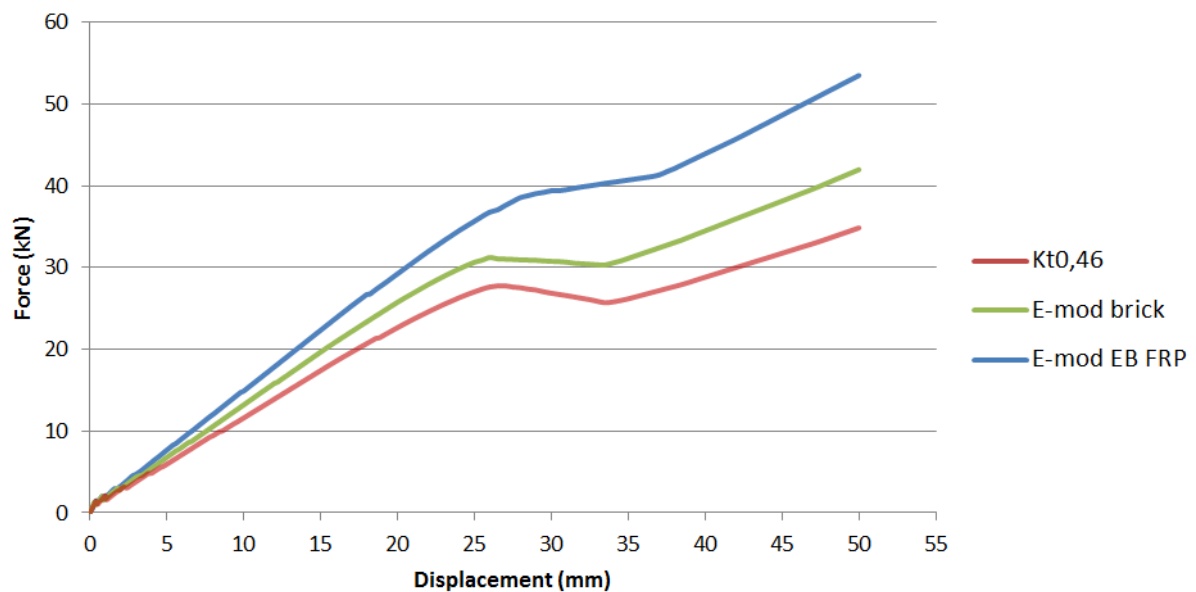


Figure 66: Model behaviour comparison, effect of E-modulus brick and EB FRP layer

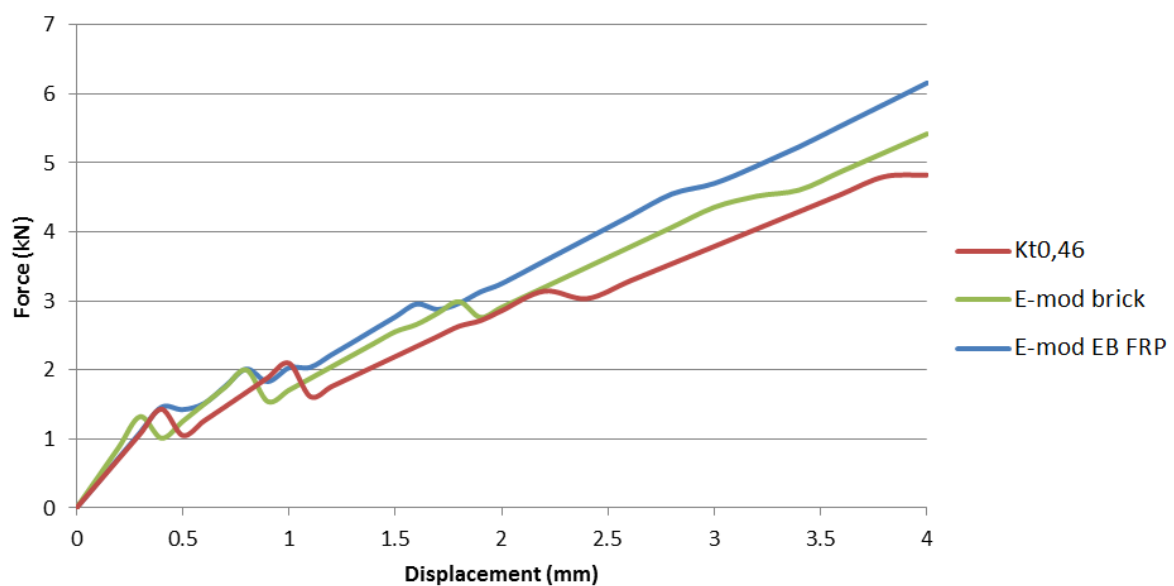


Figure 67: Same force-displacement curve as Figure 66 but only the first 4 mm displacement



### Effect of mortar tensile strength

In Figure 68 the effect of increasing the tensile strength of the mortar two times is shown. The increase in tensile strength does not have a significant influence on the overall behaviour of the model. Figure 69 shows the results of the first 4 mm displacement of the force-displacement curve. During opening of the first cracks the effect of the increased mortar tensile strength is visible. The stiffness stays about the same but the force and displacement at which the cracks initiate is increased. The load for the first crack initiation is increased 125% and 100% for the second crack. Because the stiffness stays about the same these percentages also apply for the displacement increase.

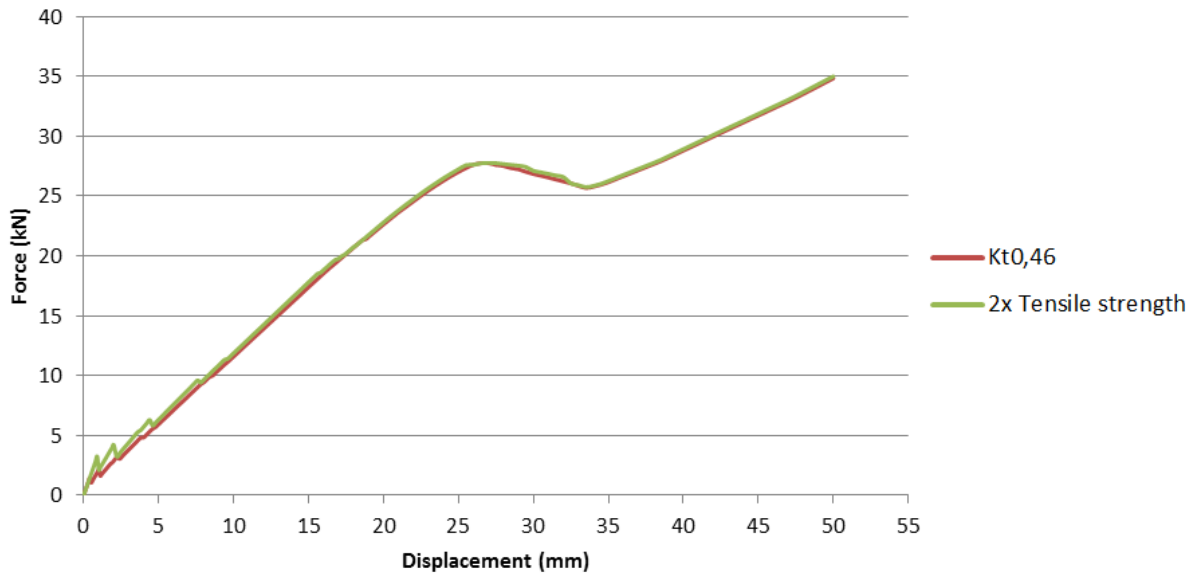


Figure 68: Model behaviour comparison, effect of mortar tensile strength

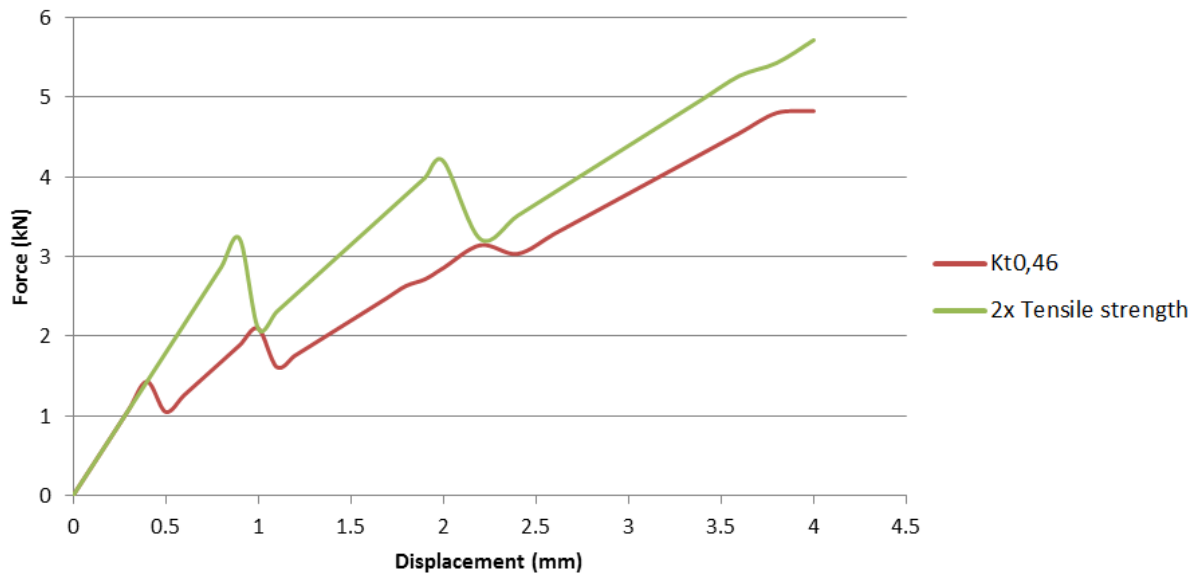


Figure 69: Same force-displacement curve as Figure 68 focused on the first 4 mm displacement

### *Effect of Kn Kt value for mortar non-linear interface*

During OP bending of the masonry sample the mortar is mainly loaded in tension. Therefore the Kn value has more influence on the stiffness and crack opening of the mortar compared to Kt. Results of the FEM model 'Kn60' has a Kn value of 60 N/mm<sup>3</sup> (Figure 70). Comparing the overall behaviour of the model if the Kn value is increased or reduced two times gives a small difference in stiffness. Reducing Kn two times (Kn30) gives a displacement increase of 15% at peak load and increasing the Kn value by two times (Kn90) gives a displacement decrease of 4% at peak load. The peak load is considered to be the horizontal plateau of the curve.

Figure 71 shows the effect of Kn on the crack initiation in the first 4 mm displacement. It is also visible that the Kn value not only has effect on the stiffness of the mortar but also on the force required to initiate the first crack in the mortar. With a higher value for Kn the stiffness is increased but the force required to initiate the first crack is reduced. The force required for crack initiation of the first crack is increased by 13% for 'Kn30' and decreased by 22% for 'kn90'. The initial stiffness before crack initiation is increased by 29% for 'Kn90' and decreased by 43% for 'Kn30'.

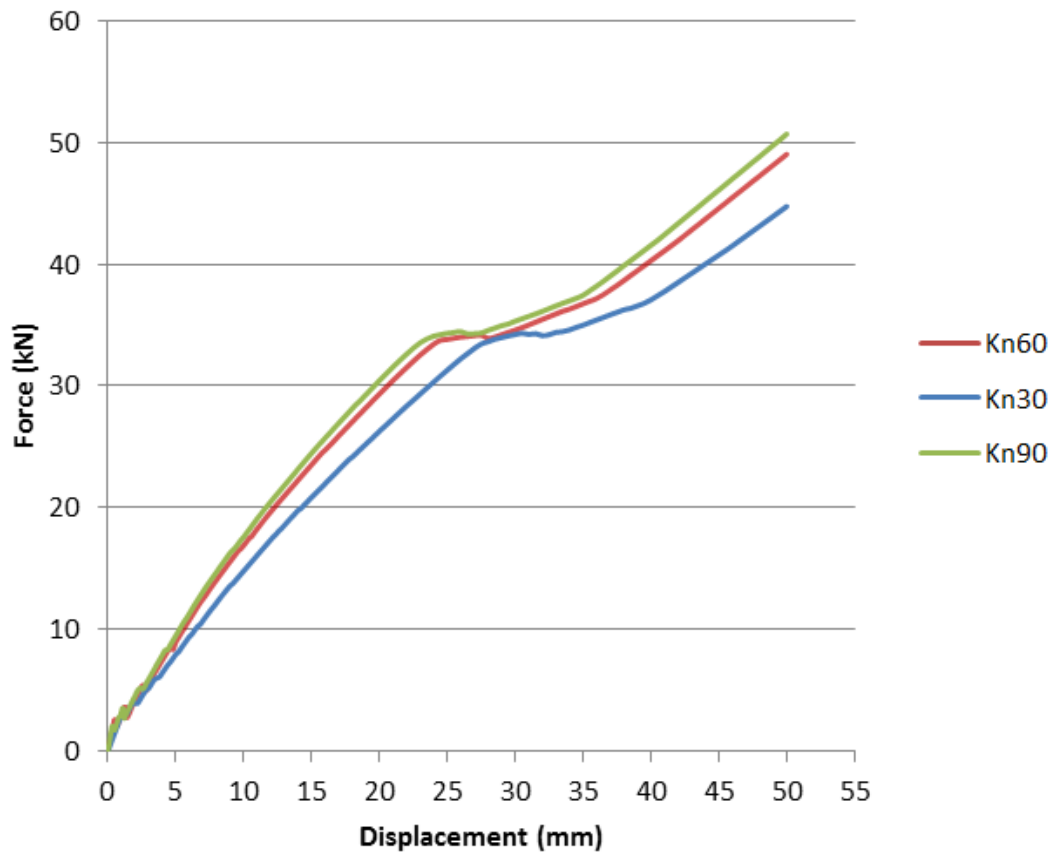


Figure 70: Model behaviour comparison, effect of Kn value if increased or reduced two times

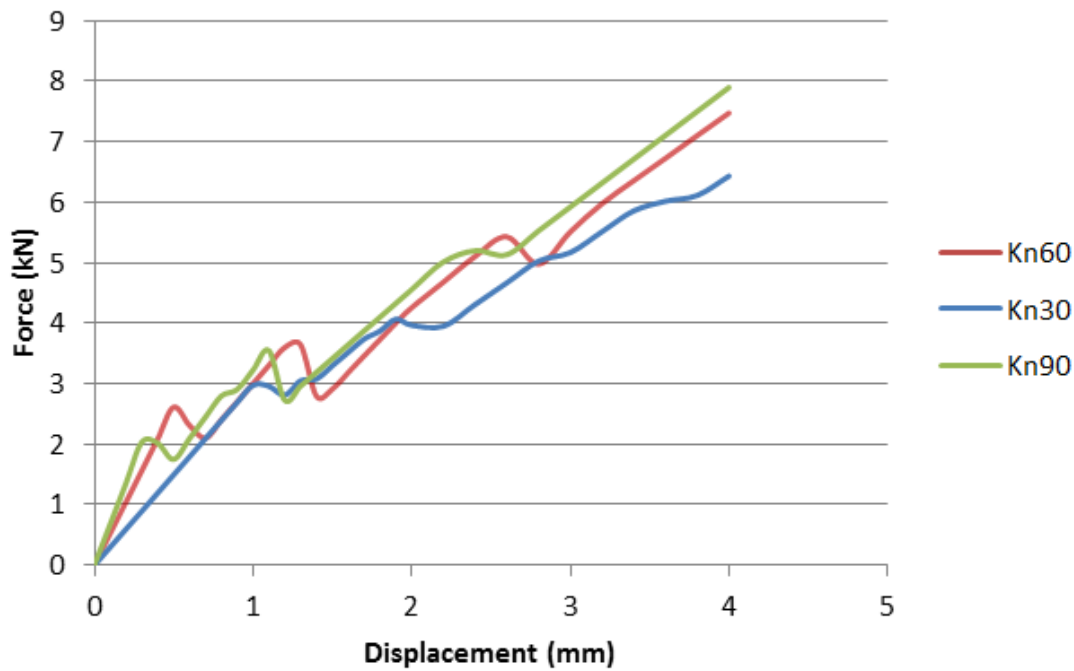


Figure 71: Same force-displacement curve as Figure 70 focused on the first 4 mm displacement

From this sensitivity study it can be concluded that the ductility of the adhesive has a large influence on the overall stiffness of the sample. By using a ductile rubber-like adhesive as used by Quake-Shield gives a 167% displacement increase compared to the stiffer epoxy used by Petersen. Using epoxy as adhesive and reducing the E-modulus of the FRP strip 2,5 times results in a 50% displacement increase.

Increasing the E-modulus of the EB FRP layer two times gives an overall strength increase of 44%.

Material properties for the mortar have mainly influence on the sample behaviour in the first 4 to 5 mm displacement. It contributes to the behaviour of initiation of the cracks. Doubling the tensile strength of the mortar will increase load at crack initiation and displacement, for the first and second crack, by respectively 125% and 100%.

Kn and Kt of the mortar contributes to the initial stiffness of the sample before the first crack initiates. This difference in initial stiffness affects also the load and displacement of the initiation of the first crack. Lowering the initial stiffness 43% results in a 15% displacement increase at peak load.

## 5 FEM model calibration & results

This Chapter contains the FEM model calibration and results of the calibrated FEM Base model compared to the test results of the Quake-Shield OP bend test.

### 5.1 FEM model calibration

As explained in paragraph 4.1.3 some material properties are uncertain due to unavailable or incomplete material property data. Some of these material properties are estimated from literature and act as reference values. In this paragraph some of these values are adjusted to get a better model result fit compared to the sample test result.

As expected and described in paragraph 4.1.3 the  $K_n$  and  $K_t$  value for the mortar interface are too high and therefore reduced to  $35 \text{ N/mm}^3$  and  $16 \text{ N/mm}^3$  for respectively  $K_n$  and  $K_t$ .

During the sensitivity study and the calibration process the EB FRP layer appears to have a reasonable influence on the overall model stiffness and influence on the peak load. By homogenising the PU and PP-mesh into a single EB FRP layer it could be that the values are overestimated both for E-modulus and yield stress. Only 3% of the EB FRP layer is PP and it could be that the iso-strain state assumption puts a too large contribution of PP properties into the homogenised EB FRP layer. Therefore it could be that taking properties closer to the PU properties is more appropriate. Material tests on the EB FRP layer could give relevant information about these material properties for modelling. Just like the pull-out tests performed by the TU/e give better insight into the mechanical behaviour of the adhesive.

The values for the E-modulus and yield stress are reduced to get a better fit compared to the sample test result. The values used are 21 MPa and 4 MPa respectively for E-modulus and yield stress of the EB FRP layer.

The E-modulus used for the EB FRP layer in the FEM model is a constant value for the first linear part. While in general a soft polymer, like in this case PU, has a relatively high initial stiffness but levels off when approaching yield stress as shown in Figure 72 (general soft polymer stress-strain curve [48]). The 'FEM EB FRP layer' curve is calculated by homogenizing the PU and PP in a single EB FRP layer as described in paragraph 4.1.3. To reduce the overestimation of the E-modulus of the homogenised polymers the secant E-modulus of PU is taken. This is 8 MPa instead of 22 MPa, this reduction of factor 2,75 is also used for the PP. Recalculating the homogenised EB FRP layer gives now an equivalent E-modulus of 21 MPa.

The same reduction factor is used for the yield stress and goes from 11 MPa to 4 MPa. This yield stress value gives a better fit for the onset of linear to non-linear transition in the force-displacement curve. Table 11 shows the material properties that have been changed during the calibration process.

Table 11: Adjusted material properties

Material properties of:	Normal stiffness modulus (Kn)	Shear stiffness modulus (Kt)
Mortar non-linear (interface)	35 N/mm <sup>3</sup>	16 N/mm <sup>3</sup>
Material properties of:	Young's modulus (E-modulus)	Yield stress
EB FRP layer (curved-shell)	21 MPa	4 MPa

In Figure 72 it is noticeable that the stress-strain curve in the FEM model stays at a constant yield stress and does not show hardening like soft polymers do. The hardening of polymers happens because of the alignment of polymer chains in the load direction. The amount of cross-links in the polymer determines the degree of hardening. This material effect is not included in the FEM model.

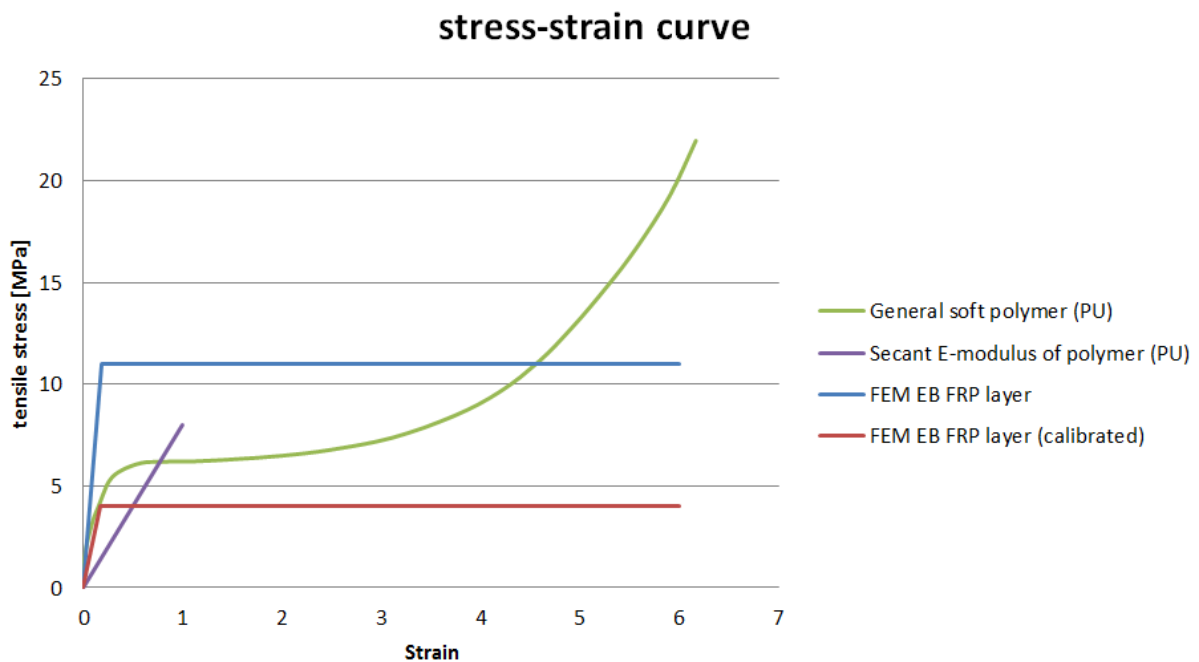


Figure 72: Stress-strain curve of PU and EB FRP layer used for the FEM model. (general soft polymer curve, source: [48])

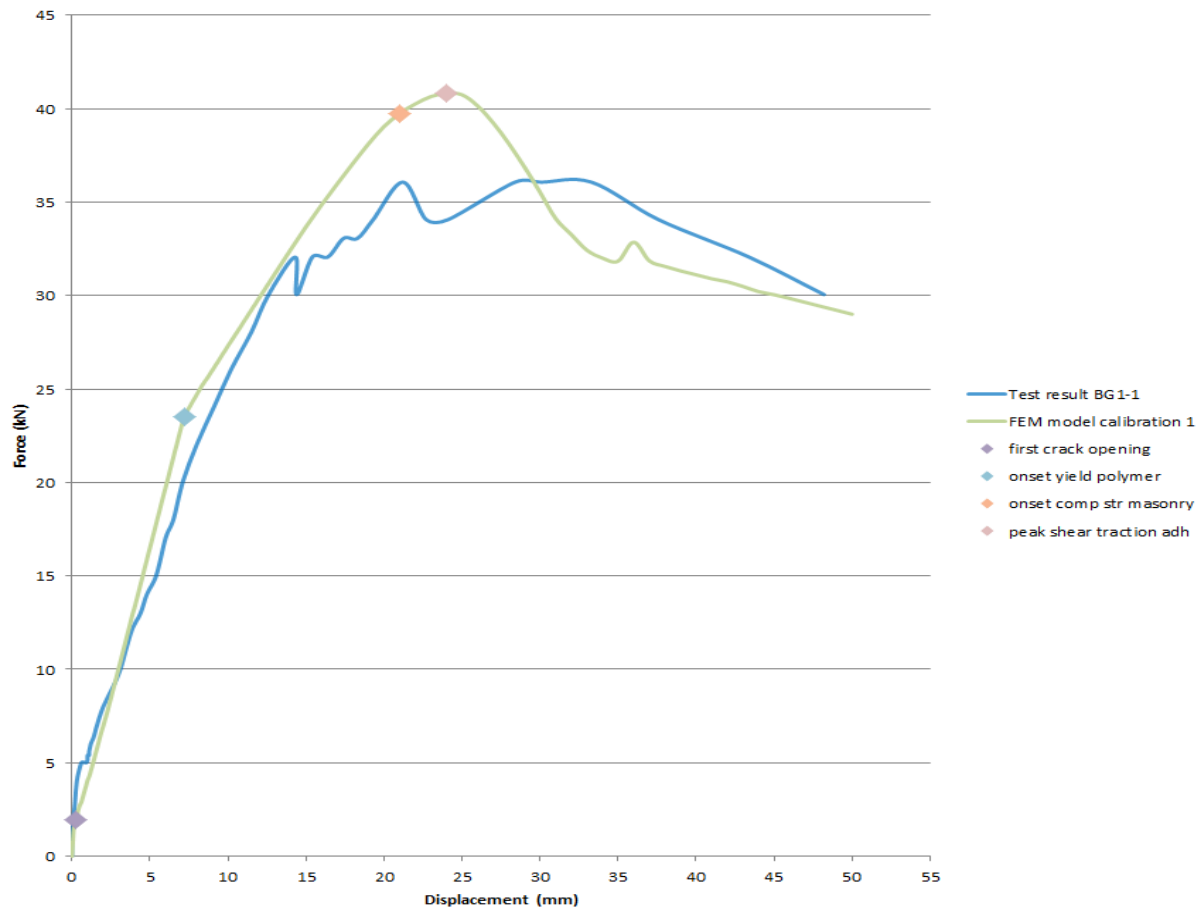


Figure 73: FEM model results after first calibration phase compared to test results of sample BG1-1

Figure 73 shows the result of the FEM model with the adjusted material properties from Table 11. The overall behaviour seems to be correct when comparing FEM model result with the test result of sample BG1-1. The peak load is 11% higher for the model compared to the test result.

The deflection from linear to non-linear behaviour at 7,2 mm displacement in the model result is the onset of yielding of the EB FRP layer. The onset of reaching ultimate compression strength of the masonry is less clear in the model result graph but takes place at 21 mm displacement. Yielding of the EB FRP layer in the test sample is hard to determine with the available information however compression failure of the masonry should initiate close to 15 mm displacement (first local peak in test result).

The displacement at peak load in the model result is also the point when the shear traction of the NSM CFRP strip in the adhesive reaches its maximum value which is also the peak of the TAUDIS curve.

From the first calibration it can be assumed the masonry has a too high compression strength. Also when looking closer to the initiation of the first crack it appears that the first crack in the model initiate at 1,4 kN instead of 5 kN. Both compression strength of the masonry and tensile strength of the mortar are adjusted. Adjusted material property values are shown in Table 12.

**Table 12: Adjusted material property values for brick1 and brick2 and mortar [15]**

<b>Material properties of:</b>	<b>Tensile strength</b>	<b>Fracture energy</b>
<b>Mortar non-linear (interface)</b>	0,6 N/mm <sup>2</sup>	0,017 N/mm
<b>Material properties of:</b>	<b>Compressive strength</b>	<b>Compressive fracture energy</b>
<b>Brick 1</b>	10 MPa	19 MPa
<b>Brick 2</b>	10 MPa	23 MPa

The tensile strength is adjusted to 0,6 MPa. This results in the first crack initiation at about 4 kN. In the book of structural masonry [15] it is indicated that a significant difference in calculated tensile strength from a tensile test could be found if not the gross cross sectional area of the brick, connected to the mortar, is taken but the net (real) cross sectional area. This actual bonded area increase the calculated tensile strength from, for example a mortar with 0,26 MPa (gross), to 0,56 MPa (net) [15]. So the 0,6 MPa tensile strength compared to the measured 0,2 MPa could be possible. Increasing the tensile strength of the mortar to 0,6 MPa results in first crack initiation at 4 kN instead of 1,4 kN.

The compressive strength of the brick is reduced until the displacement at which compressive strength is reached is close to 15 mm displacement. This is where in the test result the onset of compression failure is assumed to take place. Compressive fracture energy is dependent of the compressive strength and calculated with use of equation ( 2 ) which can be found in paragraph 4.1.3.

The initial value for compressive strength is from compression tests performed by the TU/e. The samples were made at a different time and so maybe under different conditions compared to the samples from the three point bend test. Conditions during manufacturing of the materials and masonry itself have an effect on mechanical properties of the masonry. Therefore the variation in masonry testing is high and so using a lower value for compressive strength for the model is possible. With a compression strength of 10 MPa the masonry reaches this value close to 15 mm displacement. The deviation from the graph of calibration 1 is visible at this displacement (Figure 74). By lowering the compression strength of the masonry also the peak load reduces by 5 % compared to the peak load of calibration 1 graph.

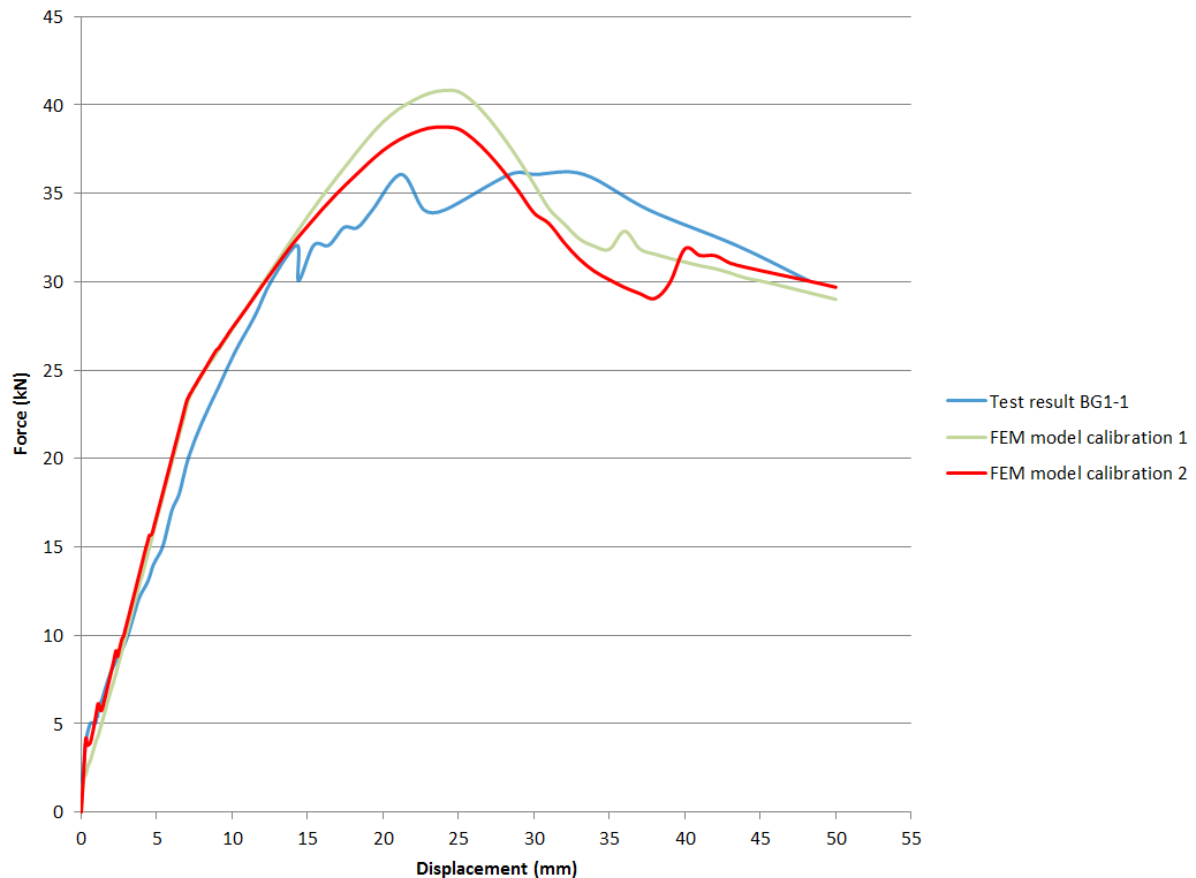


**Figure 74: FEM model results of calibration 1 and calibration 2 compared with the test result**

In Figure 74 the curve of FEM model calibration 2 shows a sudden upward deflection around 40 mm displacement. At this point there is a relatively large shift noticed in the mortar interface closest to the mid-plane of the FEM model. This shift is in the downward shear direction of the mortar interface. Increasing  $K_t$  does not prevent this effect and it is likely this effect occurs due to the fact the model tries to find equilibrium in both normal and shear direction. If it could not find it in the normal direction in the interface it tries to compensate in the shear direction. Normal and shear traction are not coupled parameters in the FEM model while in reality the load in normal direction influences the shear capacity.

Since it is an after the peak effect it is a less critical effect in the FEM model and therefore this sudden upward deflection should be ignored for the rest of the model results presented in this thesis. The curve could be assumed to continue in the same decreasing slope as just before the upward deflection. Because already activated material failure continues to progress but no new onset of material failure is found in the model or during testing in the presented displacement range.

The FEM model that produces the result of FEM model calibration 2 is from now on the result of the FEM Base model. The FEM Base model is used for the configuration analysis (Chapter 6). The result of the FEM Base model is compared to the test result more elaborated in the next paragraph.



## 5.2 FEM Base model results

Figure 75 shows the FEM Base model result compared to the test result of sample BG1-1. The overall behaviour of the model fits with the test result although there are still some points that deviate.

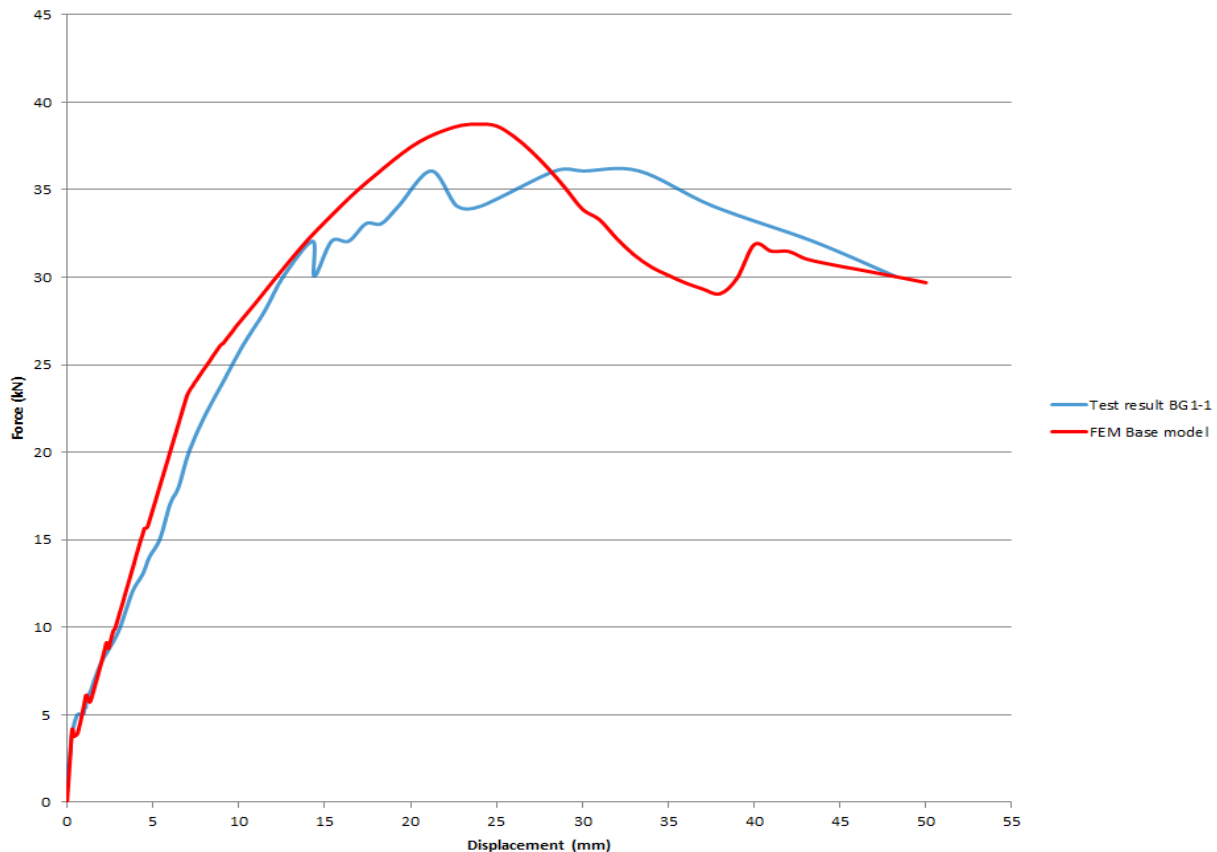
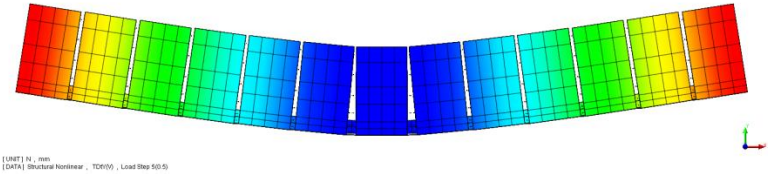
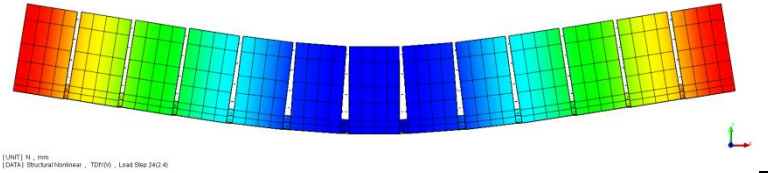
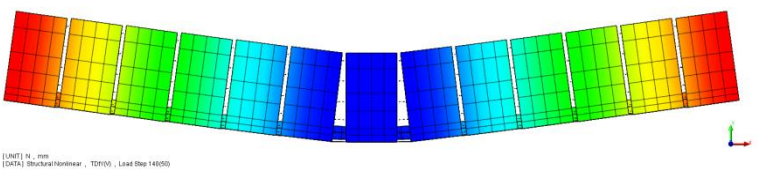


Figure 75: FEM model result compared with test result

The initial stiffness is about the same for the first 3,5 mm displacement. After this point the curve of the model result starts to deviate showing a higher stiffness. The test result shows more non-linear behaviour while the model is still in the linear elastic zone of both the EB FRP layer and masonry. After 7,2 mm displacement the EB FRP layer starts to yield and the model starts also to show non-linear behaviour. At 15 mm displacement the masonry reaches its ultimate compression strength. Compared to the model result the test result shows extra loss of stiffness after 15mm displacement. This is probably caused by the progression of compression failure of the masonry at the top side of the sample. The loss of stiffness after 15mm displacement is more gradually developing in the model. The peak load in the model is 8% higher compared to the peak load of the test result. At the peak load in the model also the shear traction of the CFRP in the adhesive has reached its ultimate strength. After this point the shear traction starts to reduce with increasing displacement resulting in a reducing load capacity at increasing displacement. The test result does not show a distinct peak load. The peak load is maintained (with a small 2 kN drop and then goes back to peak load) over a wider displacement range before decline of the load capacity really sets in.

Crack initiation starts in the mortar interfaces around the middle of the sample where the displacement is the highest and where also the tensile stress at the bottom of the sample is the highest. Table 13 shows three figures how the cracks develop at three different displacements.

Table 13: Crack opening at different displacements

 <p>[UNIT] N , mm [DATA] StructuralNonlinear , TDR050 , Load Step 5005</p>	0,5 mm displacement: initiation of the cracks at the left and right side of the middle brick
 <p>[UNIT] N , mm [DATA] StructuralNonlinear , TDR050 , Load Step 2424</p>	2,4 mm displcamenet: cracks open to the left and right side of the middle three bricks
 <p>[UNIT] N , mm [DATA] StructuralNonlinear , TDR050 , Load Step 14050</p>	50 mm displacement: all cracks have been closed except the cracks to the left and right side of the middle brick. All the crack opening that have been formed is now relocated in these two cracks

In the model most of the mortar interfaces are opened in the first 5 mm displacement where in the test sample the second crack in the mortar interface (counted from the middle brick) initiate around 5 mm displacement. Cracks form in the test sample mainly at the mortar interfaces connected to the middle three bricks (Figure 76). The brick rows to the left and right side of the three middle brick rows could be considered as undamaged masonry. From the available information it seems no cracks have formed in the interfaces of these sections of masonry.



Figure 76: Test sample (BG1-1) at 24,1 mm displacement [43]

From 7,2 mm displacement the onset of yielding of the EB FRP layer takes place, shown in Figure 77. The locations of highest stresses in the EB FRP layer are at the mortar interfaces due to crack opening in the masonry. In Figure 77 both figures are from the location of the first and second mortar interface counted from the middle brick. The fourth row of elements from the top shows a different stress, this is where CFRP strip is located. This CFRP strip resists the opening of the crack locally and therefore also reduces the stress in the EB FRP layer.

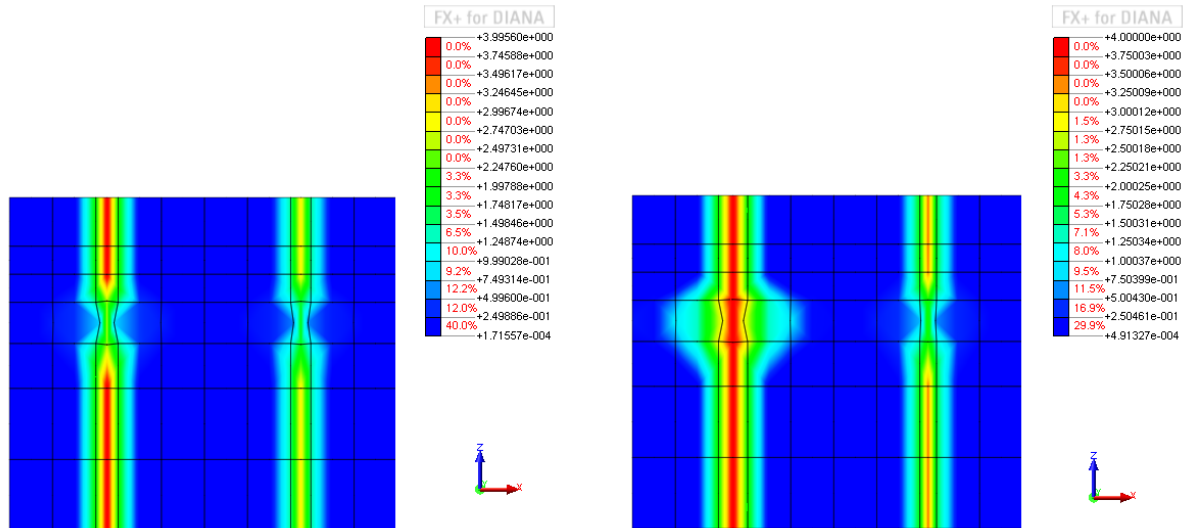


Figure 77: Von Mises stress (in MPa) in the EB FRP layer at 7,2 mm displacement (left) and 24 mm displacement (right). Both figures are from the location of the first and second mortar interface counted from the middle brick. This section is only a half brick width and where the CFRP is located (different stress level).

One of the critical failure modes of the sample is the compression failure at the top of the sample. Figure 78 and Figure 79 show the stress distribution at the top of the FEM model. The stress is mainly concentrated at the mortar interface on the left and right side of the middle brick. Figure 80 shows compression failure at the top of the test sample. Horizontal cracks are visible which is splitting of the masonry caused by a too high compression load. In the test sample the compression failure is more spread over the three middle bricks instead of the single middle brick in the model.

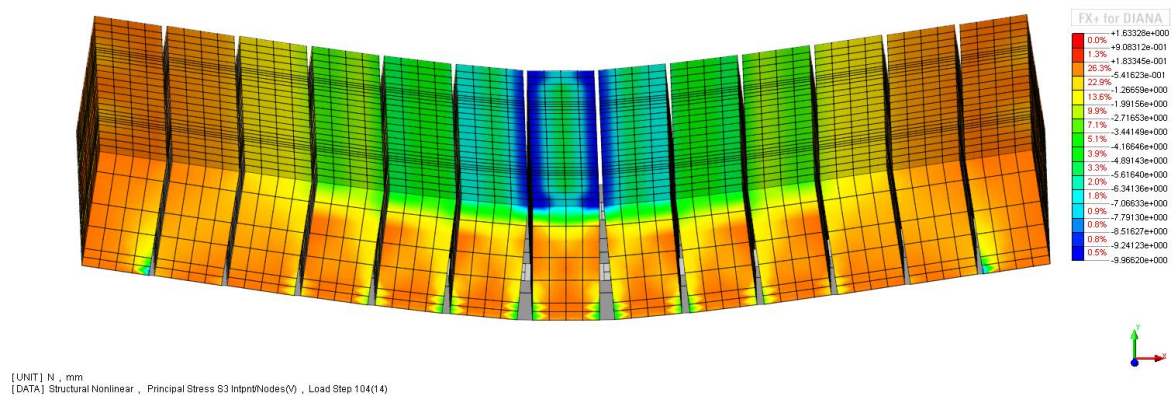


Figure 78: Stress distribution in top side of bricks at 14 mm displacement where the masonry reaches its ultimate compression strength (dark blue) (stress in MPa)

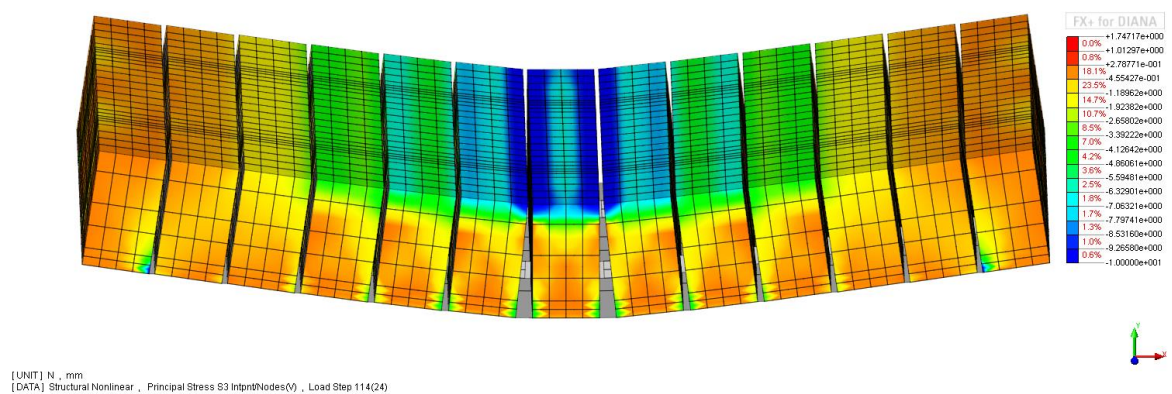


Figure 79: Stress distribution in top side of brick at 24 mm displacement (peak load). Stress is mainly concentrated to the left and right side of the middle brick (stress in MPa)



Figure 80: Test sample (BG1-1) at 33,4 mm displacement [43]

### 5.3 Discussion of FEM Base model results

After the second model calibration the model shows a good fit with the test result of BG1-1 but still has some deviations. From the initiation of the first crack till the onset of yield of the EB FRP layer the model shows close to linear behaviour. This is due to the linear elastic behaviour of the EB FRP layer and the adhesive that bonds the NSM FRP strip to the masonry. Based on the results of the sensitivity study it can be assumed the EB FRP layer is the dominant factor to the overall stiffness of the model in this displacement range.

After the onset of yielding of the EB FRP layer the NSM FRP strip takes over and stiffness of the model is reduced. The non-linear bond-slip behaviour of the adhesive before and after the peak load shows similar behaviour as the TAUDIS curve. This correlation was also found with the pull-out test model in paragraph 4.2 and is the result of the ductility of the adhesive. This ductility gives a uniform shear stress distribution between the NSM FRP strip and the adhesive. Which results in more ductile behaviour after the peak load and a more gradually loss of load bearing capacity. Ductile behaviour after peak load will increase the energy absorption and dissipation of the reinforced masonry and is important for earthquake resistant building (paragraph 2.3.1).

The model shows a more distinct peak load compared to the test result which has more of a peak load plateau. Likely compression failure in the top of the sample in combination with the reinforcing measures at the bottom result in this plateau. The masonry continues to fail in compression while the NSM CFRP strip and EB FRP layer are still carrying load and keeping the masonry together. Also imperfection in the test sample and test setup can play a role in this behaviour (paragraph 3.5). For example bond-slip behaviour due to improper bonding of the EB FRP layer to the masonry and indenting of the rubber support strips that influence displacement measurements. For proper bonding FRP to masonry multiple conditions should be considered which is described in more detail in paragraph 2.3.6.

Compression failure and crack opening in the model take place near the middle brick where in the test sample it is more spread over the three middle bricks. This could be caused by shear effects or imperfections in the masonry. By using the non-linear discrete cracking material model for the mortar interfaces some shear properties are lost compared to the CCSC material model. With the CCSC model effects like dilatancy are taken into account.

Cracks will form at the weak locations in the masonry. This is usually the mortar brick interface. Masonry is known for its large variation in mechanical properties for example due to manufacturing conditions. The mortar interfaces in the model could be considered perfect bonded and do not have 'random' weak spots. The mortar interface in the model open if the ultimate tensile strength is exceeded. The tensile strength is the highest at the bottom of the middle brick and therefore the cracks will open in the mortar interface closest to the middle brick. This is also caused by the way a slap or in this case the masonry sample is supported. The support of the three point bending test determines where the load concentration will be in the sample with corresponding failure modes (paragraph 2.2). But also the location of the sample on the test setup supports influences load introduction in the sample and failure behaviour of the sample. During testing location of the sample was done with the naked eye and not measured out accurately.



## 6 Quake-Shield configuration analysis

A configuration analysis is done to get more insight in the behaviour of Quake-Shield reinforced masonry and gain more knowledge about the FEM model. In this configuration analysis individual or sets of parameters are changed to investigate their effect on the behaviour of the model. Results from this configuration analysis can be used for future developing of the FEM model and Quake-Shield reinforcing method.

The first investigated parameter variation is removing one or both of the individual reinforcing measures from the masonry in the FEM model. Spacing between the NSM CFRP strips and dimensions of the strips are also interesting to investigate from a building application point of view. Quake-Shield uses an adhesive that shows good results for ductility and load bearing capacity. This adhesive is compared to other variations and type of adhesive. Variation on the EB layer materials are investigated as well.

### 6.1 URM, without NSM CFRP strip, without EB FRP layer

OP bend tests on Quake-Shield reinforced masonry show that the combination of two existing independent reinforcing measure provides good results for increase in stiffness, strength and overall ductility of masonry. In this paragraph the contribution of both individual reinforcing measures is investigated with use of the FEM model. Results are shown in Figure 81. Each model result is generated with the same FEM Base model but with each generated result one or both reinforcing measures are removed from the model. The models with reinforcing measures show significant improvement for load bearing capacity and ductility compared to the URM. It should be mentioned the URM model results could not be validated with use of test results of URM samples due to limitations of the three point bend test setup (paragraph 3.5). Therefore no realistic comparison can be made between URM and the results of the reinforced masonry models but it should be seen as an indication for the difference in URM and reinforced masonry in general.

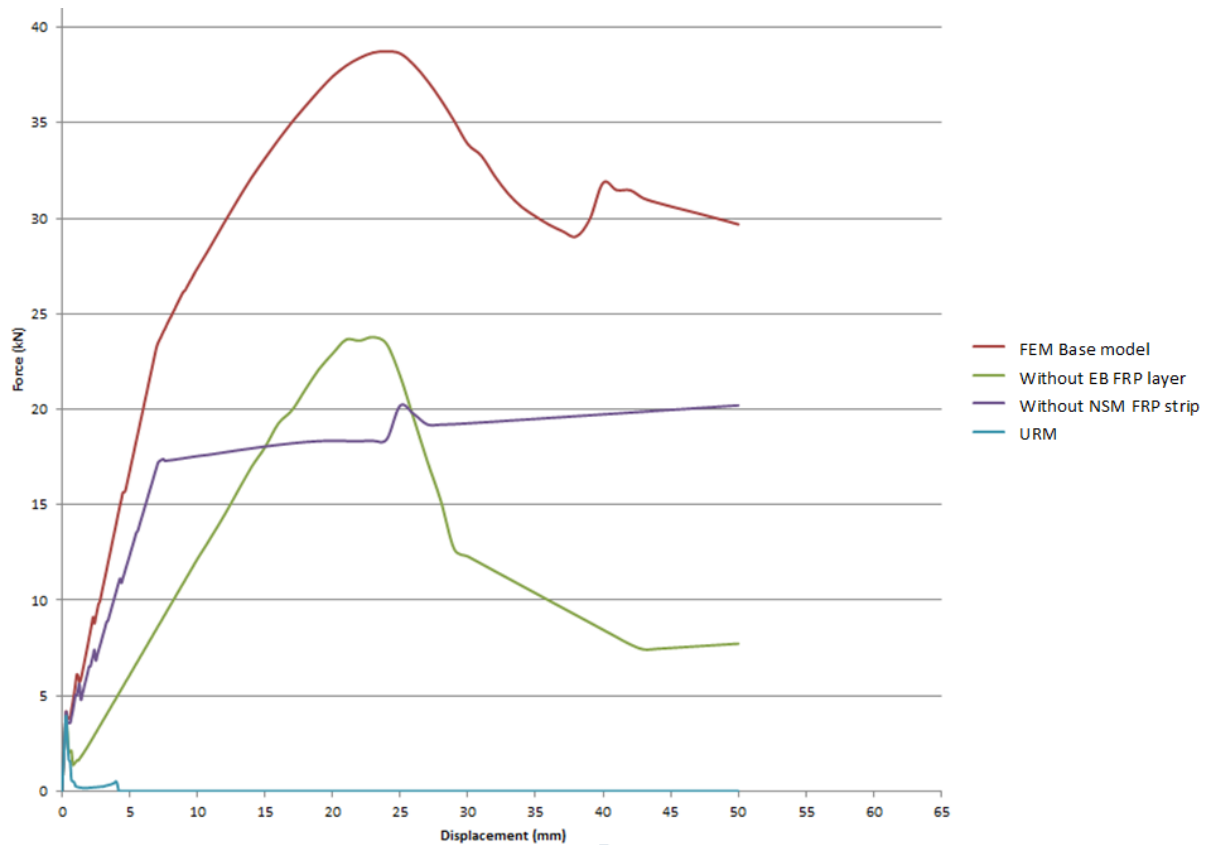


Figure 81: FEM model results of base model, without NSM FRP strips, without EB FRP layer, and URM.

When considering the linear part from at first crack initiation at 0,3 mm displacement till the onset of yielding of the EB FRP layer at 7,4 mm displacement, the stiffness contribution of the EB FRP layer is visible in the force-displacement curve (Figure 81, Without NSM FRP strip). From 7,4 mm displacement this contribution is reduced due to yielding of the EB FRP layer and the contribution of the NSM CFRP strip increase till maximum shear traction in the adhesive is reached which is visible as the peak in the force-displacement curve (Figure 81).

The model result 'without EB FRP layer' shows the same behaviour as the bond-slip behaviour of the NSM CFRP strip in the adhesive which is implemented in the model with the TAUDIS curve (Figure 64, paragraph 4.2.2). Adding the EB FRP layer as a reinforcing measure to the masonry reinforced with NSM CFRP strips gives an increase of 63% for load bearing capacity. Also the stiffness increases 175% for the linear part till the onset of yielding of the EB FRP layer.

Figure 82 shows test results of a three point bend test (series AG) comparable to the BG test series with masonry samples similar to the model variations from Figure 81, however the span between the supports was in this test series 480mm instead of 700mm, therefore the values in the force-displacement curve cannot be directly compared. The behaviour of the individual reinforcing measures can be compared to check if the individual reinforcing measure work properly in the model.

The behaviour is very similar for both cases but it could also be noticed that the transition from initial stiffness of the 'without NSM CFRP strip' test result goes more gradually to the yielding plateau in the test result. This is due to the fact that the elastic-plastic behaviour of the EB FRP layer in the model is simplified as discussed in paragraph 5.1.

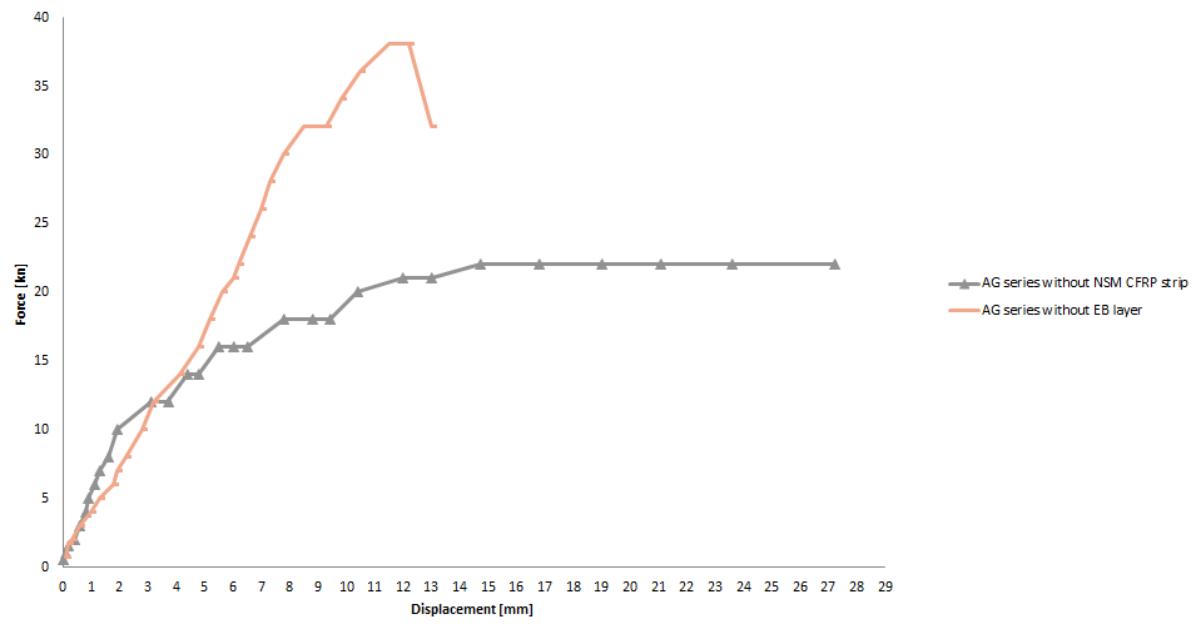


Figure 82: Test results of three point bend tests (Series-A) performed by Quake-Shield on masonry samples similar to the sample as in the BG series but without NSM CFRP strips or without the EB FRP layer.



## 6.2 Geometrical variations

### 6.2.1 Spacing of NSM CFRP strips

The effect of increasing strip spacing from 250 mm to 500 mm and 1000 mm is shown in Figure 83. For this variation the model had to be scaled up to fit in one NSM CFRP strip every 1000 mm. The scaled up model has a width of 1000 mm instead of 550 mm (Figure 84). So the strip spacing could also be considered as number of strips per meter masonry being four strips per meter is 250 mm spacing etc.

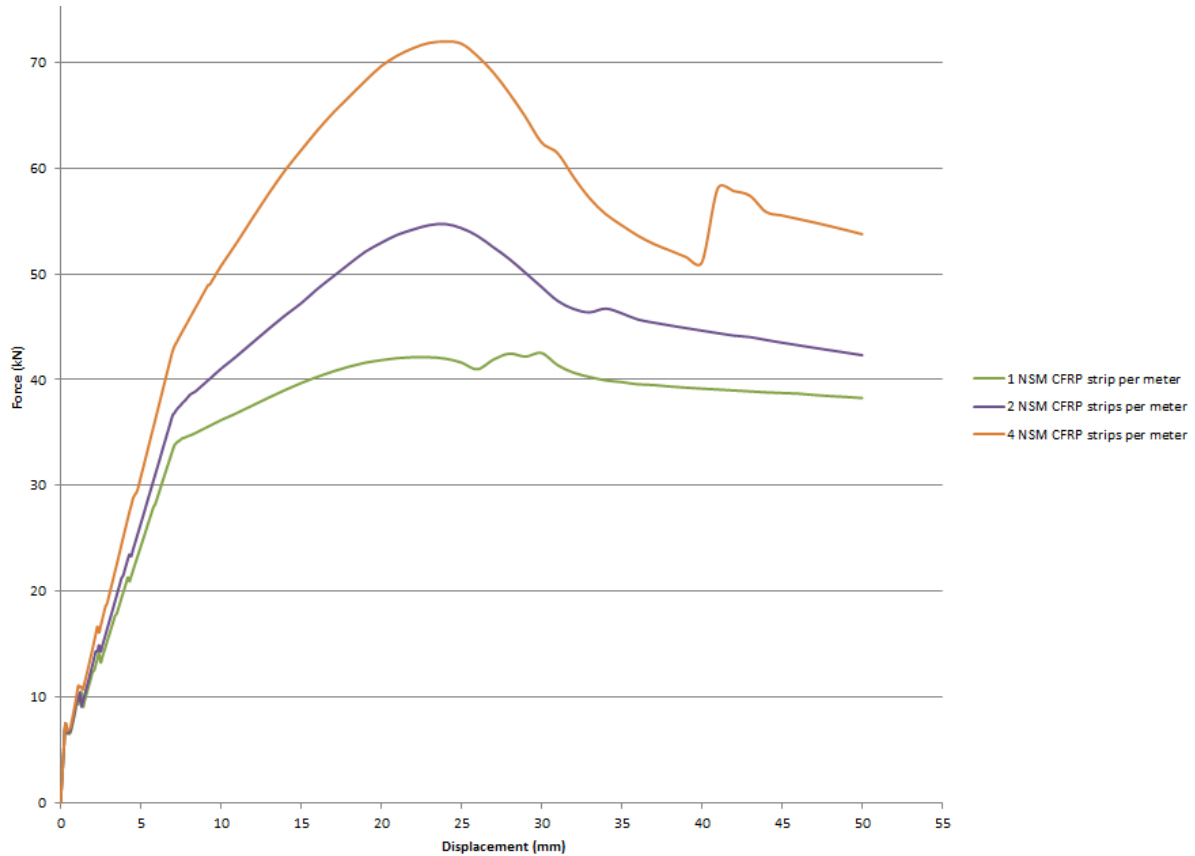


Figure 83: model results of scaled up model with different number of NSM CFRP strips per meter

The difference in test results when using one, two or four strips per meter is mainly visible in the load bearing capacity. Using two strips instead of one gives a load bearing capacity increase of 31%, and an increase of 71% when using four strips instead of one. The stiffness till the onset of yielding of the EB FRP layer is not significantly influenced by the number of strips per meter masonry. This again indicates the EB FRP layer is dominant in this first linear part. However the ratio EB FRP material to NSM FRP material is different in these three variants. More NSM FRP material gives a more distinctive peak with similar behaviour as was observed in the FEM Base model. When the portion of EB FRP material increases the behaviour of the FEM model is more similar to the model from the previous paragraph where only the EB FRP layer is applied.

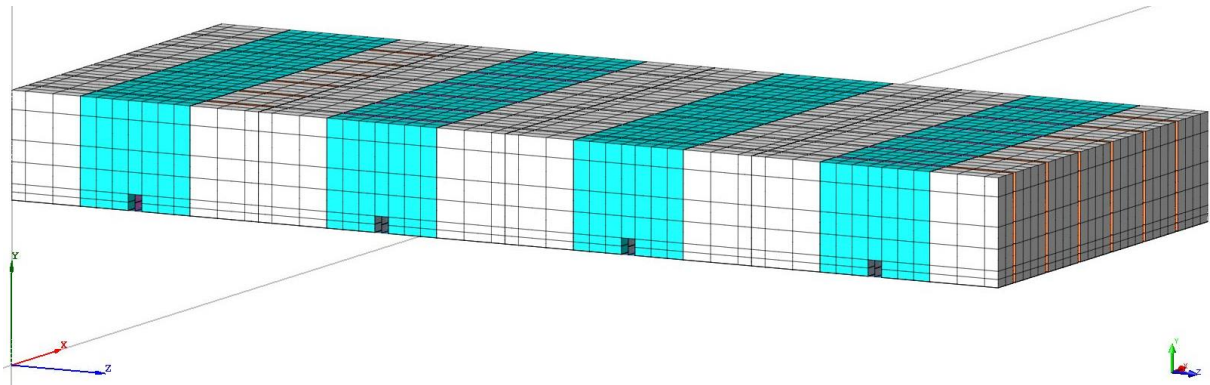


Figure 84: Scaled up model with four NSM CFRP strips per meter

### 6.2.2 Dimensions of the CFRP strips

The width of the NSM CFRP strips have an influence on the stiffness and the load bearing capacity as can be seen in Figure 85. The width of the strips do not only determine the amount of reinforcing material applied to the masonry, but also influence bending resistance due to the way the strips are positioned and loaded. The amount of bonded surface area between the strip, adhesive and masonry is determined by the width of strip and influences ductile behaviour of the reinforced masonry. All strips used for this parameter variation have a thickness of 2,5 mm which is the same as for the FEM Base model.

The stiffness of the almost linear part of curve is mainly caused by the change in bending resistance of the strip. The non-linear part till peak load is changed due to the extra bond area of the adhesive. Compared to the FEM Base model, which has a 15 mm width CFRP strip, a 30 mm width CFRP strip results in a load bearing capacity increase of 57%. Also the displacement at peak value is increased 21%. A 30 mm width strip is 30% of the width of the brick which is according to research from the literature study (paragraph 2.3.4) the recommended maximum percentage of strip width compared to the brick width. Wider strips and corresponding groove depth can result in splitting in through thickness of the masonry sample along the strip. With the current FEM model this splitting failure cannot be simulated due to the used elements and material models and therefore the maximum of 30% is used.

When using 7,5 mm width CFRP strips the load bearing capacity is decreased by 25% compared to the FEM Base model. In this case the displacement at peak load is decreased by 8%.

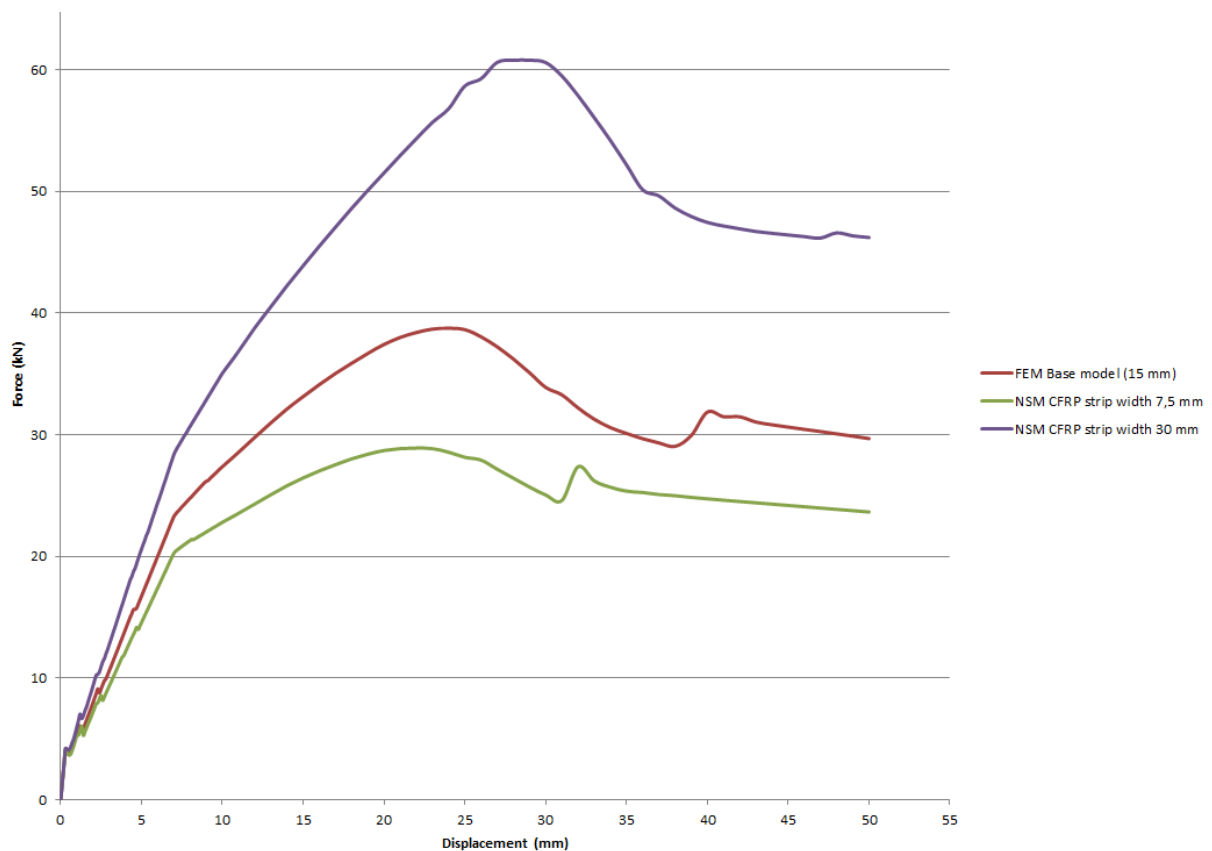


Figure 85: Model results of different NSM CFRP strip widths (7,5 mm, 15 mm, 30 mm)

The minimum required thickness of the strips can be calculated using the maximum tensile stress found in the FEM model for the NSM CFRP strip. It should be considered that the quality of the NSM CFRP strips can deviate, therefore usually a safety factor is used. The CFRP strips used for Quake-Shield are factory made so in this case a safety factor of 1,2 can be used [49]. The minimum thickness of the CFRP strips with different widths can be found in Table 14. The minimum required thickness of the CFRP strip with a width of 30 mm should be increased to 2,73 mm compared to the currently used 2,5 mm thickness to meet the safety factor requirements.

**Table 14: Maximum tensile stress in different width CFRP strips and their minimum required thickness**

<b>NSM CFRP strip width</b>	<b>Maximum tensile stress</b>	<b>Percentage of ultimate tensile strength CFRP</b>	<b>Minimum thickness of CFRP strip</b>
<b>7,5 mm</b>	1134 MPa	41%	1,23 mm
<b>15 mm</b>	1724 MPa	62%	1,86 mm
<b>30 mm</b>	2543 MPa	91%	2,73 mm

## 6.3 Material variations

### 6.3.1 Different types of NSM FRP reinforcing materials

CFRP is used as NSM strip material in the Quake-Shield reinforcing method. Other commonly used reinforcement FRP materials are Glass FRP (GFRP) and Aramid FRP (AFRP). Table 15 shows the general material properties of the commonly used FRP reinforcing material [41].

Table 15: Material properties of different FRP reinforcing materials [50] [41]

Material properties of:	Young's modulus (E-modulus)	Poisson's ratio	Density	Ultimate tensile strength	Specific strength
Carbon FRP	165000 MPa	0,3	1600 kg/m <sup>3</sup>	2800 MPa	1750 kNm/kg
Glass FRP	40000 MPa	0,25	1900 kg/m <sup>3</sup>	1000 MPa	530 kNm/kg
Aramid FRP	75000 MPa	0,34	1400 kg/m <sup>3</sup>	1300 MPa	930 kNm/kg

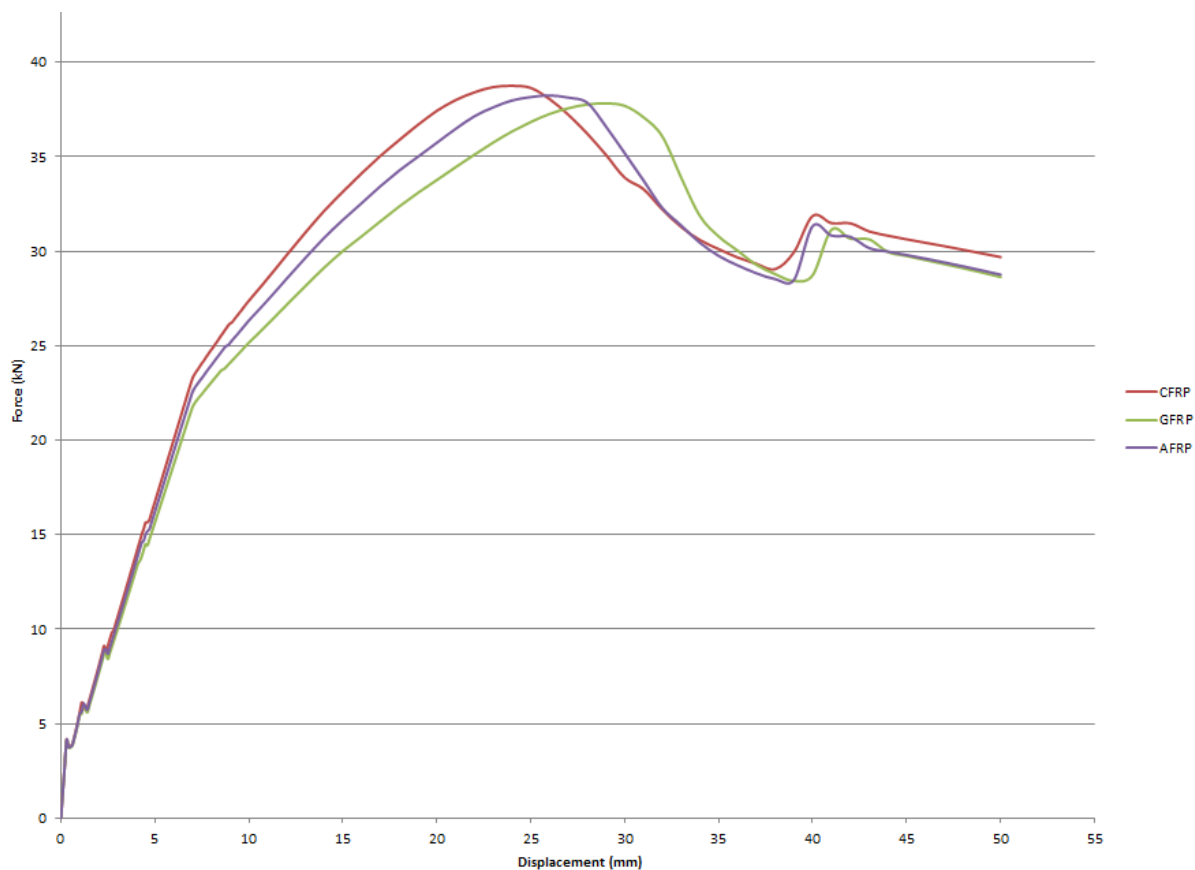


Figure 86: Model results using different types of NSM FRP strip materials (carbon, glass, aramid)

The key material property that influences the model result is the E-modulus of the FRP material. The three FRP materials could be ranked according their stiffness as: carbon, aramid, glass. With carbon the one with the highest stiffness. This is also visible in the force-displacement curve in Figure 86, where the model result with aramid is situated between carbon and glass. Related to the change in stiffness also the peak load shifts, changing overall ductility. Displacement at peak load is increased

8% for aramid and 21% for glass when comparing to carbon. The load bearing capacity is not significantly changed because for all three cases the same type of adhesive and EB FRP layer is used.

### 6.3.2 Different types of adhesive

From the sensitivity study (paragraph 4.3), the OP three point bend tests and model results it is clear the type of adhesive to bond the NSM CFRP strip to the masonry has a large contribution to the overall behaviour of the reinforced masonry. Some different adhesive variants are applied to the FEM Base model to get a better understanding of its effect.

**Table 16: Properties of the adhesive variants used for the FEM model**

Material properties of:	Shear stiffness modulus (Kt)	Diagram Shear direction
FEM Base model	0,345 N/mm <sup>3</sup>	TAUDIS function see Figure 87
2 times stronger and stiffer	0,69 N/mm <sup>3</sup>	TAUDIS function see Figure 87
2 times less strong	1,38 N/mm <sup>3</sup>	TAUDIS function see Figure 87
epoxy	65 N/mm <sup>3</sup>	TAUDIS function see Figure 87

Note: For all models the Kn and SIGDIS curve are the same as the FEM Base model

Table 16 gives the properties used for the different adhesive variants and Figure 87 shows the TAUDIS curves used for each adhesive variant. Two variants are a modification of the bond-slip curve used for the FEM Base model. The shear strength and initial stiffness are increased two times and for the other variant the strength is decreased two times. The latter could be the case if for instance the adhesion between the adhesive and masonry has some imperfections so the ultimate shear strength could not be reached due to premature debonding. The stiffness of the adhesive is in this case the same till the debonding takes place and therefore the stiffness is kept the same as in the FEM Base model. Results of these two variants can be found in Figure 89.

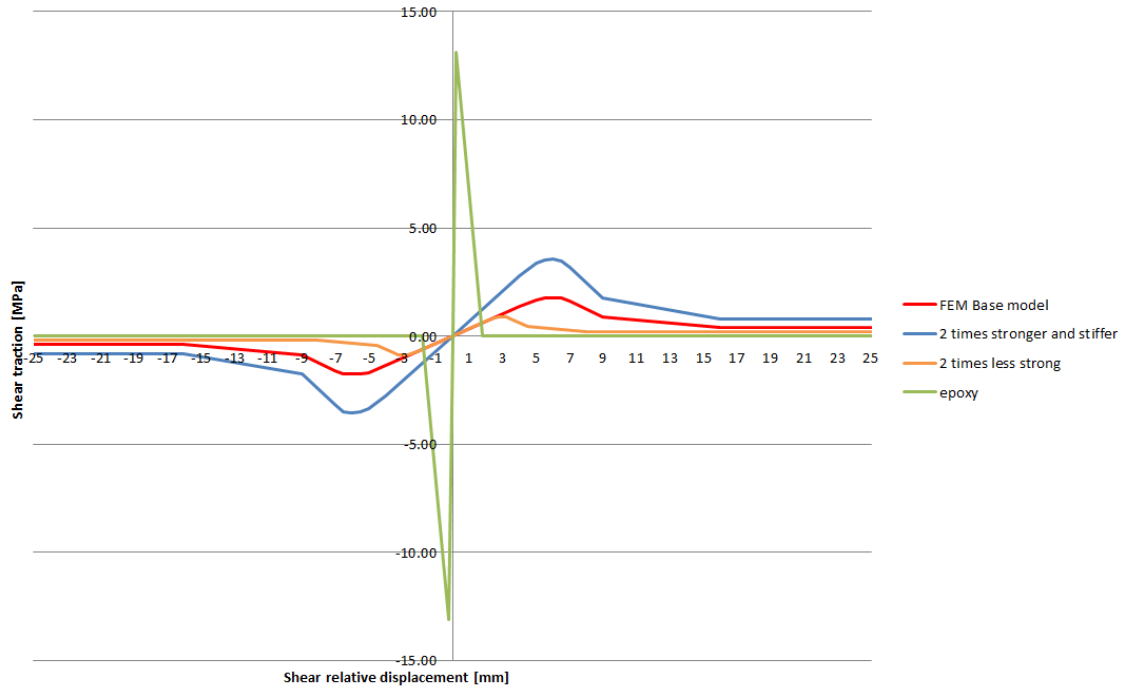


Figure 87: TAUDIS curves used for the different adhesive variants

The 'Bilinear refined' curve in Figure 88 is the same curve as the 'epoxy' curve in Figure 87.

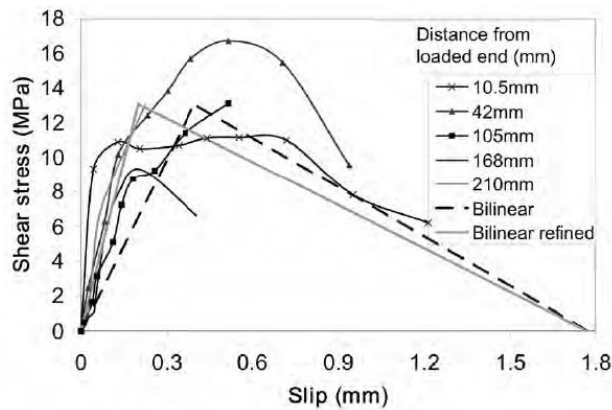


Figure 88: Bond-slip curves from Petersen research fitted with a bi-linear curve to be implemented in a FEM model [24]

Stiffness after first crack initiation is only increased 22% when stiffness of the adhesive is increased two times compared to the FEM Base model (Figure 89). The load bearing capacity is 49% increased and 28% decreased when increasing or decreasing respectively the ultimate shear strength of the adhesive two times. The displacement at peak load is shifted from 24 mm to 27 mm (13% increase) for the two times stronger and stiffer adhesive compared to the FEM Base model. For the two times less strong adhesive the displacement at peak load is 12 mm (50% decrease).



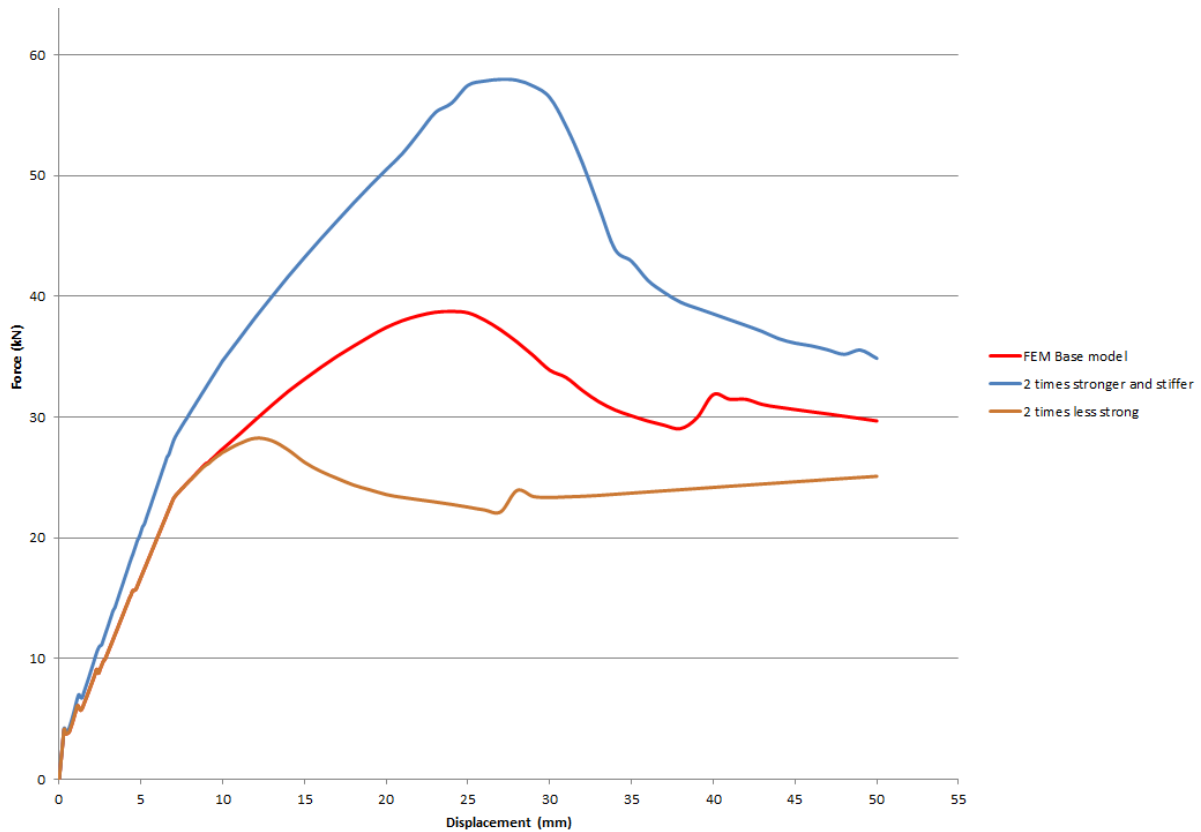


Figure 89: Force-displacement curves of the different adhesive variants

Also the epoxy used by Petersen's research is one of the variants [24]. The bond-slip curve of the epoxy used by Petersen is shown in Figure 88. This epoxy is also used in the sensitivity study in paragraph 4.3. The model in this sensitivity study and the FEM Base model cannot be directly compared due to geometrical and material model differences. However the same behaviour of the epoxy and a more ductile adhesive can be also seen in Figure 90. The epoxy results in a much higher overall stiffness and has a sudden drop after peak load which could be considered as total failure of the reinforced masonry where in the case of the FEM Base model after peak load there is still a certain amount of load bearing capacity available. Comparing the stiffness of the linear part from first crack till 7 mm displacement, the epoxy provides a 182% higher stiffness compared to the FEM Base model. The peak load of the epoxy is also 177% higher but due to the higher stiffness this peak load is already at 15 mm displacement instead of the 24 mm of the FEM Base model.

The large differences in model results for the peak load and the stiffness can also be found when comparing the bond-slip curves of the epoxy and the adhesive used in the FEM Base model.  $K_t$  is  $65 \text{ N/mm}^3$  for epoxy compared to  $0,345 \text{ N/mm}^3$  for the FEM Base model adhesive which is a factor of 188. Also the ultimate shear strength is 7,4 times higher for the epoxy.

The force-displacement curve of the epoxy levels off at about 20 kN. This is the EB FRP layer that takes over. In reality the high force and sudden debonding of the NSM CFRP strip after peak load will cause for a high energy release which will likely result in tensile failure of the EB FRP layer. After the peak load the force-displacement curve of epoxy should continue to decline in the same rate and total failure of the reinforced masonry is assumed.

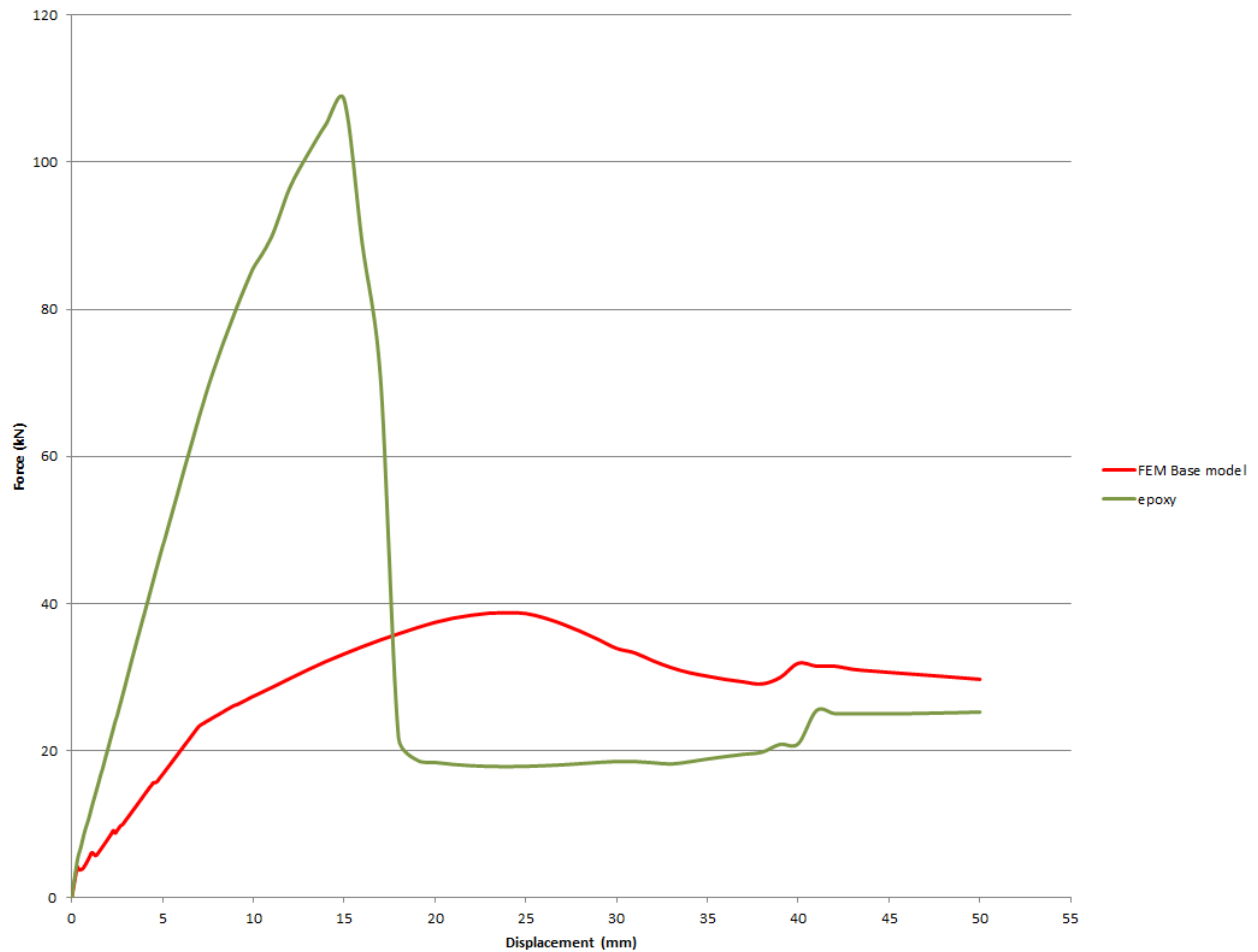
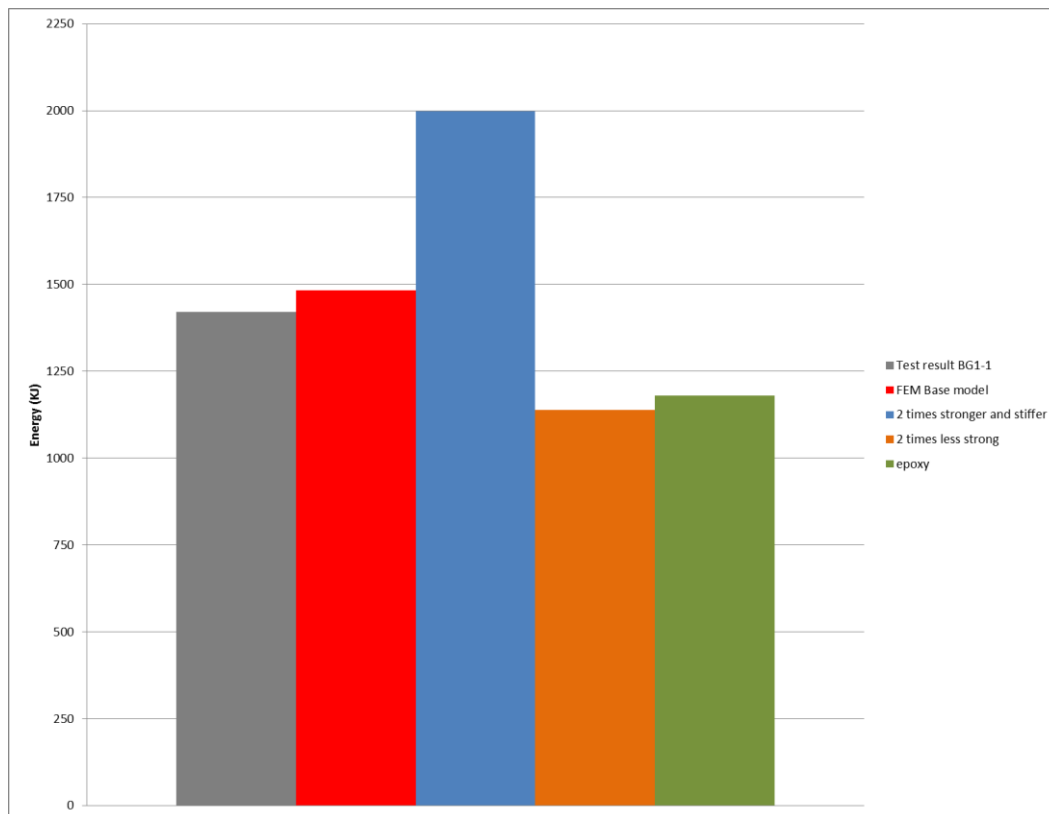


Figure 90: Epoxy compared with FEM Base model

From the comparison between epoxy and the more ductile adhesive from the FEM Base model one could assume that epoxy is a better adhesive from a stiffness and load bearing capacity point of view. In paragraph 2.3.1 of the literature study it is explained that stiffness, strength and ductility play a critical role in the amount of energy that can be absorbed and dissipated by the reinforced masonry. The lack of ductility in epoxy limits this energy absorption and dissipation, i.e. limited area under the force-displacement curve due to the sudden failure (collapse) after peak load.

Figure 91 shows a bar diagram with a comparison of taken up energy by the reinforced masonry with different types of adhesives that are shown in the force-displacement curves of Figure 89 and Figure 90.

The area under the force-displacement curves are calculated till 50 mm displacement. This was also about the maximum displacement that could be measured during the OP bend test due to the limited measuring range of the displacement measuring system. For this energy absorption comparison it should be kept in mind that in all the models and also for the OP bend test no total collapse is observed. It is therefore uncertain to what displacement the area under the force-displacement curve should extent till total failure could be assumed. The available measuring data is the range over which the area under the curve is calculated. The area for the epoxy variant is calculated till 18mm displacement assuming the decline of this force-displacement curve continues till zero force due to total failure.



**Figure 91: Comparison of energy taken up by the reinforced masonry with different types of adhesive**

For comparison of the FEM base model also the area of the BG1-1 force-displacement curve is added to the bar diagram in Figure 91. The FEM Base model takes up 4% more energy compared to the results of the BG1-1 sample. The '2 times stronger and stiffer' variant takes up 35% more energy compared to the FEM Base model. The FEM Base model takes up 23% and 20% more energy compared to 2 times less strong and the epoxy variant respectively.

### 6.3.3 Different types of EB layer

Multiple Quake-Shield reinforced masonry EB FRP layer variations are tested with the OP bend test. Besides the PU+PP-mesh (BG1 series) used for the FEM Base model also a cementitious carbon reinforced (AC+C-mesh) EB FRP layer is investigated. Homogenising these two very dissimilar materials into one layer gives problems for the model. For the EB FRP layer variation in the configuration analysis the two materials in the EB FRP layer are modelled separately. The Base material, PU or AC, are modelled with the same curved shell elements that are also used for the single homogenised EB FRP layer used in the FEM Base model. The PP-mesh or C-mesh is modelled with embedded grid reinforcement elements, because the PP-mesh and C-mesh are grid like reinforcement materials. The grid reinforcement is located at the same location as the curved shell elements, i.e. at the mid-plane of the base layer.

Table 17 shows the four individual materials used for the EB layer variations and the corresponding material properties used for the FEM model. For the PU and PP-mesh the same material properties values are used as with the calculated homogenised EB FRP layer (paragraph 5.1).

**Table 17: Materials used for the EB layer variations and the corresponding material properties [51] [52] [41]**

<b>Material properties of:</b>	<b>Young's modulus (E-modulus)</b>	<b>Poisson's ratio</b>	<b>Density</b>	<b>Yield stress</b>	<b>Maximum strain</b>	<b>Ultimate tensile strength</b>
<b>PU*</b>	8 MPa	0,486	1110 kg/m <sup>3</sup>	4 MPa	3,3	23 MPa
<b>Armo-Crete (AC)</b>	26000 MPa	0,2	2090 kg/m <sup>3</sup>	-	0,00021	5,5 MPa
<b>PP-mesh (PP)*</b>	436 MPa	0,45	920 kg/m <sup>3</sup>	8,7 MPa	6	30 MPa
<b>C-mesh (CM)</b>	160000 MPa	0,3	1790 kg/m <sup>3</sup>	-	0,004	650 MPa

\* With the 2,75 reduction factor included from paragraph 5.1

First the EB layer variations with the C-mesh model results are compared with the FEM Base model (Figure 92). The higher stiffness of AC and C-mesh are visible in the first linear part till the first crack initiation. The load at first crack initiation is increased with 175%. This load increase in the first linear part has an effect on the load bearing capacity for the PU+C-mesh variant, which is increased 22% compared to the FEM Base model. For the AC+C-mesh variant the load bearing capacity is about the same. When AC cracks its contribution to the reinforced masonry becomes almost zero. From this point it functions mainly as bonding material for the C-mesh to the masonry. The C-mesh takes over the load in combination with the NSM CFRP strip.

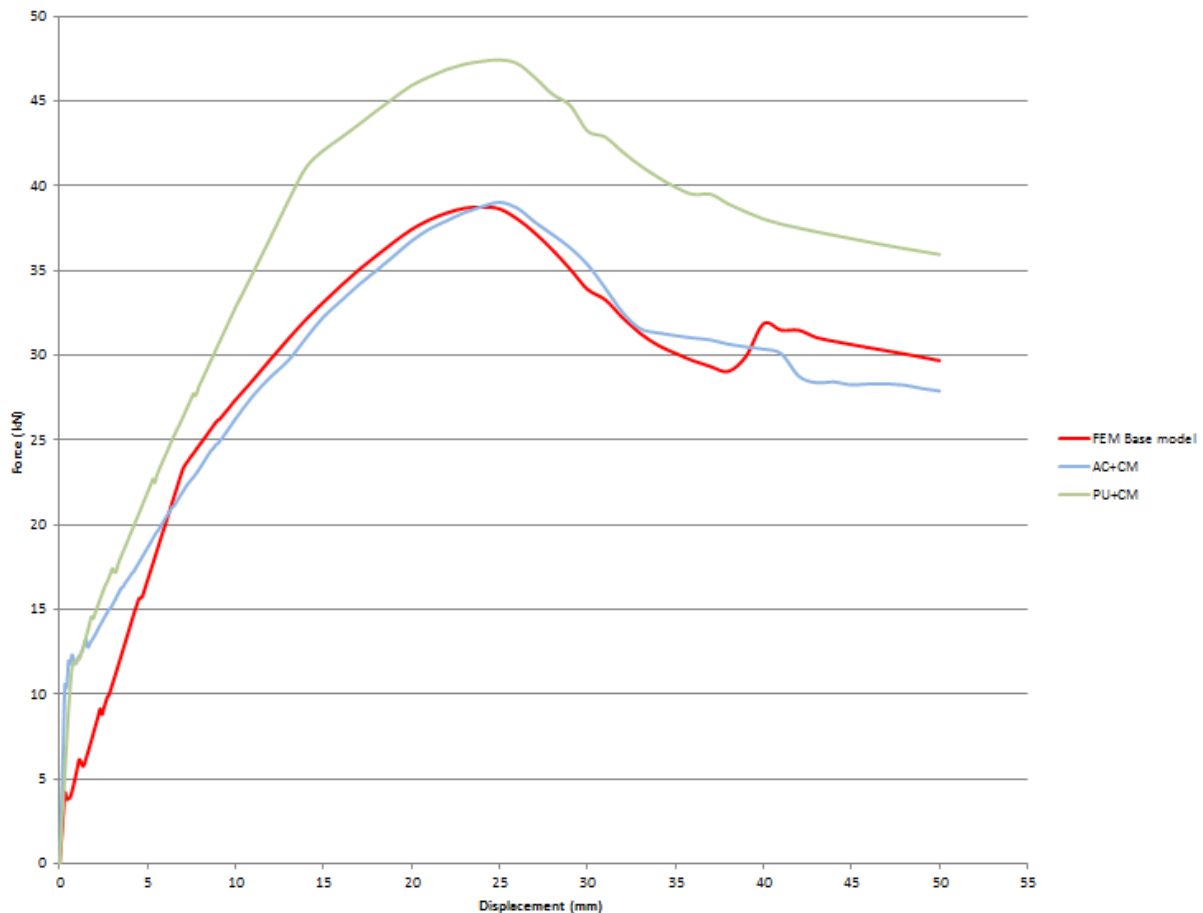


Figure 92: FEM model results of the AC+C-mesh and PU+C-mesh variant compared to the FEM Base model

In the case of PU+C-mesh the PU does not crack but starts to yield at a certain load. PU can cope with a higher strain compared to AC due to its elastic properties. Therefore its contribution to the reinforced masonry is much larger till yielding of the PU starts.

Figure 93 shows the first 5 mm displacement of the same force-displacement curve as shown in Figure 92. The difference in AC and PU in the first linear part till first crack initiation is more clearly visible. The more ductile behaviour of PU causes for a shift of the displacement at which the first crack takes place, from 0,3 mm to 0,7 mm, a 133% increase. This means compared to the FEM Base model with PP-mesh, the C-mesh has larger contribution to preventing cracks in the masonry to initiate.

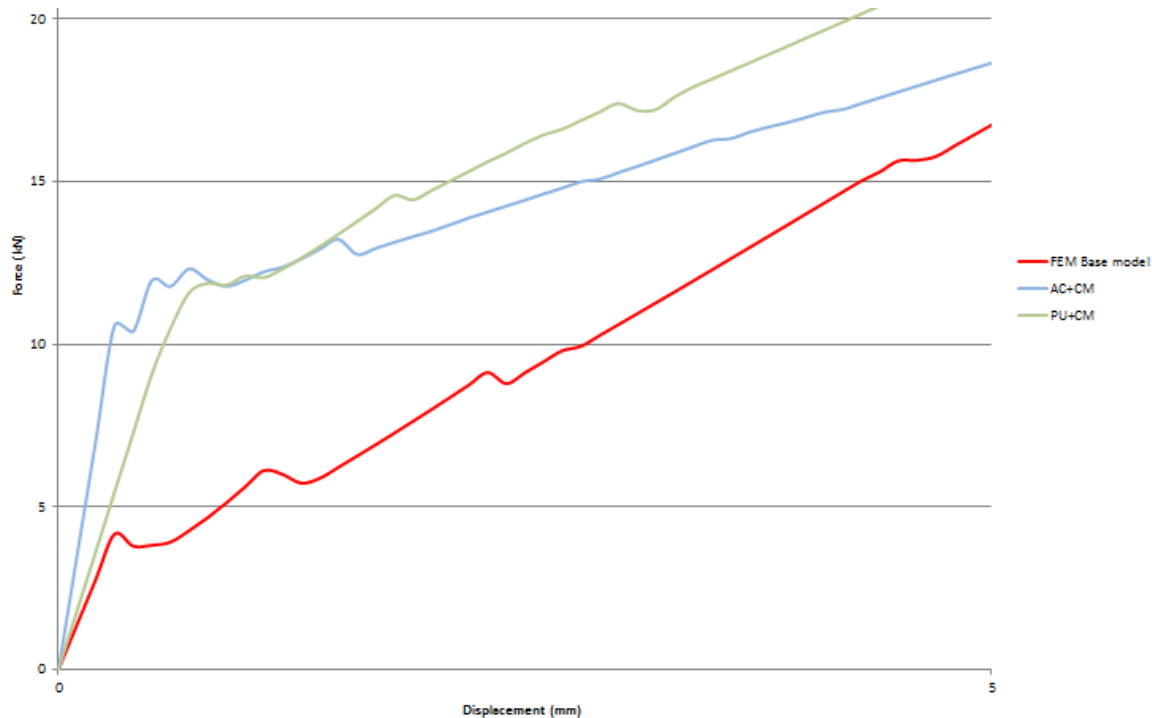


Figure 93: First 5 mm displacement of the same force-displacement curve as in Figure 92

The combination of PU+C-mesh is also tested by Oosterhof Holman with the IP tests but not yet with an OP bend test. This combination looks promising based on the FEM model results. However the contribution of C-mesh could be overestimated in this model. The reason for this is the material behaviour of carbon and how it is now implemented in the FEM model.

In reality carbon in the form of a strip or thread has a linear stress-strain curve which suddenly fails when reaching its maximum strain. From information and observations based on other OP three point bend test performed on Quake-Shield, involving the AC+C-mesh variant, it appeared that there is large crack opening or displacement in the C-mesh possible before total failure of the C-mesh takes place. This could be due to slip of the C-mesh threads in the AC layer or slip of carbon strands in the carbon threads itself. The latter one could be visible in Figure 94 which shows the threads that have become a sort of 'fluffy' which indicates some strands have broken in the thread but the thread still has some load bearing capacity. At this point the behaviour of the C-mesh in the AC or PU is not known and should be investigated to get more accurate FEM model results when C-mesh is used.



Figure 94: An opened crack in the AC layer with CM threads visible

Also variants on the PU EB layer are modelled. Since the model is slightly adapted for the EB layer variations also the PU+PP-mesh variant is compared to the homogenised single EB FRP layer of the FEM Base model. Results are shown in Figure 95 and it is clear that the two separate layers for PU and PP-mesh result in less stiff behaviour from the first crack initiation till 15 mm displacement.

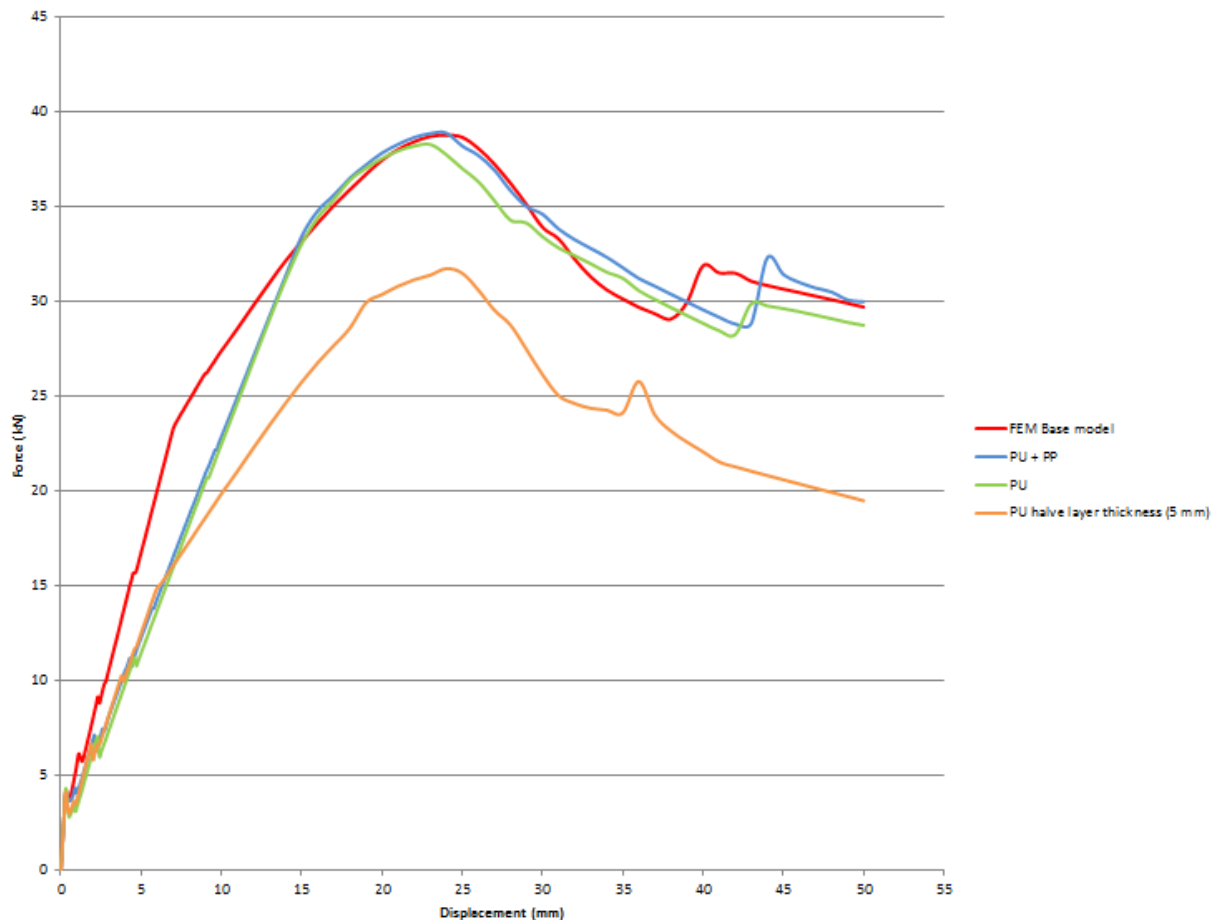


Figure 95: FEM model results of the PU EB layer variants compared to the FEM Base model

In Figure 96 it can be seen the EB layer variations do not affect the stiffness before the first crack initiate. This is due to the fact that the masonry stiffness is much higher compared to the PU and PP. The relatively low stiffness of PU and PP will not have an effect on this overall stiffness behaviour. Between the initiation of the first crack and yielding of PU the PP does have a significant contribution to the stiffness of the EB layer. This is observed when comparing the results of the PU+PP-mesh with the PU variant. PP starts to yield at 0,6 mm displacement. From this point the stiffness contribution of PP to the EB layer is reduced and PU provides mainly the stiffness after this point and is therefore comparable to the PU variant.

The load bearing capacity is not significantly different because in both cases the EB layer is yielded and the maximum shear traction of the adhesive bonded to NSM CFRP dominant resulting in about the same peak load. The small difference of 1 kN between the PU and PU+PP-mesh variant could be the contribution of the PP-mesh because after yielding the PP-mesh still keeps a contribution to the reinforced masonry

If only PU is applied as EB layer and this layer is reduced to 5 mm thickness, which is halve the thickness used in the other variants and FEM Base model, than the load bearing capacity is significantly reduced. Compared to the FEM Base model this is an 18% reduction in load bearing capacity.

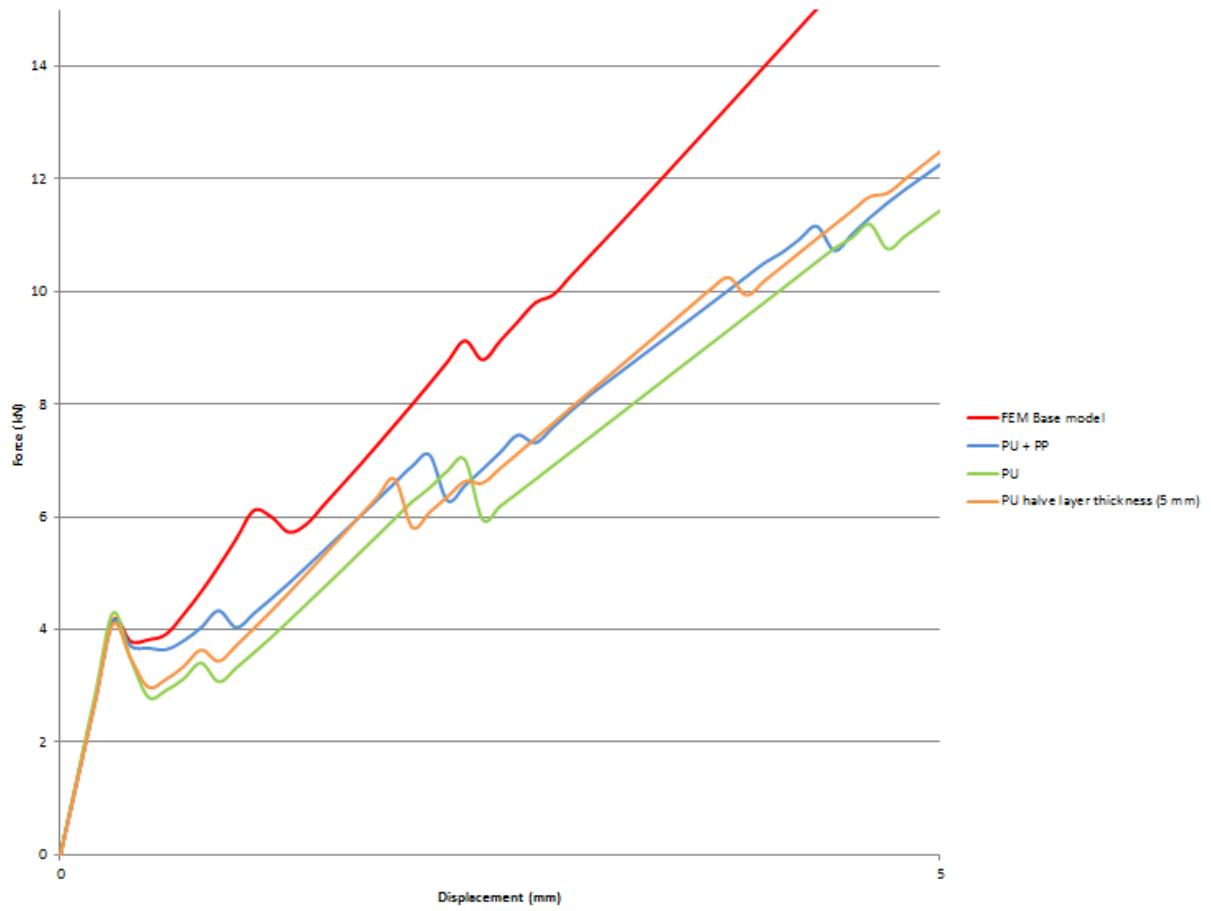


Figure 96: First 5 mm displacement of the same force-displacement curve as in Figure 95



## 6.4 Discussion of configuration analysis results

Considering the model results when only one of the two reinforcing measures is applied, the contribution of these individual measures becomes more clear. As described in the Chapter 5 the EB FRP layer is dominant from the first crack initiation till the onset of yielding of this layer. From this point the NSM CFRP strip becomes dominant and the mechanical properties of the adhesive determine in great extent the ductile behaviour of the reinforced masonry. Comparing the model results to the AG test series similar behaviour is observed when only one of the two individual reinforcing measures is applied.

Changing the spacing between the NSM FRP strips has a significant effect on the load bearing capacity which is increased with 31% and 71% using two or four strips per meter masonry. More strips per meter masonry will give a higher load bearing capacity with a more distinctive and sharper peak. The behaviour of one of the two individual reinforcing measures becomes more dominant if the ratio between the two reinforcing measures moves to one of the reinforcing measures. The stiffness of the first linear part of the force-displacement curve is not significantly affected by the ratio between the reinforcing measures. The significant increase in load bearing capacity when applying more strips per meter masonry was also found in a research described in the literature study (paragraph 2.3.5).

Not only strip spacing but also the dimensions of the NSM FRP strips effect the mechanical behaviour of the masonry. Using a CFRP strip with a 30 mm width increases load bearing capacity by 57% compared to the 15 mm wide strip used in the FEM Base model. This is because of the increase of reinforcing material and by adding more bending resistance due to the effect of increased area moment of inertia. The increased bonding area between adhesive, strip and masonry results in more ductility due to the ductile material properties of the adhesive used with Quake-Shield. With a CFRP strip that has a width of 30 mm the displacement at peak load is increased with 21% compared to the 15 mm strip.

The model can be used to calculate minimum required NSM FRP strip dimensions to prevent FRP rupture which is an unwanted failure mode because of its sudden loss of load bearing capacity.

The type of NSM FRP strip material used results in a small difference in model behaviour. Less stiff FRP material provides a little more ductility which is visible in a displacement increase at peak load of 21% for GFRP compared to CFRP.

Variations in adhesive properties have an effect on the TAUDIS curve in the model. Increasing stiffness and shear strength of the adhesive two times results in a 49% increase in load bearing capacity and a 13% increase in displacement at peak load. Comparing the ductile adhesive to a more commonly used stiff epoxy shows clear differences. Epoxy gives a high initial stiffness and a high load bearing capacity but has a sudden drop after the peak load has been reached. Overall ductility and also a gradual decline in load bearing capacity after the peak load are critical when considering reinforced masonry. The sudden drop of load bearing capacity after peak load reduces energy absorption and can result in a sudden collapse of a building. Also stiff behaviour in the first initial part of the force-displacement curve is not always beneficial from a dynamic point of view. If the natural

frequency of a building gets close to the frequency of the earthquake resonance can occur which results in more severe loading on the building (paragraph 2.3.1).

An high peak load with very ductile behaviour after the peak is favourable because this gives a large area under the curve which is the amount of energy that the reinforced masonry can take up during an earthquake.

Different variations on the EB layer gives better insight in the contribution of this layer and the effects of different types of EB FRP layer materials. Using C-mesh instead of PP-mesh gives a much stiffer behaviour in the first initial part till first crack initiation. After cracking AC losses its contribution to the reinforced masonry. An elastic polymer like PU keeps its contribution to the reinforcing measure even after yielding although the contribution is reduced after this point. C-mesh is stiffer than PP-mesh therefore crack opening will be reduced. A stiffer EB FRP layer can cause for an increased compression zone at the top (non-reinforced) side of the masonry. This can have a negative influence on the overall behaviour of the reinforced masonry because the masonry is usually the weakest material compared to the reinforcing materials. By increasing the compression zone more stress is focussed on the masonry. This could lead to lower overall mechanical properties of the reinforced masonry although a stiffer and stronger EB FRP material is used.

For the PU+PP-mesh variant the question could be asked how large the contribution of the PP-mesh is. An EB layer variant with only the base layer PU is used to determine the contribution of the PP-mesh. If the two separate layers are used for the PU+PP-mesh variant the contribution is minimal and it could be concluded that the PP-mesh could also be removed from the EB FRP layer to get almost the same mechanical behaviour of the reinforced masonry. Compared to the FEM Base model the PP-mesh has a contribution in the stiffness which is noticed in the displacement range from first crack initiation till about 10 mm displacement. As explained in Chapter 5, the homogenised EB layer with PU and PP-mesh is likely to overestimate the stiffness of this layer. Concluding from this the PP-mesh likely has a contribution to the EB FRP layer but the dominant material is the base layer which is in this case PU.

The thickness of the PU layer has and significant effect on the load bearing capacity. Using a 5 mm thick EB layer instead of 10 mm reduces the load bearing capacity with 18%. This decrease is mainly caused by a reduced contribution of the EB layer and the earlier onset of yielding of this layer. This is because with the same load on the EB layer at a certain displacement, and half a thickness of this layer, this means the stress will be two times higher and the yield stress is reached at a much lower displacement.

## 7 Conclusions & Recommendations

### Conclusions

In the last decade, the earthquakes in Groningen receive more attention from the government, researchers and engineers. Research has shown that potentially heavier earthquakes with PGA values of up to 0,42g can occur in the future. Houses build up out of single leaf masonry walls have to be reinforced to prevent collapse if an earthquake of 0,42g takes place. Quake-Shield provides a reinforcing method in which the combination of two independent seismic reinforcing measures are used to make masonry earthquake resistant. Quake-Shield increases the stiffness, load bearing capacity and ductility of the masonry. These three increased factors result in an increased energy absorption and dissipation of the masonry wall. A FEM model is used to get more insight in the behaviour of Quake-Shield reinforced masonry and the contribution of the two independent reinforcing measures to the stiffness, strength and ductility of masonry.

The following conclusions can be drawn from the results found with use of the FEM model:

- 3D FEM modelling Quake-Shield reinforced masonry with DIANA gives good model behaviour compared to the Quake-Shield test results.
- Modelling the NSM CFRP discreetly and use the TAUDIS function (DIANA) for bond-slip behaviour gives good model control over the bond-slip behaviour of the NSM CFRP strip in combination with a ductile adhesive as with the Quake-Shield adhesive.
- CCSC material model for the mortar interfaces cannot be combined with embedded reinforcement elements in combination with bond-slip. (DIANA) (Appendix A, Figure A - 7)
- Homogenising two different types of polymers into a single layer gives a stiffness overestimation. This is also partly caused by the simplified elastic-plastic material model that is used in DIANA. (Paragraph 5.1, Figure 72).
- Using embedded grid reinforcement elements for mesh type materials in combination with shell elements for the base layer appears to work properly to simulate the EB FRP layer. (DIANA)
- Both independent seismic reinforcing measures show increased stiffness, strength and ductility if applied separately. If combined the EB FRP layer is in the beginning dominant, reducing the stress on the NSM FRP strip, and determines mainly the behaviour of the reinforced masonry. After the onset of yielding of the EB FRP layer the NSM FRP strip becomes dominant, determining the load bearing capacity and behaviour of the reinforced masonry post peak. (Paragraph 6.1, Figure 81)
- The bond-slip behaviour of the ductile adhesive to bond the NSM CFRP to the masonry determines mainly the pre and post peak behaviour of the reinforced masonry with a gradual decline in load bearing capacity after the peak load.
- The ultimate shear strength of the adhesive determines mainly the peak load of the reinforced masonry.
- The EB FRP layer bonds the individual bricks and provides stiffness to the reinforced masonry from the first crack initiation till yielding of the EB FRP layer.
- Small imperfections in the test samples and test setup have likely influenced the test results. The model does not contain these imperfections and therefore the model results could be slightly overestimated.

- Spacing and dimensions of the NSM CFRP strips have a significant influence on the maximum load bearing capacity of the reinforced masonry. (Paragraph 6.2.1, Figure 83)
- Epoxy as an adhesive for bonding NSM FRP gives a high stiffness and load bearing capacity but a reduced ductility after peak load compared to the adhesive of Quake-Shield. Resulting in a lower energy absorption and therefore epoxy is a less favourable earthquake reinforcing material. (Paragraph 6.3.2, Figure 90)
- A cementitious base layer like Armo-Crete only has a contribution to an increased stiffness of the reinforced masonry till the Armo-Crete base layer cracks.
- C-mesh reduces crack opening by increasing stiffness of the reinforced masonry. Combined with the PU base layer the onset of yielding of PU is delayed and also the stress on the NSM FRP strip is reduced resulting in a higher load bearing capacity for masonry when the ultimate shear strength of the adhesive is reached (peak load).

### *Recommendations*

The FEM model used for this project shows good behaviour compared to the test result of BG1-1. However the model could still be improved or more details could be included to get even a better fit with test results. This can also provide more insight in the smaller effects that are present in the test sample, like debonding of FRP from masonry. Also improvements can be made for the test setup and how the samples are tested. Experimental material tests have supported this project with critical information like the pull-out tests performed by the TU/e. Experimental material tests could also be done on the EB FRP layer to get better information and knowledge about the mechanical behaviour of this layer. Below some recommendations could be listed that are interesting for future research:

- Research into the adhesion and debonding of the NSM FRP strip adhesive and the EB FRP layer to the masonry. Improper adhesion or debonding could reduce the mechanical properties of the reinforced masonry significantly.
- Use separate layers for the EB FRP layer. Using embedded grid reinforcement elements for mesh type materials appears to work properly.
- Improve masonry behaviour of the model by improving non-linear behaviour of the masonry when compression loaded and implement more extensive shear effects in the mortar interfaces.
- It is desirable to test masonry in vertical position with an applied normal force to the sample to get more realistic loading conditions. Also URM could be tested properly in this position which can then be used to compare results with Quake-Shield reinforced masonry.
- Gain more information about the used masonry for the Quake-Shield reinforced masonry samples by performing small scale material tests. Like for example a compression test.
- The amount of displacement or drift is limited for an OP loaded masonry wall. On the small scale masonry wall used in this project this limit cannot be determined. Vertical loaded full size Quake-Shield reinforced masonry wall tests and correlating FEM models are able to determine this drift limit.
- Use static-cyclic or dynamic time dependent FEM analysis to introduce more realistic earthquake loading into the model. Hysteresis graphs give a better view of how much energy

is absorbed and dissipated by the reinforced masonry. The ideal initial stiffness can only be determined when dynamic loading is used due to factors like natural frequency of the reinforced masonry.

- Improve the three point bend test setup with displacement measuring that automatically logs test data and measure directly the displacement for example with a laser displacement meter.
- Extend measuring and loading range so samples can be tested till complete failure. Same accounts for the pull-out tests.
- Improve supports by reducing the chance of indenting the supports or incorporate this in the model to eliminate this effect.
- Place all test samples exactly in the same position in the test setup.
- Use and computer controlled hydraulic pump to apply the load more gradually.
- For optimization of the Quake-Shield geometry, like strip spacing, use a 2D model of a full size masonry wall that could be scaled up to a house or building.
- More research on alternative FRP materials for future improvement and more environmental friendly masonry reinforcing solutions.

## Bibliography

- [1] "RTV Noord - Aardbevingsbestendig behang' is voor het eerst toegepast," RTV Noord, 2016. [Online]. Available: <http://www.rtvnoord.nl/nieuws/159175/Aardbevingsbestendig-behang-is-voor-het-eerst-toegepast>. [Accessed 2016].
- [2] B. Dost, D. Kraaijpoel, T. v. Eck and M. Caccavale, "Seismicity induced due to gas production: Groningen Seismic Hazard Analysis," Bilt, 2015.
- [3] "KNMI," [Online]. Available: [http://www.nlog.nl/nl/reserves/Groningen\\_clip\\_image006.png](http://www.nlog.nl/nl/reserves/Groningen_clip_image006.png). [Accessed August 2015].
- [4] "KNMI," [Online]. Available: <http://www.knmi.nl/cms/viewimage.jsp?number=23031>. [Accessed 2015].
- [5] "Nederlandse praktijkrichtlijn (NPR 9998)," February 2015.
- [6] "RTVNoord - Minister Kamp bezoekt Jarino-woningen," [Online]. Available: <http://www.rtvnoord.nl/artikel/artikel.asp?p=148019>. [Accessed 19 June 2015].
- [7] Arup, "Arup Project Title: Groningen 2013: Implementation Study," Arup, nov 2013.
- [8] B. v. d. Broek and S. Wijte, "Analyse resultaten metselwerkproeven Oosterhof Holman (dossier 9032) [PRIVATE CONVERSATION]," Adviesbureau Hageman B.V., Rijswijk, 2015.
- [9] C. Konthesingha Muhandiramlage, "Earthquake Protection of Masonry Shear Walls Using Fibre Reinforced Polymer Strengthening," Newcastle, Australia, October 2012.
- [10] A. Coburn, "Death Tolls in Earthquakes".
- [11] T. Inglesby, "Mixing Mortar for Properties — The Prescription Mortar Method," [Online]. Available: <http://www.masonrymagazine.com/9-02/mixing.html>. [Accessed 18 June 2015].
- [12] M. A. ElGawady, P. Lestuzzi and a. M. Badoux, "Static Cyclic Response of Masonry Walls Retrofitted with Fiber-Reinforced Polymers," 2007.
- [13] J. G. Tumialan, N. Galati and A. Nanni, "FRP Strengthening of URM Walls Subject to Out-of-Plane Loads," Missouri–Rolla.
- [14] C. W. Dolan and J. M. Gilstrap, "Out-of-plane bending of FRP-reinforced masonry walls," Laramie, USA, 1998.
- [15] J. G. Rots, R. v. d. Pluijm, A. Vermeltfoort and H. Janssen, "Structural Masonry – An Experimental/Numerical Basis for Practical Design Rules.," Balkema, Rotterdam, The Netherlands, 1997.
- [16] M. C. Griffith, J. Kashyap and M. M. Ali, "Flexural displacement response of NSM FRP retrofitted masonry walls," Adelaide, Australia, 2012.
- [17] C. Willis, Q. Yang, R. Seracino and M. Griffith, "Damaged masonry walls in two-way bending retrofitted with vertical FRP strips," *Construction and Building Materials*, vol. 23, 2007.
- [18] D. Dizhur et al., "Out-of-plane strengthening of unreinforced masonry walls using near surface mounted fibre reinforced polymer strips," *Engineering Structures*, pp. 330-343, 2014.
- [19] "Eurocodes - EN 1998: Design of structures for earthquake resistance," [Online]. Available: <http://eurocodes.jrc.ec.europa.eu/showpage.php?id=138>. [Accessed 18 June 2015].
- [20] R. Steenbergen, "Dynamica en Aardbevingen - TNO - NEN training Ontwerpen Gebouwen op Aardbevingen," Groningen, 2015.
- [21] F. L. Mantia and M. Morreale, "Green composites: A brief review," Italy, 2011.

- [22] H. Patil, "Introduction to Fracture Mechanics," [Online]. Available: <http://www.slideshare.net/HarshalPatil7/introduction-to-fracture-mechanics>. [Accessed July 2015].
- [23] T. Zimmermann, A. Strauss and B. Konrad, "Energy dissipation and stiffness identification of unreinforced masonry," Florianópolis – Brazil, 2012.
- [24] R. B. Petersen, "In-plane Shear Behaviour of Unreinforced Masonry Panels Strengthened with Fibre Reinforced Polymer Strips," Newcastle, Australia, oct, 2009.
- [25] "elitemodels," [Online]. Available: <http://www.elitemodelsonline.co.uk/images/products/Materials/Carbon/~RelatedImageGallery/~LightBox-Batten.jpg>. [Accessed June 2015].
- [26] D. Dizhur, M. Griffith and J. Ingham, "Pullout strength of NSM CFRP strips bonded to vintage clay brick masonry," *Engineering Structures*, no. 69 (2014), 2014.
- [27] J. Poulis, "Adhesive Bonding AE4 ASM107 TU Delft," Delft, 2015.
- [28] C. Willis, Q. Yanga, R. Seracino and M. Griffith, "Bond behaviour of FRP-to-clay brick masonry joints," 2009.
- [29] T. Stratford, G. Pascale, O. Manfroni and B. Bonfiglioli, "Shear Strengthening Masonry Panels with Sheet Glass-Fiber Reinforced Polymer," 2004.
- [30] "NEN-EN 1052-2 Methods of test for masonry - Part 2: Determination of flexural strength," Nederlands Normalisatie-instituut, Delft, maart 2016.
- [31] R. B. Petersen, M. J. Masia and R. Seracino, "Bond Behavior of Near-Surface Mounted FRP Strips Bonded to Modern Clay Brick Masonry Prisms: Influence of Strip Orientation and Compression Perpendicular to the Strip," June 2009.
- [32] M. d. Boer, "Ontwerpen van gebouwen onder aardbevingsbelasting," NEN, Groningen, 20 april 2015.
- [33] P. Lourenço, "proefschrift: Computational Strategies for Masonry Structures," Delft, 1996.
- [34] J. Manie, "Concrete and Masonry Analysis User's Manual release 9.6," TNO Diana, Delft, 2014.
- [35] G. Godevenos, "Preliminary analyses on strengthened masonry [PRIVATE CONVERSATION]," TU Delft, Delft, 2015.
- [36] H. Köksal, O. Jafarov, B. Doran and C. Karakoç, "Modeling of the Shear Behavior of Unreinforced and Strengthened Masonry Walls," Turkey, 2012.
- [37] L. Macorini and B. Izzuddin, "A Nonlinear Interface Element for 3D Mesoscale Analysis of Brick-Masonry Structures," London, 2010.
- [38] J. Manie and W. P. Kikstra, "Diana User's manual Material Library release 9.6," TNO Diana, Delft, 2014.
- [39] "IHS Engineering 360," [Online]. Available: Source: <http://cr4.globalspec.com/thread/20315>. [Accessed June 2015].
- [40] J. G. Rots, "Smeared and discrete representations of localized fracture," Delft University of Technology, Faculty of Civil Engineering, 1990.
- [41] "Performance Composites - Mechanical Properties of Carbon Fibre Composite Materials," Performance Composites LTD, [Online]. Available: [http://www.performance-composites.com/carbonfibre/mechanicalproperties\\_2.asp](http://www.performance-composites.com/carbonfibre/mechanicalproperties_2.asp). [Accessed sept 2015].
- [42] A. V. Amirkhiz et al., "Constitutive Modeling and Experiments on Polyurea," San Diego.
- [43] Quake-Shield, "youtube - Metselwerk versterkt met Quake-Shield Poly," Quake-Shield, [Online]. Available: <https://www.youtube.com/watch?v=PEFmqgrtfzw>. [Accessed 2015].

- [44] J. Manie and W. P. Kikstra, "DIANA – Finite Element Analysis User's Manual release 9.6 Element Library," Delft, 2014.
- [45] B. d. Vries, "Samenvatting Schaduwproeven," Eindhoven (TUE), 2016.
- [46] A. T. Vermeltfoort, "Uittrekproeven op koolstof strips in gleuven metselwerk," Eindhoven (TUE), 2015.
- [47] W. D. Callister, Materials science and engineering an introduction, John Wiley & Sons, inc., 2007.
- [48] C. Roland, J. Twigg, Y. Vu and P. Mott, "High strain rate mechanical behavior of polyurea," Washinton DC, US, 2006.
- [49] T. Triantafillou et.al., "Externally bonded FRP reinforcement for RC structures," fib, July 2001.
- [50] "Technische gegevens CFK-lamellen van S&P," S&P, Aalsmeer.
- [51] S&P, "S&P Armo-crete w(4)," Aalsmeer.
- [52] "S&P ARMO-System FRCM Design Guidelines fiber reinforced cementitious matrix," 2013.



## Appendix A

### *OP three point bend test masonry prism model*

The model described in this Appendix is based on a research by Dmytro Dizhur, et al. [18]. The results from this research can be used to check if the FEM model produces satisfying results to be used for the Quake-Shield reinforced masonry FEM model. If this is the case than the EB FRP layer can be added to the model and eventually scaling up the model to the sample size of the OP bend test of Quake-Shield reinforced masonry (described in Chapter 3).

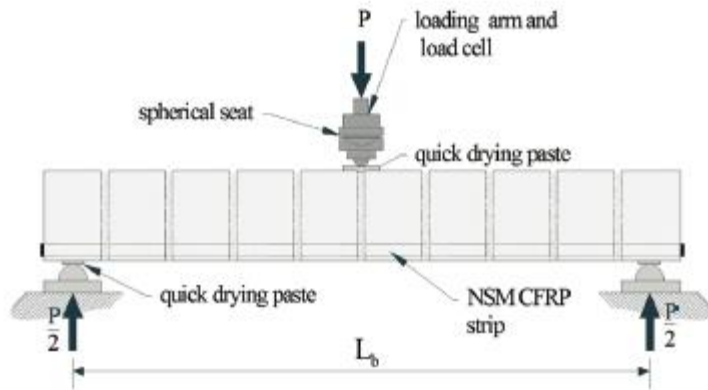
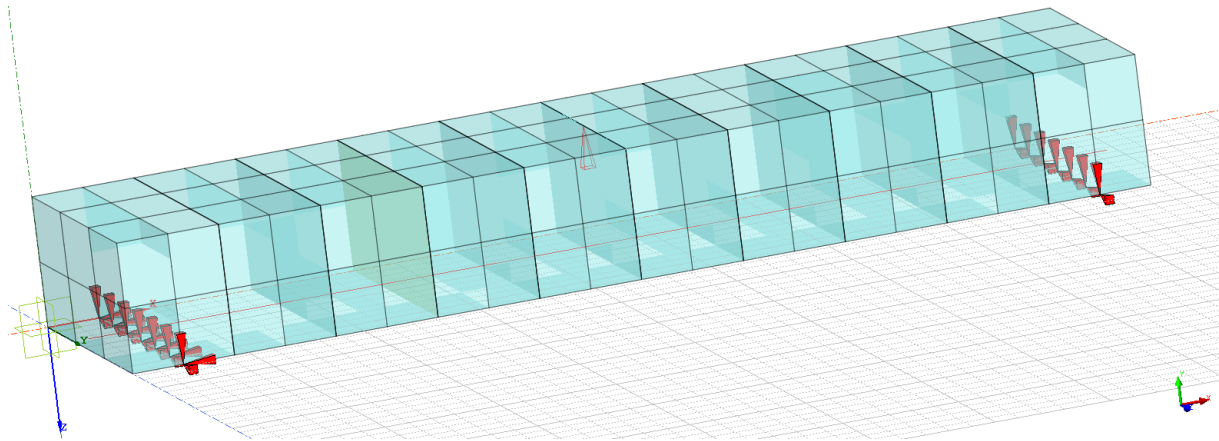


Figure A - 1: Three point bend test on a reinforced masonry prism [18]

The model consists out of a prism of 10 bricks reinforced with a NSM CFRP strip is OP loaded with a three point bend test (Figure A - 1). The bricks are twenty-node isoparametric solid elements (CHX60) with isotropic linear elastic properties and a default 3×3×3 Gauss integration scheme [44]. The mortar joints are zero-thickness interface elements (CQ48I) with a default 3×3 Newton-cotes integration scheme. Cracking of the mortar layer in the mid-plane of the prism is most likely. Therefore only this mortar interface has non-linear behaviour modelled with the CCSC material model [38]. The other mortar interfaces are modelled with linear elastic material properties. For the models that are OP loaded the extra interface at the mid-plane of the brick unit to simulate a potential crack as recommended in literature is not included [15] [24]. This is done because crack forming in OP loaded masonry is likely to take place in the bed joints and not in the length direction of the masonry sample. This is also based on observations during the Quake-Shield OP tests. The NSM CFRP strip is modelled using 1D embedded reinforcement (beam) elements (CL18B) with isotropic material properties, bond-slip behaviour and a default 2-point Gauss integration scheme.



**Figure A - 2: Reinforced masonry prism (10 bricks) model (50% element transparency) with support and displacement load**

Figure A - 2 shows the model as described. The solid (brick) elements are divided into 12 elements. More than one element is recommended so load distribution over the thickness gives better results. The 1D embedded reinforcement elements are located in the longitudinal mid-plane of the prism at 10 mm from the bottom side (shown in Figure A - 2). DIANA automatically divides the single reinforcement element in multiple elements corresponding to the number of solid elements where the reinforcement elements are embedded in. Every reinforcement element has three nodes.

The prism is supported on two locations as can be seen in Figure A - 2. The prism could be considered as a simply supported beam. The supports in the experiment are round metal bars that provide some free rotation and some displacement in longitudinal direction.

On the top side the nodes of the mid-plane mortar interface are connected to a single node (master) using tyings. A displacement is applied to this single node and so the connected nodes (tyings) move in exact the same way as the master node.

### ***Reinforced masonry prism model dimensions and material properties***

The material parameters shown in Table A - 1 till Table A - 5 are chosen from the research paper of this reinforced masonry prism test and other literature. The information on material properties from the research paper are limited so other sources had to be used. These others sources are mentioned at the corresponding material properties tables in this paragraph.

**Table A - 1: Dimensions used in FEM model of prism, brick, mortar joint and CFRP strip**

	<b>Dimensions [mm ]</b>
<b>prism</b>	880x230x110 (lxwxh)
<b>brick</b>	230x110x88 (lxwxh)
<b>mortar joint</b>	230x110x0 (lxwxh)
<b>CFRP strip</b>	15x1.2 (wxt)

The bricks used in the experiment are solid clay bricks. The brick is expanded in the model with the thickness of the mortar joint (13 mm) because the mortar joint will be modelled with a zero-thickness interface, like recommended in literature [15] [24].

Table A - 2: Material properties of brick [15]

Material properties of:	Young's modulus (E-modulus)	Poisson's ratio	Density
Brick (solid)	6050 MPa	0,2	1880 kg/m <sup>3</sup>

Brick material properties are taken from the book Structural Masonry [15]. In this book the clay brick units with these properties are called Vijf Eiken (VE) and are likely to be similar to the bricks used in the research but the VE bricks in the Structural Masonry book have more FEM relevant material properties available. So these material properties are used for this model.

Table A - 3: Material properties of mortar (non-linear, CCSC material model) [23]. Values marked with \* are not original values from Petersen research anymore.

Material properties of:	Normal stiffness modulus (Kn)	Shear stiffness modulus (Kt)	Cohesion (C)	Internal friction angle
Mortar non-linear (interface)	*82 N/mm <sup>3</sup>	*36 N/mm <sup>3</sup>	1 MPa	42 <sup>0</sup>
	Dilatancy angle	Residual friction angle	Confining normal stress	degradation coefficient
	35 <sup>0</sup>	42 <sup>0</sup>	-1.8 MPa	2,2
	Tensile strength (ft)	Fracture energy mode-I (Gf I)	Fracture energy mode-I (Gf I) factor (a)	Fracture energy mode-I (Gf I) factor (b)
	*1,1 MPa	0,012 N/mm	0 mm	0,34 N/mm
	Compression strength (fc)	Shear traction contribution (Cs)	Compressive fracture energy (Gfc)	Peak Equiv. plastic relative disp. (kp)
	32 MPa	9	25 N/mm	0,024 mm

Most of the parameters of the CCSC material model cannot be found in the paper of the research where this model is based on. Therefore the Structural Masonry book and a research by Petersen are used [15] [24]. The parameter values for the CCSC material model from the book and the research of Petersen could be considered as reference values and some are changed during calibration of the model as indicated in Table A - 3.

Kn and Kt values are also used for the zero-thickness interfaces in the FEM model that represent the mortar joints in masonry. Equation ( 5 ) and ( 6 ) can be used to determine the Kn and Kt values for the zero-thickness interface for the mortar joints [15].

$$k_n = \frac{E_{unit}E_{joint}}{h_{joint}(E_{unit} - E_{joint})} \quad (5)$$

$$k_t = \frac{G_{unit}G_{joint}}{h_{joint}(G_{unit} - G_{joint})} \quad (6)$$

$K_n$  = Normal stiffness modulus

$K_t$  = Shear stiffness modulus

$E_{unit}$  = E-modulus of brick

$E_{joint}$  = E-modulus of mortar

$G_{unit}$  = Shear modulus of brick

$G_{joint}$  = Shear modulus of mortar

$h_{joint}$  = Height of mortar joint

In this case the shear modulus G can be calculated from the E-modulus and the Poisson ratio (Equation ( 7 )). The same Equation applies for the joint in which case the material parameters of the unit is substituted with the material parameters of the joint.

$$G_{unit} = \frac{E_{unit}}{2(1 + \nu_{unit})} \quad (7)$$

$\nu_{unit}$  = Poisson ratio of brick

$E_{unit}$  = E-modulus of brick

$G_{unit}$  = Shear modulus of brick

The Kt value is the relation between the shear traction and the shear relative displacement [38]. The dimension of the Kt (and also Kn) value is N/mm<sup>3</sup> which means it is a force per area per length (stress per length).

**Table A - 4: Material properties of mortar (linear) [15]**

Material properties of:	Normal stiffness modulus (Kn)	Shear stiffness modulus (Kt)
Mortar linear (interface)	82 N/mm <sup>3</sup>	36 N/mm <sup>3</sup>

\*Same value taken for Kn and Kt as in the Mortar non-linear (interface) (Table A - 3).

Table A - 5: Material properties of NSM CFRP strip (Beam + bond-slip interface) [41] [38]

Material properties of:	Young's modulus (E-modulus)	Poisson's ratio	Density	Bond-slip function
NSM CFRP strip (Beam+bond-slip interface)	165000 MPa	0,3	1600 kg/m <sup>3</sup>	1
	Normal stiffness modulus (Kn)	Shear stiffness modulus (Kt)	Parameter C of bond-slip function	Shear slip at max shear traction
	1000 N/mm <sup>3</sup>	10 N/mm <sup>3</sup>	1,1 MPa	0,06 mm

The Young's modulus of the CFRP is from the research paper. The Poisson's ratio and density are general values for unidirectional carbon Fibre composites [41]. Parameter C and shear slip at max shear traction define the Cubic bond-slip function (Figure A - 3) which is activated with number 1 for the bond-slip function [38]. In the materials library manual of DIANA it is recommended to choose parameter C equal to the tensile strength of the mortar (ft) which is 1,1 MPa. And take for the shear slip at max shear traction 0,06 mm.

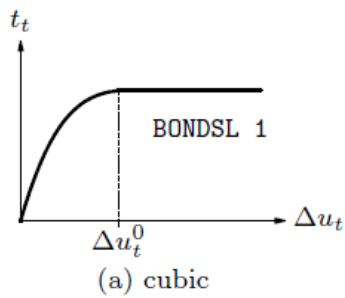


Figure A - 3: Cubic bond-slip function for reinforcement elements [38]

### Results for the reinforced masonry prism model

The research paper contains a force-displacement curve of the three point bending test which will act as a reference to model the same reinforced masonry behaviour as is shown by the force-displacement curve (Figure A - 4).

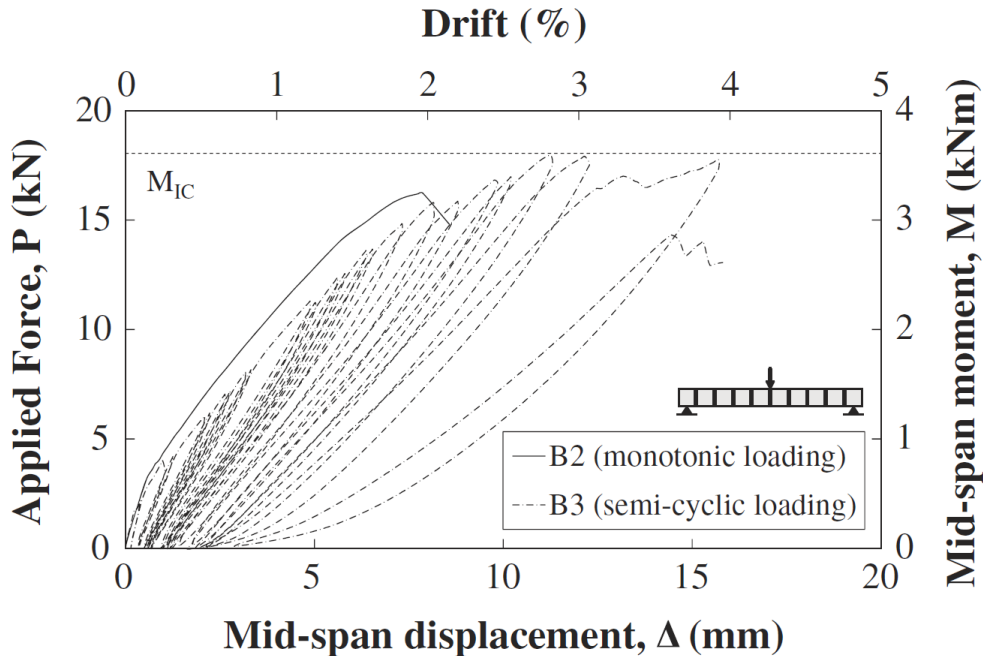


Figure A - 4: Force-displacement curve of the three point bend test [18].

For this model the focus is only on the monotonic loading curve in Figure A - 4. From the curve origin to about 0,5 mm mid-plane displacement (3 kN) the curve shows a linear trend indicating the masonry is in the elastic zone and no major cracks have formed (assumed uncracked state). From this point till the peak load, non-linear behaviour is visible (parabolic like curve development) and likely cracks are forming in the masonry. Usually the assumption is made that the NSM CFRP strip is only loaded when cracks start to initiate.

The NSM CFRP strip provides more ductile behaviour of the reinforced masonry and extends the non-linear part of the curve until peak load is reached. At peak load it is likely that the adhesive reaches its ultimate shear strength and the strip starts to debond from the masonry losing overall stiffness and strength. Or the masonry is severely damaged in the compressive zone due to exceeding ultimate compressive strength of the masonry, so the overall structure loses its stiffness and strength. When comparing the model results with the experimental results, focus is only on the simulation of the behaviour and the force-displacement values due to the large variation in masonry and limited material properties available in the research paper.

Figure A - 6 shows results of two FEM models compared to the test results from paper of Dmytro Dizhur, et al. [18]. Beam bend test model v1 is as described in this Appendix (Figure A - 2 & Figure A - 5). This model showed non-linear behaviour and bond-slip of the embedded reinforcement elements. After a large crack had developed in the mid-plane mortar interface a lot of convergence problems occurred in the model calculations. Beam bend test model v2 is the same model with two model alteration. The mesh is refined (two time increase of elements in all directions) and the non-linear CCSC material at the mid-plane mortar interface is also used for all the other mortar

interfaces instead of using linear mortar interfaces so cracks could form at multiple mortar interfaces.

The model is able to keep analysing after non-convergence steps although still a lot of non-convergence steps were still present in the model result (Figure A - 6).

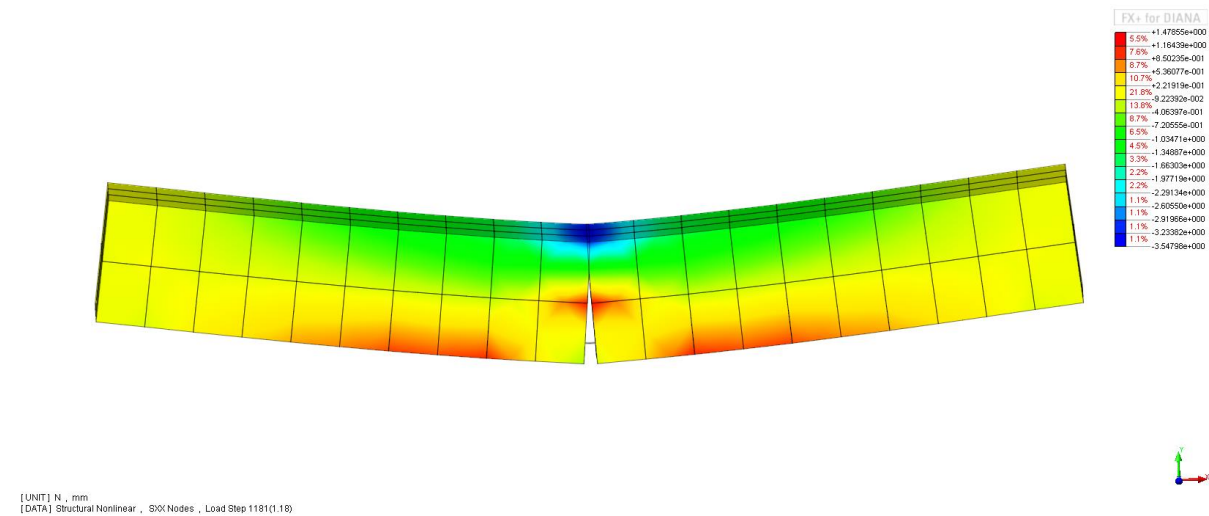


Figure A - 5: Beam bend test model v1

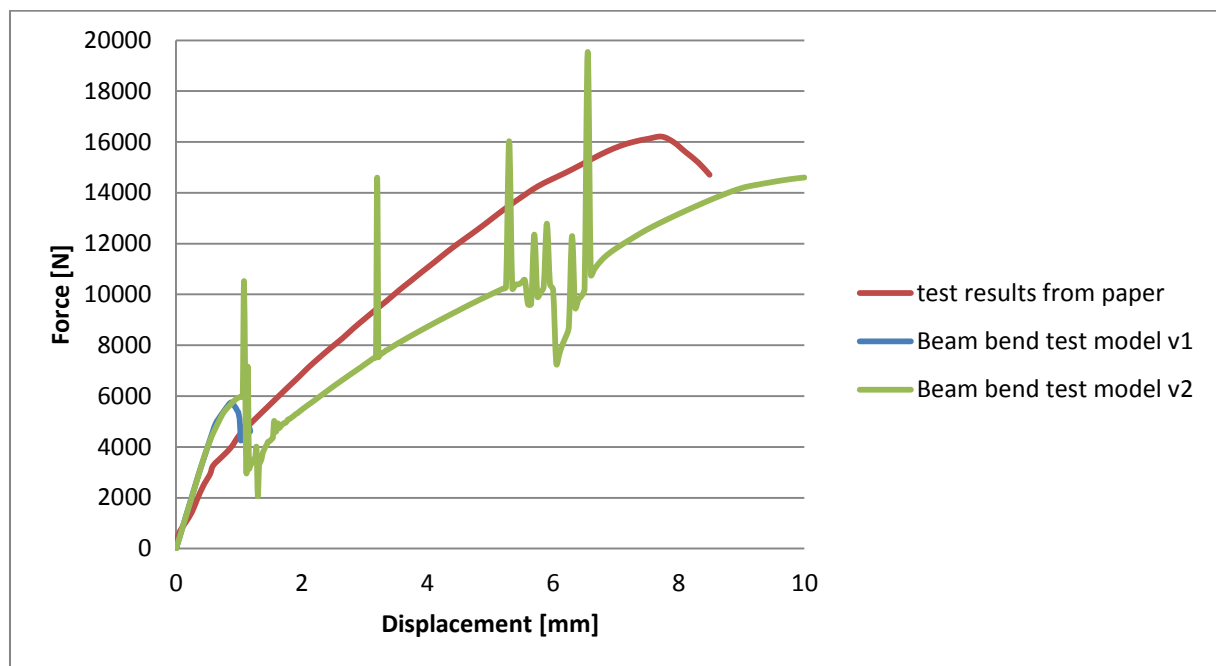
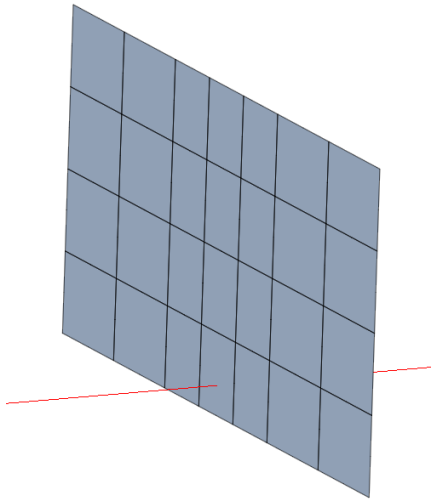


Figure A - 6: Force-displacement curves of Beam bend test model v1 & v2 compared with test results from paper of Dmytro Dizhur, et al. [18]

The problems occurring with these two models are likely to take place because of using embedded reinforcement elements with bond-slip behaviour. The bond-slip function will add interface elements around the reinforcement element to provide slip behaviour. The intersection between these interface elements with the mortar interface elements gives problems (Figure A - 7). After this finding the FEM model based on the Quake-Shield OP bend test does not have reinforcement elements for the NSM CFRP strips but is modelled discrete with shell elements for the NSM CFRP strip and interface elements for the adhesive. Details about this model are described in Chapter 4.



**Figure A - 7: Reinforcement element intersecting a mortar interface element**



## Appendix B

Reduced .DAT file of FEM Base model. Node and element numbers are removed to reduce the number of lines of the file (indicated by dotted lines).

: Diana Datafile written by Diana 9.6

Translated from FX+ for DIANA neutral file (version 1.2.0).

'UNITS'

LENGTH MM

FORCE N

TEMPER CELSIU

'DIRECTIONS'

1 1.00000E+00 0.00000E+00 0.00000E+00

2 0.00000E+00 1.00000E+00 0.00000E+00

3 0.00000E+00 0.00000E+00 1.00000E+00

'MODEL'

GRAVDI 3

GRAVAC -9.81000E+03

'COORDINATES'

20706 2.21827E-13 7.49884E+00 1.50625E+02

.....

44445 3.43750E+02 -3.48253E-03 2.78125E+02

'MATERI'

1 NAME "brick"

MCNAME CONCR

MATMDL TSCR

ASPECT

POISON 8.00000E-02

YOUNG 7.88600E+03

DENSIT 1.78600E-06

TOTCRK ROTATE

TENCRV ELASTI

COMCRV PARABO

CNFCRV NONE

COMSTR 1.00000E+01

GC 1.90000E+01

2 NAME "adhesive"

MCNAME INTERF

MATMDL NONLIF

ASPECT

DSTIF 1.00000E+03 3.45000E-01

SIGDIS -1.00000E+03 -1.00000E+03 -1.00000E+03 -1.00000E+00

0.00000E+00 0.00000E+00 1.00000E+03 1.00000E+00

1.00000E+03 1.00000E+03

TAUDIS -4.00000E-01 -1.00000E+03 -4.00000E-01 -1.60000E+01

```

-8.70000E-01 -9.00000E+00 -1.59000E+00 -7.00000E+00
-1.74000E+00 -6.50000E+00 -1.77000E+00 -6.00000E+00
-1.75000E+00 -5.50000E+00 -1.68000E+00 -5.00000E+00
-1.38000E+00 -4.00000E+00 0.00000E+00 0.00000E+00
1.38000E+00 4.00000E+00 1.68000E+00 5.00000E+00
1.75000E+00 5.50000E+00 1.77000E+00 6.00000E+00
1.74000E+00 6.50000E+00 1.59000E+00 7.00000E+00
8.70000E-01 9.00000E+00 4.00000E-01 1.60000E+01
4.00000E-01 1.00000E+03
3 NAME "mortar"
MCNAME INTERF
MATMDL DISCRA
ASPECT
DSTIF 3.50000E+01 1.60000E+01
DCRVAL 6.00000E-01
DISCRA 1
MODE1 2
MO1VAL 1.70000E-02
MODE2 0
UNLO1 1
4 NAME CFRP
YOUNG 1.65000E+05
POISON 3.00000E-01
DENSIT 1.60000E-06
5 NAME "poly_int"
DSTIF 1.00000E+06 1.00000E+06
6 NAME "PU_shell"
MCNAME MCSTEL
MATMDL TRESCA
ASPECT
POISON 4.86000E-01
YOUNG 2.10000E+01
DENSIT 1.00000E-06
TRESSH NONE
YIELD VMISES
YLDVAL 4.00000E+00
7 NAME "brick2"
MCNAME CONCR
MATMDL TSCR
ASPECT
POISON 8.00000E-02
YOUNG 7.88600E+03
DENSIT 1.78600E-06
TOTCRK ROTATE
TENCRCV ELASTI

```

```

COMCRV PARABO
CNFCRV NONE
COMSTR 1.00000E+01
GC 2.30000E+01
'GEOMET'
1 NAME "mortar"
2 NAME "adhesive"
XAXIS 1.00000E+00 0.00000E+00 0.00000E+00
3 NAME "poly_int"
XAXIS 0.00000E+00 0.00000E+00 1.00000E+00
4 NAME "PU_shell"
THICK 1.00000E+01
5 NAME "frp"
THICK 2.50000E+00
6 NAME "brick"
'DATA'
1 NAME "brick"
8 NAME "brick2"
5 NAME "PU_shell"
7 NAME "frp"
2 NAME "adhesive"
3 NAME "mortar"
4 NAME "poly_int"
'ELEMENTS'
SET "brick"
CONNECT
CHX60 .....
MATERIAL 1
GEOMETRY 6
DATA 1
SET "mortar"
CONNECT
CQ48I.....
MATERIAL 3
GEOMETRY 1
DATA 3
SET "adhesive"
CONNECT
CQ48I.....
MATERIAL 2
GEOMETRY 2
DATA 2
SET "PU int"
CONNECT
CQ48I.....

```

MATERIAL 5  
 GEOMETRY 3  
 DATA 4  
 SET PU  
 CONNECT  
 CQ40S.....  
 MATERIAL 6  
 GEOMETRY 4  
 DATA 5  
 SET FRP  
 CONNECT  
 CQ40S.....  
 MATERIAL 4  
 GEOMETRY 5  
 DATA 7  
 SET "brick2"  
 CONNECT  
 CHX60 .....  
 MATERIAL 7  
 GEOMETRY 6  
 DATA 8  
 SET "Element set 7"  
 CONNECT  
 CQ48I.....  
 MATERIAL 3  
 GEOMETRY 1  
 DATA 3  
 SET "Element set 8"  
 CONNECT  
 CQ48I.....  
 MATERIAL 5  
 GEOMETRY 3  
 DATA 4  
 SET "Element set 9"  
 CONNECT  
 CQ40S.....  
 MATERIAL 6  
 GEOMETRY 4  
 DATA 5  
 SET "Element set 10"  
 CONNECT  
 CQ48I.....  
 MATERIAL 3  
 GEOMETRY 1  
 DATA 3

```

SET "Element set 11"
CONNECT
CQ48I.....
MATERIAL 5
GEOMETRY 3
DATA 4
SET "Element set 12"
CONNECT
CQ40S.....
MATERIAL 6
GEOMETRY 4
DATA 5
'LOADS'
CASE 1
NAME "disp"
DEFORM
36956 TR 2 -1.00000E+00
'GROUPS'
ELEMEN
  155 "Copied-Mesh" / "Element set 7" "Element set 8" "Element set 9" /
  156 "Copied-Mesh-1" / "Element set 10" "Element set 11" "Element set 12" /
'SUPPOR'
NAME "sym".....
NAME "rot".....
NAME "disp".....
NAME "sym2".....
NAME "L_disp"
36956 TR 2
'TYINGS'
NAME "Link Element"
FIX TR 2.....
'END'

```